2007-12-13

Pyridinium Bis-Retinoids A2-Dopamine and A2-Cadaverine: Implications in Age-Related Macular Degeneration and Cancer

McKenzie Ruth Pew
Brigham Young University - Provo

PYRIDINIUM *BIS*-RETINOIDS A2-DOPAMINE AND A2-CADAVERINE: IMPLICATIONS IN AGE-RELATED MACULAR DEGENERATION AND CANCER

by

McKenzie Ruth Pew

A thesis submitted to the faculty of

Brigham Young University

in partial fulfillment of the requirements for the degree of

Master of Science

Department of Chemistry and Biochemistry

Brigham Young University

December 2007

BRIGHAM YOUNG UNIVERSITY

GRADUATE COMMITTEE APPROVAL

of a thesis submitted by

McKenzie Ruth Pew

This thesis has been read by each member of the following graduate committee and by majority vote has been found to be satisfactory.

Date	Heidi R. Vollmer-Snarr, Chair
Date	Steven A. Fleming
Date	Matt A. Peterson
Date	Craig D. Thulin

BRIGHAM YOUNG UNIVERSITY

As chair of the candidate's graduate committee, I have read the thesis of McKenzie R. Pew in its final form and have found that (1) its format, citations, and bibliographical style are consistent and acceptable and fulfill university and department style requirements; (2) its illustrative materials including figures, tables, and charts are in place; and (3) the final manuscript is satisfactory to the graduate committee and is ready for submission to the university library.

Date	Heidi R. Vollmer-Snarr Chair, Graduate Committee

Accepted for the Department

Date	Paul B. Farnsworth Professor and Chair

Accepted for the College

Date	Thomas W. Sederberg College of Physical and Mathematical Sciences

ABSTRACT

PYRIDINIUM *BIS*-RETINOIDS A2-DOPAMINE AND A2-CADAVERINE: IMPLICATIONS IN AGE-RELATED MACULAR DEGENERATION AND CANCER

McKenzie Ruth Pew

Department of Chemistry and Biochemistry

Master of Science

Age-related macular degeneration (AMD) is the leading cause of blindness in the United States of America. The pyridinium *bis*-retinoid A2-ethanolamine (A2E) has been implicated to play a role in AMD. We have observed novel pyridinium *bis*-retinoids through melanolipofuscin and human RPE extractions that may also play a role in the pathology of AMD. We have begun the construction of an amino-retinoid library in order to identify these ocular compounds. The compounds from the amino-retinoid library are also used in a targeted and triggered drug delivery system for treating cancer. Folic acid is coupled with the amino-retinoids to specifically target cancer cells. The first two amino-retinoids to be synthesized and characterized were A2-dopamine (A2D) and A2-cadaverine (A2C). Both pyridinium *bis*-retinoids were shown to generate cytotoxic oxidation products similar to A2E. Successful coupling of folic acid to A2C was

achieved to form the folic acid-A2-cadaverine (FA-A2C) product. Preliminary irradiation results suggest that the FA-A2C product may be more photoreactive than initially anticipated. This could mean less drug and light exposure required to induce apoptosis and could eventually lead to a less invasive and toxic cancer treatment.

ACKNOWLEDGEMENTS

I would first and foremost like to thank Dr. Vollmer-Snarr for her support, guidance, kindness, and understanding throughout my graduate career. I am especially grateful to her for taking a chance on me four years ago by mentoring me as an undergraduate in her lab. This enabled me to fulfill a lifelong dream of doing cancer research and it was in her lab that I truly came to love organic chemistry.

I am forever indebted to Dr. Xue for his patience in teaching me everything I know about working in an organic chemistry research lab.

I would also like to extend thanks to all of my undergraduate associates, especially Mathew Sparks and Bryce Harbertson, who were so kind in helping me during my last couple of months at BYU when I was unable to perform certain tasks for myself.

I am also extremely grateful for the support of my family and for the sacrifices that they have made on my behalf in order to make this thesis a reality.

Most of all I would like to extend my appreciation to my husband, Jefferson, for his extensive help with this thesis. I would also like to especially thank him for the long nights he spent with me in a dark lab while I did research. If not for his love, encouragement, support, and belief in me this thesis would not have been possible. It is to him and our darling daughter Madison, photographed in Chapter 1, that I dedicate this thesis.

TABLE OF CONTENTS

LIST OF FIGURES

LIST OF SCHEMES

LIST OF TABLES

CHAPTER 1. INTRODUCTION TO PYRIDINIUM *BIS*-RETINOIDS

1.1 Age-Related Macular Degeneration

Age-related macular degeneration (AMD) is the leading cause of blindness in the civilized world.[1,2,3] The disease robs the elderly of their central vision, leaving them unable to perform simple tasks such as cooking, driving, reading, watching television, or recognizing faces (Figure 1). Unfortunately, despite much research, the exact cause remains elusive partly due to its multifactorial nature involving a mesh of metabolic, environmental, and genetic contributing factors.[1,4] Consequently, there is no cure for the disease to date.

Figure 1. Vision with Advanced AMD (left) and Normal Vision (right)

AMD can be classified into two subgroups: exudative (wet form) and atrophic (dry form) pictured in Figure 2. Exudative AMD is typified by neovascularization, accompanied by bleeding and fluid leakage, resulting in significant rapid vision loss.[1,2,3] Atrophic AMD is characterized by a slow deterioration of the retinal pigment epithelium (RPE) and photoreceptor cells (Figure 3). The work related to this part of the thesis focuses on the most common form of AMD, atrophic AMD, which represents approximately 90% of the cases.

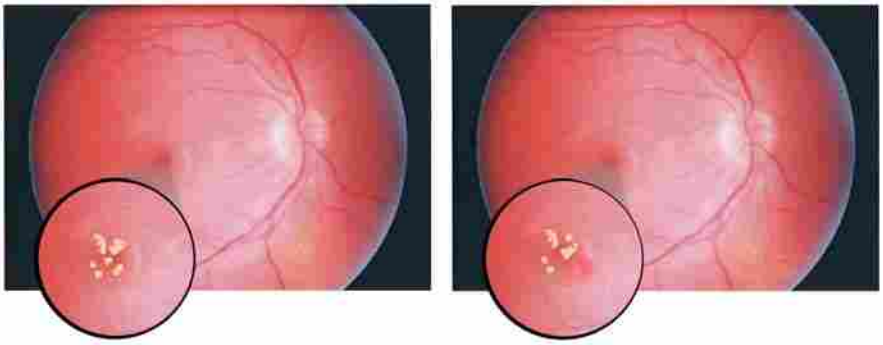

Figure 2. Depiction of Dry (left) and Wet (right) Forms of AMD

Both RPE and photoreceptor cells, which are largely affected in atrophic AMD, are postmitotic and have a symbiotic relationship. Photoreceptor outer segments are replete with light absorbing chromophores responsible for phototransduction. Due to constant light exposure causing oxidative stress, photoreceptor cells are dependent on RPE cells for the phagocytosis of their discarded outer segments.[5,6] The death of one of these cells leads to the permanent loss of the other. While not much is known about the pathogenesis of AMD and precisely what causes the atrophy of the RPE and photoreceptor cells, it is known that at least two processes contribute to its progression: formation of lipofuscin and drusen.[1,2,4,7-10]

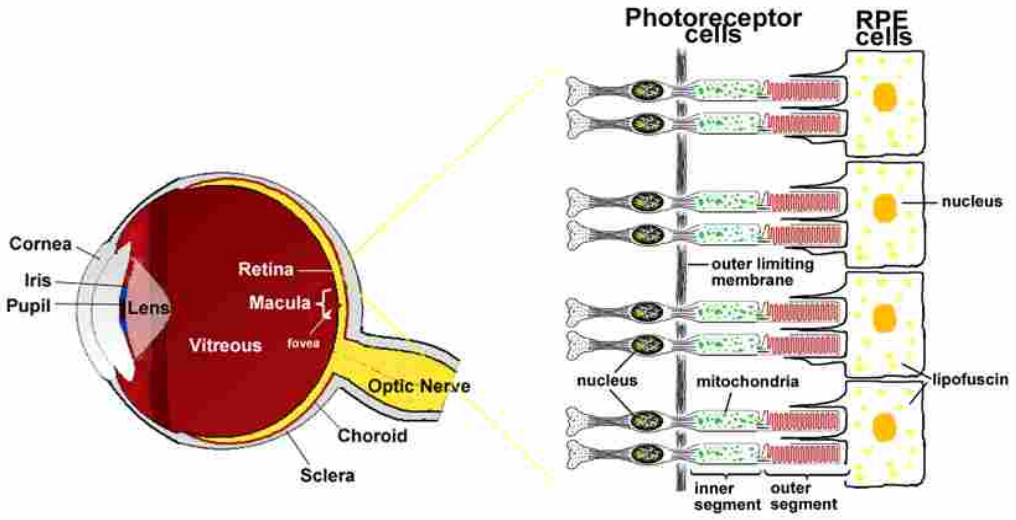

Figure 3. Anatomy of the Eye and Retina

Drusen are amorphous yellow deposits that accumulate in the space between the RPE and choroid and are considered to be the signature trait of AMD.[1,3,11,12] Numerous large drusen deposits are considered to be a major risk factor in developing advanced forms of AMD.[1,11,12] Drusen is thought to negatively impact the health of photoreceptors and RPE by physically displacing these layers, activating the immune system, and causing inflammation.[7]

Another biomarker to the onset of AMD is the accumulation of fluorescent pigments in the RPE known as lipofuscin.[13,14] Lipofuscin is classified as "cellular junk" composed of approximately 50% lipids and 44% proteins[9,10,15] resulting from incomplete digestion of cellular debris from RPE phagocytosis of photoreceptor outer segments.[16,17,18] Evidence suggests that lipofuscin deleteriously affects the RPE by generating toxic singlet oxygen, superoxide anion, and H_2O_2 when irradiated with blue light.[19,20,21] The identification of the responsible chromophores could potentially help in determining the etiology of AMD. One blue absorbing pigment has been extensively characterized; the pyridinium *bis*-retinoid A2E (2-[2,6-dimethyl-8-(2,6,6-trimethyl-1-cyclohexen-1-yl)-1*E*,3*E*,5*E*,7*E*-octatetraenyl]-1-(2-hydroxyethyl)-4-[4-methyl-6-(2,6,6-trimethyl-1-cyclohexen-1-yl)-1*E*,3*E*,5*E*-hexatrienyl]-pyridinium) (**1**, Figure 4).

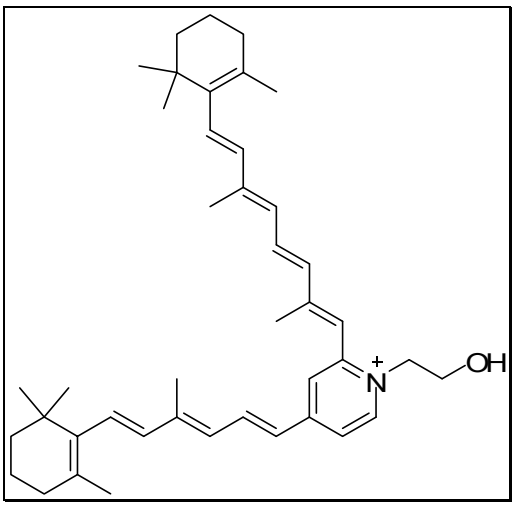

Figure 4. Structure of A2E (**1**)

1.2 Identification and Synthesis of A2E

Eldred and Katz[22] were the first to report a series of blue absorbing fluorophores from 250 RPE eye extracts. Eldred *et al.*[23] used a series of silica gel column chromatography and preparative thin layer chromatography (TLC) purifications to successfully isolate one of the fluorophores. It was hypothesized that this fluorophore was responsible for the fluorescence of RPE lipofuscin. An initial structure of the fluorophore was proposed based on mass spectrometry (MS) and basic chemical analysis of the 100 μg collection. However, structural ambiguities and inconsistencies from the miniscule sample led Sakai *et al.*[24] to reevaluate the proposed structure with the aid of a synthetic standard. The synthetic fluorophore was made from all-*trans* retinal (**2**) and ethanolamine (**3**) in 0.5 % yield (Figure 5). Nuclear magnetic resonance spectroscopy (NMR) structural analysis revealed the structure to be a pyridinium *bis*-retinoid, named A2E (**1**) for the two vitamin A substituents and one ethanolamine moiety.

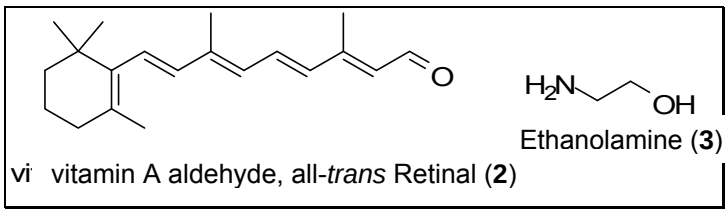

Figure 5. Components of A2E

Since this original discovery, great improvements have been made in A2E synthesis. Significant headway from the original 0.5% yield synthesis has enabled further characterization and study of this molecule and its relationship to lipofuscin's role in AMD. Ren *et al.*[25] were the first to report a seven step total synthesis of A2E. However, this multi-step synthesis only provided modest yields and was not stereo-selective, producing a 4:3:3:2 mixture of A2E isomers. The isomers could be almost entirely converted to the all-*trans* product by heating in nitromethane.

Shortly after the report of the first total synthesis of A2E, Parish *et al.*[26] published a biomimetic one-step preparation of A2E, combining two equivalents of all-*trans* retinal with one equivalent of ethanolamine and acetic acid in ethanol. This methodology was a marked improvement over previously reported syntheses, giving A2E in 49% yield. The significant increase in yield was attributed to the addition of catalytic acetic acid. This one pot process allowed for A2E preparations to be made on a much larger scale, preparing up to 50 mg of material.

The most recent A2E synthesis to be reported was a total synthesis by Sicre *et al.*[27] This A2E total synthesis is an improvement over the original in that it is stereoselective for the all-*trans* isomer. However, this method requires ten steps and still only gives A2E in 14 % yield. Thus, the biomimetic approach remains the most efficient route to synthesize substantial quantities of A2E.

1.3 Age-Related Macular Degeneration and the Visual Cycle

A genetic predisposition to AMD has been postulated, but specific genes have not been directly linked to the disease. However, several genes associated with juvenile macular degeneration have been implicated to play a role in the pathology of AMD. Some of these include the *SOD2, APOE, FIBL-6, RDS, ELOVL4,* and *ABCA4* genes.[28,29] The functions of these genes vary widely and underscore the complexity of AMD. For instance, the *RDS* gene encodes a protein responsible for maintaining the flattened shape of disks in the photoreceptor outer segments.[30] Mutations in the *ELOVL4* gene, predicted to play a role in the elongation of very long-chain fatty acids in photoreceptor cells,[31,32] present a phenotype that closely resembles that seen in atrophic AMD. The phenotype includes photoreceptor degeneration, accumulation of lipofuscin and A2E, and geographic atrophy of RPE cells.[33]

The most frequently studied gene in connection with AMD is the *ABCA4* or *ABCR* gene. The *ABCR* gene is responsible for the recessive form of the childhood macular degeneration, Stargardt's disease,[34,35] and it has been hypothesized that a heterozygous mutation might result in a predisposition to AMD. Heterozygous $abcr^{+/-}$ mice have been shown to experience delayed dark adaptation, along with accumulation of lipofuscin and A2E.[36] The *ABCR* gene encodes rim protein (RmP), a photoreceptor specific ATP-binding-cassette transporter.[37,38,39] During normal phototransduction, as shown in Figure 6, a photon of light hits opsin bound 11-*cis* retinal to yield free all-*trans* retinal (**2**) and opsin. All-*trans* retinal, in the form of N-retinylidene-phosphatidylethanolamine (NRPE, **4**), is then transferred by RmP from

the interior membrane disk to the cytoplasmic surface of the photoreceptor outer segment where it is reduced to all-*trans* retinol (**5**) by all-*trans* retinol dehydrogenase.[40] The newly reduced chromophore is then transferred to the RPE where it is subsequently esterified (**6**), reisomerized to the 11-*cis* conformation (**7**), and finally oxidized back to the original 11-*cis* retinal (**8**).[41] However, when *ABCR* encodes a defective protein, NRPE (**4**) accumulates in the disk membrane where it can combine with an additional molecule of all-*trans* retinal, eventually leading to formation and buildup of A2E within the RPE cell.[36,40,42]

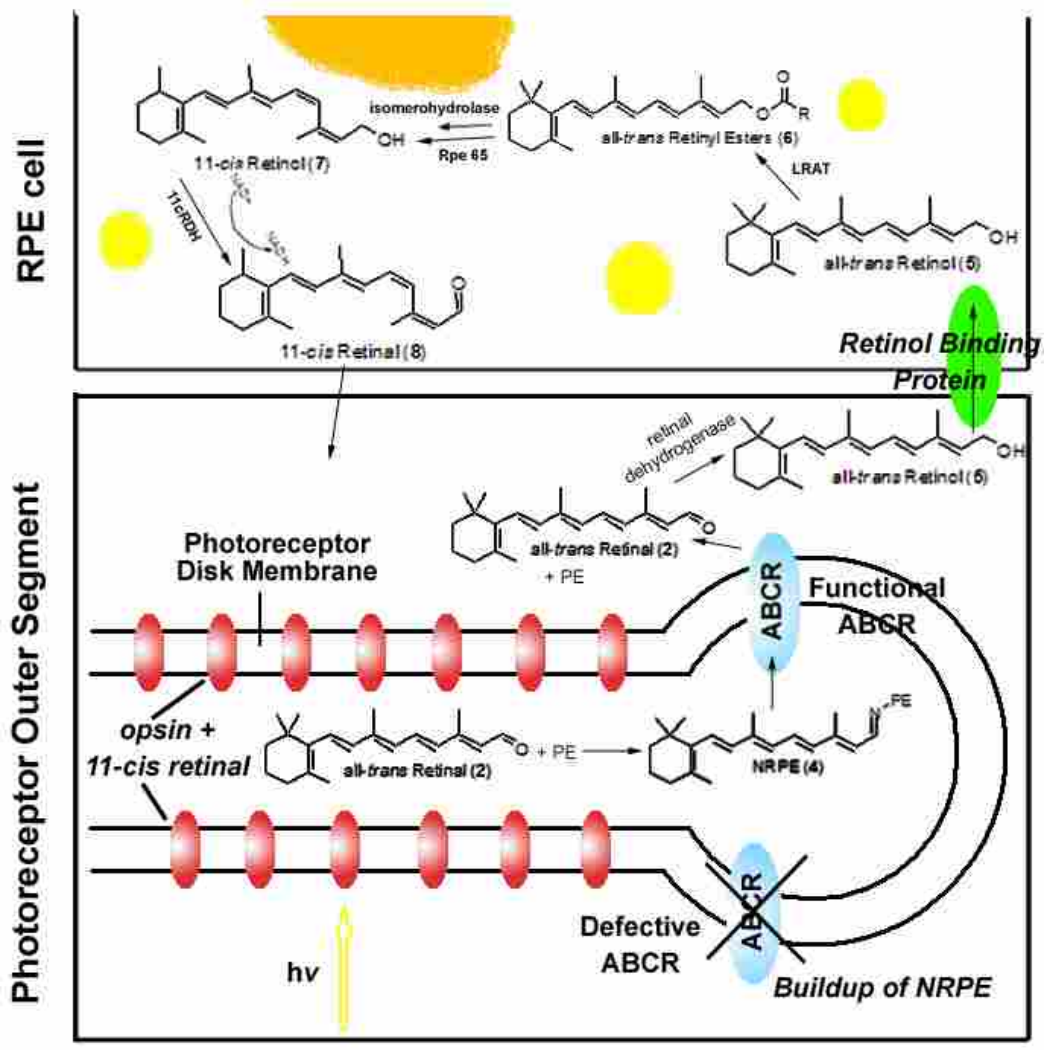

Figure 6. Enlargement of the Retina and the Visual Cycle

1.4 Biosynthesis of A2E

The biosynthesis of A2E has drawn a great deal of interest. Knowledge of how this lipofuscin pigment forms, could potentially lead to targets for AMD prevention and remedies. To this end, Mata *et al.*[42] set out to determine the biosynthetic precursors to A2E using *abcr*$^{-/-}$ mice as a model for AMD. The authors claim to have identified three new compounds involved in the biosynthesis of A2E. The first two precursors of A2E are NRPE (**4**), the Schiff base formed between all-*trans* retinal (**2**) and phosphatidylethanolamine (**9**), and A2PE-H_2 (**10**), formed from reaction of NRPE with all-*trans* retinal. Both precursors appeared to form in mice outer segments, and were found to accumulate with age. *In vitro* incubation of the purported A2PE-H_2 in acidic and oxidizing conditions mimicking the RPE lysosome environment, where lipofuscin accumulates, yielded A2PE (**11**) and A2E (**1**).[42] The biosynthesis of A2E is pictured in Scheme 1.

Lui *et al.*[43] also identified A2E precursors NRPE (**4**) and A2PE (**11**) through the incubation of all-*trans* retinal (**2**) in rod outer segments. The resulting precursors were identified by high performance liquid chromatography (HPLC) analysis with synthetic standards. NRPE and A2PE were also shown to accumulate in photoreceptor outer segments of rat retinal tissues. The biosynthesis of these molecules proved to be dependent on light induced release of all-*trans* retinal.[44] The authors also hypothesized that the hydrolysis of A2PE (**11**) resulted by enzymatic processes rather than by acid hydrolysis. To prove this, A2PE (**11**) was incubated with phospholipase D. HPLC analysis revealed A2E (**1**) formation after two hours, a

significantly faster rate compared to acid hydrolysis. This finding doesn't preclude acid hydrolysis, but lends support to the possibility of enzymatic cleavage.[43,44]

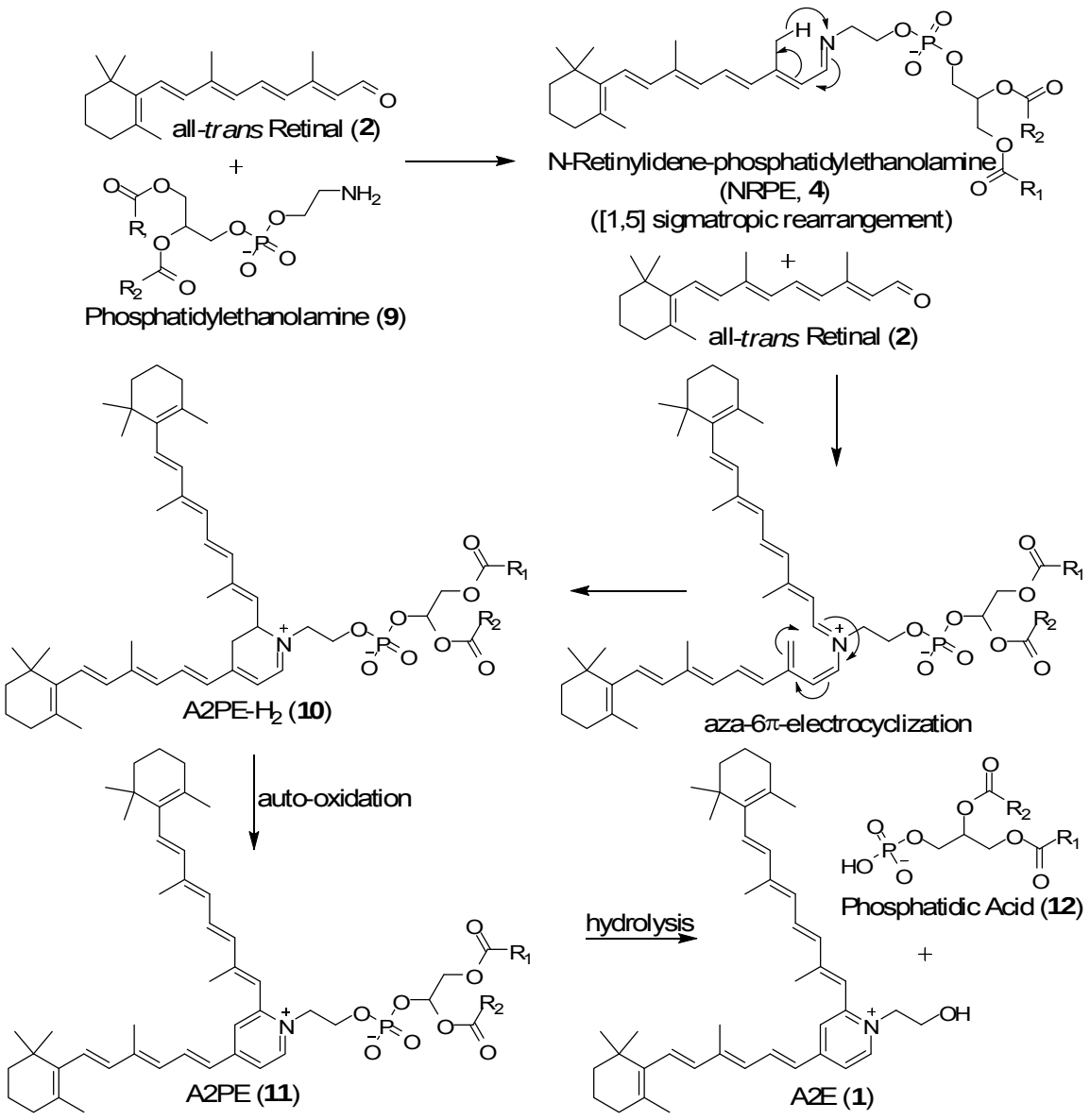

Scheme 1. Biosynthesis of A2E

1.5 Toxicity of A2E

A2E has been attributed to four different modes of RPE cell toxicity. The first proposed mode of A2E toxicity was the disruption of cell membranes. A2E's ampiphilic nature enables it to insert into the lipid bilayer acting as a detergent to disrupt cell membranes. To demonstrate A2E's potential detergent-like nature, Sparrow *et al.*[45] incubated RPE cells with extracellular A2E. Two methods were used to determine loss of membrane integrity: measuring the levels of cytoplasmic enzyme lactate dehydrogenase (LDH) and fluorescence of a nucleic acid stain. A2E was shown to disrupt RPE cell membranes and cause LDH leakage at concentrations of 50 and 100 μM. Nucleic acid staining revealed that exposure to 100 μM A2E for six hours compromised 15% of nuclei. Similarly, De *et al.*[46] used model membranes to demonstrate that A2E caused a decrease of membrane fluidity and membrane solubility. The amount of A2E required for the onset of membrane solubilization depended on the membrane lipid composition. While both of these experiments did demonstrate A2E's potential toxicity as a detergent, the levels of the pyridinium *bis*-retinoid required for the effect were well above those found in human RPE cells. However, work by Schutt *et al.*[47,48] showed that A2E disrupted organelle membranes at low physiologically relevant concentrations. Mitochondria, lysosome and microsome leakage was observed at 1, 2, and 5 μM of A2E, compared to more than 100 μM required for cellular membranes.

A2E and lipofuscin have both been shown to localize in the lysosomes of RPE cells.[45,49] Accordingly, lysosomes would be a logical target for A2E toxicity and Finnemann *et al.*[49] explored this relationship. RPE cells incubated with 100 μM A2E

showed slower outer segment degradation compared to control RPE cells. The authors found that while A2E loaded lysosomes did not inhibit protein degradation, it did impair outer segment lipid degradation, specifically phosphatidylcholine. It was hypothesized that the lack of lipid degradation was a result of A2E's selective inhibition of lipid hydrolases or blocking of lipid trafficking into subcompartments. The end result would be a build up of undigested lipids in RPE cells over time. Bergman *et al.*[50] used isolated intact A2E fed lysosomes to demonstrate ATPase activity, a measurement of lysosomal proton pump activity, was reduced by 50 % at 1 μM A2E and 90 % at 2 μM A2E concentrations. The proton pump was also shown to be affected by A2E through the increase of lysosomal pH. It was concluded that A2E directly interacts with the proton pump and inhibits its activity, eventually resulting in decreased photoreceptor outer segment phagocytosis and degradation.

A third reported A2E toxicity mechanism is disruption of mitochondrial function. It was thought that because mitochondria establish a negative charge inside their inner membrane that it would drive lipophilic cations, like A2E, into the organelle. Suter *et al.*[51] incubated cerebellar granule cells, known for their high mitochondria content, with 5-20 μM A2E. Apoptosis, along with release of the proapoptotic proteins cytochrome *c* and apoptosis inducing factor (AIF), was observed in cells with concentrations >10 μM of A2E. Isolated mitochondria from the cells showed decreased oxygen consumption. Specifically, A2E was found to bind tightly, but non-covalently, to cytochrome *c* oxidase. Exposure to light increased A2E's inhibition of the enzyme and permanently altered its function. Ultimately, A2E's binding with cytochrome *c* oxidase prevented the binding with

cytochrome *c*, interrupting the electron flow, increasing oxidative stress, and resulting in apoptosis.[52] While it was demonstrated that A2E did inhibit mitochondria function at low biologically relevant concentrations, it has also been shown that A2E does not accumulate in RPE mitochondria.[45]

The majority of A2E research has centered on its potential phototoxicity. If A2E is the major blue absorbing fluorophore in lipofuscin, then it should also be responsible for the induced phototoxicity. Because of this hypothesis, Sparrow *et al.*[53] tested the blue light phototoxicity of A2E on human adult RPE cells free of endogenous A2E. Cell cultures were incubated with 10, 50, and 100 μM A2E, resulting in intracellular accumulation at levels measured from healthy human donor eyes, and then irradiated with blue light. After irradiation, RPE cell viability was assayed and showed that 100 μM A2E killed 75% of the cell culture, while 10 μM A2E did not have a measurable impact. Cell apoptosis was demonstrated to be a function of both A2E concentration and light exposure.

The executioners responsible for A2E apoptosis were additionally investigated. Cells incubated with A2E showed caspase-3 activity five hours after irradiation. Furthermore, addition of the caspase-3 inhibitor, Z-DEVD-fmk, decreased A2E photoinduced apoptosis by 55%. To determine if Bcl-2, an antiapototic protein, expression could also attenuate cell death, RPE cells were transfected with a plasmid containing cDNA for human *Bcl-2*. The transfected cells showed a 50% reduction in apoptotic nuclei, suggesting that A2E photoinduced apoptosis is executed by a caspase cascade which is regulated by Bcl-2.[54]

DNA is known to be damaged by reactive oxygen species, and therefore considered a potential target of A2E phototoxicity. Once again, Sparrow *et al.*[55] incubated human RPE cells with 20 μM A2E and exposed the incubated cells to blue light. Comet assays showed over 95% of the cells suffered DNA damage and the number of strand breaks was proportionate to the duration of light exposure. Addition of sodium azide, a singlet oxygen quencher, to A2E containing cells reduced the number of DNA strand breaks, which indicates that singlet oxygen plays a role in A2E blue light toxicity. Additional evidence for the role of singlet oxygen was provided by DNA repair enzymes that showed cells suffered from oxidized purine and pyrimidine bases. Avidin and monoclonal antibodies specifically identified formation of the common oxidative DNA lesion 8-oxo-deoxyguanosine (**13**, Figure 7). Finally, it was also observed that the ability of RPE cells to repair damaged DNA declined with increasing severity of injury. Not only does this evidence suggest A2E is capable of causing photoinduced DNA damage, and eventually apoptosis, but it also indicates damage is mediated through singlet oxygen.

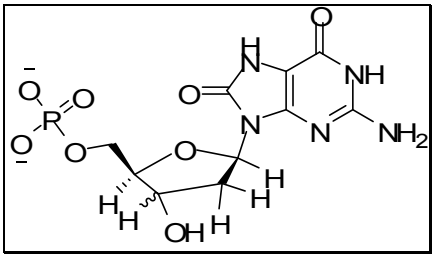

Figure 7. 8-Oxo-deoxyguanosine (**13**)

To further elucidate A2E's mechanism in blue light photoinduced toxicity, Ben-Shabat *et al.*[56] directly irradiated the pyridinium *bis*-retinoid with blue light. MS analysis of the sample after ten minutes of blue light exposure revealed a series of *m/z* +16 oxidative product peaks corresponding to the addition of oxygen atoms to the

carbon-carbon double bonds of A2E. Up to nine oxidation products were observed by MS, meaning that potentially nine oxygen atoms were added to one molecule of A2E. Upon NMR studies of a synthetic A2E oxidation product generated by reaction with *meta*-chloroperoxybenzoic acid (MCPBA), the authors assigned the structure to be a *bi*s-oxirane (**14**).

It was hypothesized that singlet oxygen might be responsible for the formation of these polyoxidation products. To test this theory, A2E was irradiated in the presence of singlet oxygen enhancer D_2O. HPLC analysis demonstrated the disappearance of A2E to be 3 fold greater in D_2O compared to H_2O. It was concluded that the excited states of A2E were quenched by triplet oxygen producing singlet oxygen, which in turn was efficiently quenched by A2E to form the observed polyoxidated products. The highest molecular ion product purportedly corresponded to the formation of a nonaoxirane (**15**).

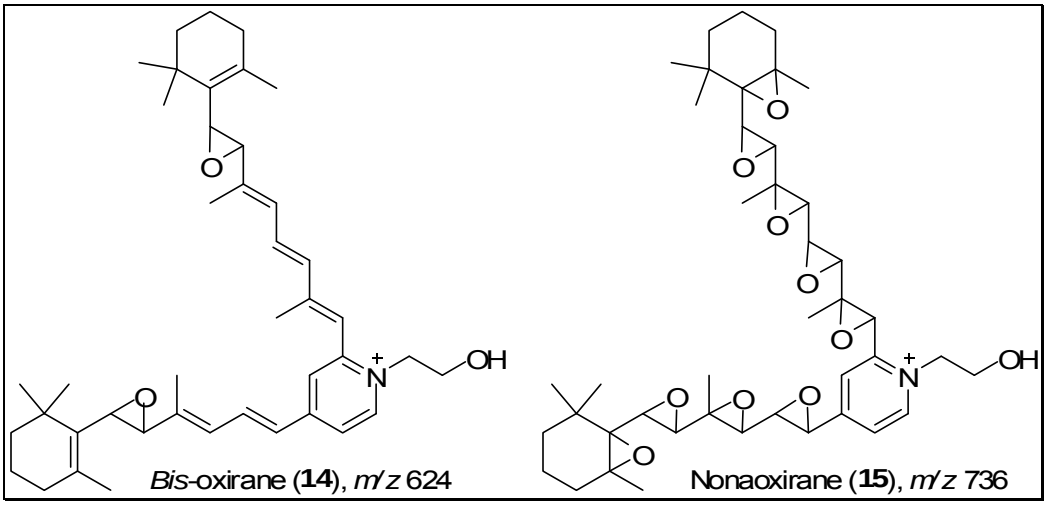

Bis-oxirane (**14**), *m/z* 624 Nonaoxirane (**15**), *m/z* 736

Figure 8. A2E Photooxidation Products

The A2E epoxide investigation was extended to generation of photooxidation products in human RPE cells. RPE cells were incubated with A2E, followed by

exposure to blue light. The irradiated culture was then extracted and subjected to MS analysis. As previously seen with irradiated A2E solutions, the RPE cellular extracts also contained a series of polyoxidative products. The involvement of singlet oxygen in the formation of these photooxidation products was further implicated when A2E containing cells in deoxygenated media were exposed to blue light. RPE cell death was decreased by 98%. Cell death could also be attenuated by incubating A2E containing cell cultures with singlet oxygen quenchers such as sodium azide and histidine. A 43% decrease in cell death was observed with 1 mM of sodium azide, while a 23% reduction in nonviable cells resulted from 10 mM of histidine incubation. Addition of D_2O to cell cultures exhibited the opposite effect and an increase of 66% in nonviable cells was observed.[57] Photooxidation of A2E was also shown to take place *in vivo*. Albino *abcr* $^{-/-}$ mice lacking melanin, the pigment responsible for absorbing extrapupillary and scattered light, were exposed to cyclic light. The mice eyecups were subsequently isolated and the resulting organic material extracted. While both albino and pigmented mice had a similar amount of A2E, albino mice presented a 1.5 fold higher level of oxidized A2E. The greater amount of oxidized A2E present in albino mice suggests that the biosynthesis of A2E and its conversion to polyoxidated products is dependent on increasing amounts of light.[58]

DNA was once again revisited as a potential target of A2E photochemistry, but with A2E epoxides directly reacting with DNA. To test this interaction, A2E epoxides were generated through irradiation and then incubated with human RPE cells. The comet assay was used to test for epoxide reactions with DNA. Only cells

incubated with the oxidized A2E showed a significant amount of DNA strand breaks compared to control cells containing unoxidized A2E. DNA cleavage was also observed in cells that were incubated with synthetic *bis*-oxo-A2E made from reaction with MCPBA. The use of monoclonal antibodies revealed that cells incubated with oxidized A2E tested positive for the common oxidative DNA lesion 8-oxo-deoxyguanosine (**13**). Furthermore, the antioxidants vitamins E and C were proven to suppress the formation of A2E oxidation products and blue light induced DNA strand breaks in RPE cells. This evidence, combined with the knowledge that DNA repair mechanisms and antioxidants decrease with age, implies that DNA and other cellular macromolecules may be targets for A2E-epoxide elicited cell death.[59]

Recently the validity of the formation of a nonaoxirane (**15**) was brought into question due to its instability and the structure of the A2E oxidation product was reevaluated.[60] Jang *et al.*[61] reacted A2E with MCPBA to generate the partially oxidized A2E. Heteronuclear single quantum correlation (HSQC) NMR clarified the structure to be a 5,8,5′,8′-*bis*-furan-A2E (**16**, Figure 9) instead of the previously suggested 7,8-epoxide. Reaction with the singlet oxygen generator 1,4-dimethylnaphthalene yielded a product corresponding to the addition of four oxygens, but with an ultraviolet-visible (UV-Vis) absorption spectrum showing addition occurring at only one double bond on both long and short arms of A2E. Subsequent proton and HSQC-NMR analysis revealed the structure to be 5,8,5′,8′-*bis*-peroxy-A2E (**17**).

In order to better characterize the A2E oxidation products previously seen in cellular environments, human RPE cells were once again incubated with A2E and

irradiated with blue light. Liquid chromatography-mass spectrometry (LC-MS) analysis of chloroform extracts showed two product peaks of *m/z* 608 and 624 with similar UV-Vis spectra having hypsochromic shifts occurring only on the shorter arm of A2E. On the basis of the new structural assessments of oxo-A2E products, these cellular oxidation products were assigned to be the *mono*-furanoid and *mono*-peroxide, respectively. The *mono*-furan-A2E (**18**) and *mono*-peroxy-A2E (**19**) were also shown to occur *in vivo* as they were found in both human donor RPE and *abca4/abcr* $^{-/-}$ mice posterior eye extracts. According to the new structural assignments it appears that upon oxidation, A2E initially forms an epoxide at the electron rich 5,6 double bond, and then depending on the environment, such as the acidic environment of lysosomes or MCPBA, likely rearranges to the more stable 5,8-furanoid product in the RPE. Instead of epoxidation occurring at every double bond of A2E, as presumed with the nonaoxirane (**15**), a more likely explanation is that the higher molecular weight oxidation products result from a [4+2] cycloaddition with singlet oxygen. The newly observed A2E-endoperoxides are relatively unstable and are anticipated to promote reactivity within the cell, causing significant RPE death.[61]

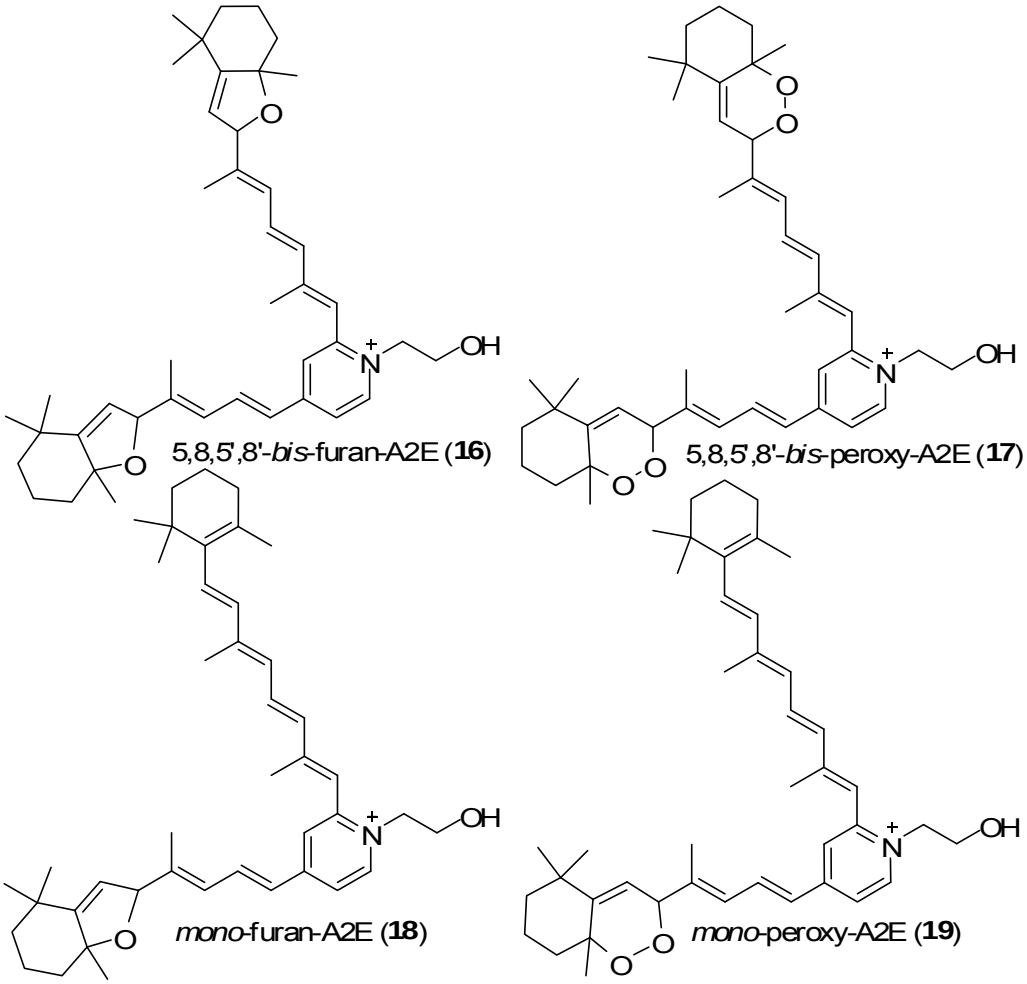

Figure 9. Revised A2E Oxidation Products

1.6 Photophysical and Photochemical Properties of A2E

In order to better understand the relationship between A2E and lipofuscin phototoxicity in AMD, the photophysical and photochemical properties of A2E have been extensively studied. The primary photophysical properties of A2E were first studied by Lamb *et al.*[62] wherein they calculated the emission quantum yield in ethanol to be 0.01. From this it was concluded that A2E's main relaxation process was through a nonradiative mechanism. Comparison of A2E photoacoustic signals to a standard solution indicated that the absorbed energy is almost quantitatively

converted into heat. Contrary to the nonexponential decay observed for lipofuscin, the emission decay for A2E was found to be exponential with a 12 picosecond (ps) time constant, leaving little time for energy transfer to singlet oxygen. The authors also calculated the quantum yield for generation of molecular singlet oxygen from emission intensities to be 0.02 and concluded that A2E is not an efficient generator of singlet oxygen or the major phototoxin of lipofuscin.

The generation of singlet oxygen was directly measured by Kanofsky *et al.*[63] using steady state irradiation and cholesterol as a singlet oxygen trap. Singlet oxygen phosphorescence detection for A2E showed the quantum yield to be 0.013. Cholesterol hydroperoxide (ChOOH) measurements showed A2E singlet oxygen generation to be small compared to a known singlet oxygen generator standard. A2E singlet oxygen generation was also compared to its retinal precursor. Solutions of A2E and all-*trans* retinal dissolved in liposomes both demonstrated photoproduction of ChOOH from cholesterol. However, all-*trans* retinal consumed oxygen at 20.6 times the rate of A2E. An interesting observation gleaned from this experiment is that while photoexcited all-*trans* retinal generated only singlet oxygen, A2E produced both singlet oxygen and free radicals, although inefficiently. From the comparison of the photoreactivity of all-*trans* retinal and A2E, Pawlek *et al.*[64] concluded that the generation of singlet oxygen and free radicals by A2E is insufficient to account for the photoreactivity of lipofuscin. Moreover, they claimed that A2E is an efficient protective agent against all-*trans* retinal phototoxicity.

To further study the potential phototoxicity of A2E, Pawlek *et al.*[65] monitored the photoconsumption of oxygen by lipofuscin, lipofuscin extracts, and A2E.

Lipofuscin granules, liposomes containing lipofuscin extract, and the chloroform insoluble lipofuscin material all showed similar photoinduced oxygen uptake. Thus, the lipofuscin granule photoactive materials were also present in lipofuscin extracts. A2E's oxygen consumption was measured and found to follow the absorbance spectra. However, it did not resemble the action spectra for lipofuscin. The authors proposed that A2E is not a significant contributor to lipofuscin's photoinduced uptake of oxygen. Additionally, the photoreactivity of A2E was directly compared to that of lipofuscin by irradiating liposome dissolved samples with blue light. Extracts were measured to consume a significant amount of oxygen, while the oxygen consumption of A2E was undetectable. At most, A2E could only account for 25% of the oxygen consumption of the lipofuscin extract. The above results postulate that there must be other more prevalent and toxic blue absorbing chromophores responsible for the generation of reactive oxygen species in lipofuscin.

1.7 Detection of New Lipofuscin Fluorophores and Amino-Retinoid Library

While the photophysical and photochemical properties of A2E argue that it does not play a role in the pathology of AMD, the evidence from multiple cellular assays demonstrating A2E's photoinduced apoptosis cannot simply be ignored.[53,54,55,59] The photophysical findings do not preclude the role of A2E in the etiology of AMD. However, the comparison of the photoreactivity of A2E and lipofuscin does illustrate the need for further identification and study of all of lipofuscin's components. To this end, one of the goals of our research is to identify

the remaining blue absorbing chromophores of lipofuscin, specifically new pyridinium *bis*-retinoids.

Originally, Eldred[22,23] isolated the first fluorophore from pooled lipofuscin extractions. Similarly, we have found new unidentified lipofuscin components through organic extractions and HPLC purification. Extractions were also performed on human donor RPE for comparison. Initial structural investigations of the new fluorophores were conducted using a combination of MS and HPLC analysis. Just as the final structural elucidation of A2E required the use of a synthetic standard,[24] an amino-retinoid library was constructed in our laboratories using biogenic amines commonly found in the eye for the final characterization of the extracted amino-retinoids.

1.8 Targeted and Triggered Drug Delivery System

The formation of an amino-retinoid library serves a dual purpose in our research. In addition to identifying fluorophores implicated in the pathology of AMD, the standards are also used to create compounds for the development of a targeted and triggered cancer treatment. Current cancer chemotherapies are invasive and mostly indiscriminant and thus highly toxic to both healthy and cancerous cells. Recent evidence suggests that folic acid may offer a way to specifically target cancer cells, leaving normal cells reasonably unharmed. The folate receptor has been shown to have increased expression in certain malignant tissues, up to two orders of magnitude greater than found in normal tissue.[66] Folate receptor α has a higher expression in ovarian,[67] brain,[68] kidney,[66] cervical,[69,70] breast,[71] and pancreatic[72]

cancers. Another isoform, folate receptor β, is mostly associated with leukemia, specifically chronic myelogenous leukemia[73] and acute myelogenous leukemia.[74] Both folate receptor isoforms are known to bind and uptake folic acid with high affinity at low physiological concentrations.[75] This, combined with the evidence that most normal tissues virtually lack the folate receptor, along with folic acid's ease of modification, ready availability, low cost, and stability during storage, make the folate receptor an attractive target.[76] An additional mechanism of protection for healthy cells expressing the folate receptor is provided by the cell's polarization wherein the folate receptor is attached to the apical surface of epithelial cells, out of direct contact with circulating folic acid labeled toxins.[77] However, cancer cells typically lose their polarization, making the folate receptor accessible to folates in circulation.[77,78] Several drugs have shown increased success through the targeting of the folate receptor,[79-84] and it is this way that we plan to target our treatment. Pyridinium *bis*-retinoids from our synthetic library will be tethered to folic acid by standard coupling procedures, shown in Scheme 2, to selectively kill malignant tissues.

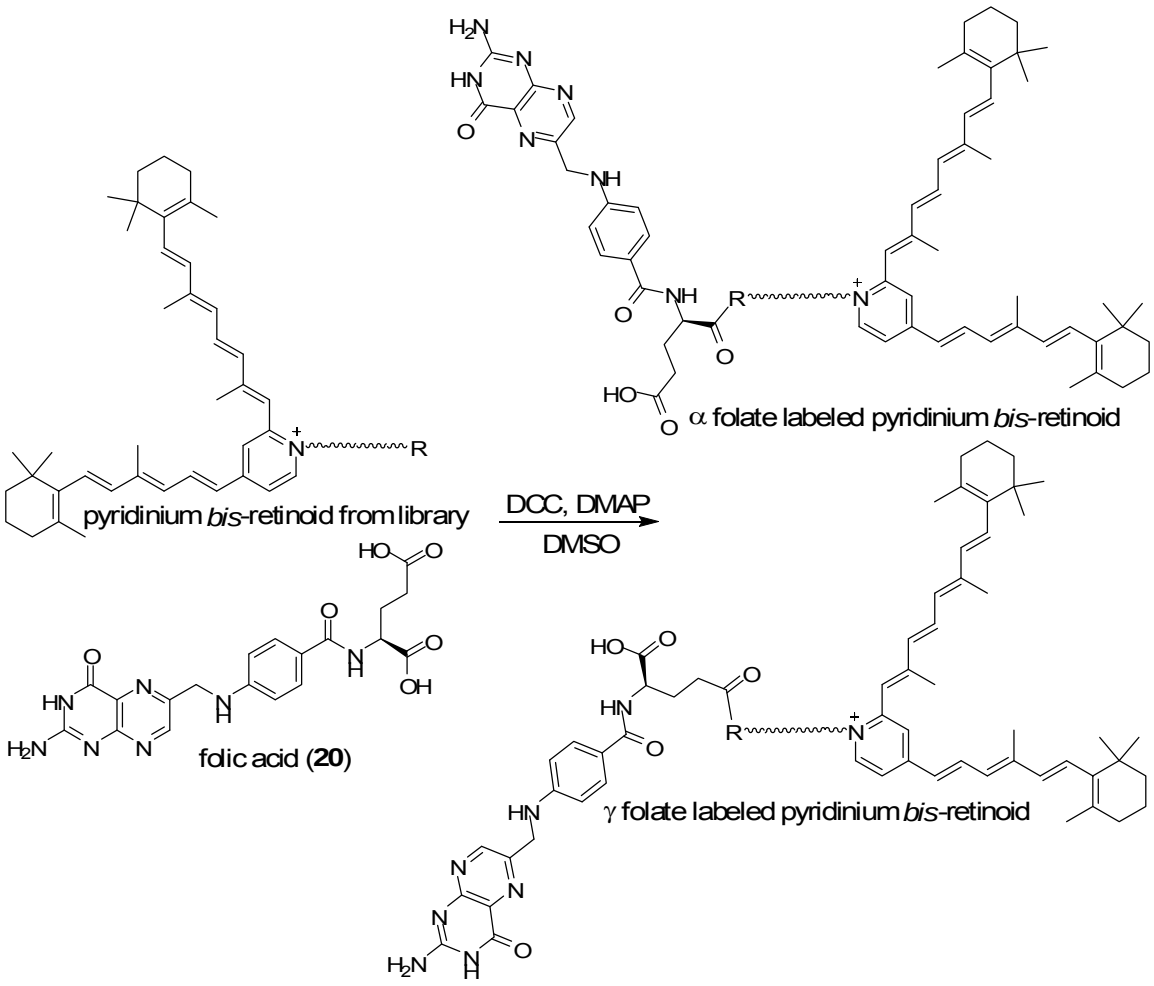

Scheme 2. Targeting Pyridinium *Bis*-Retinoids with Folic Acid

The trigger for our system is light. Our targeted and triggered drug delivery system is based on principles of photodynamic therapy. Photodynamic therapy involves the administration of a photosensitizer which, through various mechanisms, localizes into the tumor tissue.[85,86] In our targeted and triggered drug delivery system the photosensitizer is selectively taken up by folate receptor positive malignant cells. The photosensitizer is then activated by light which transforms the drug into an excited state. From this point the drug can interact with surrounding cellular components transferring a hydrogen atom or electron to form radicals, which can then

react with oxygen to produce oxygenated products. Alternatively, the excited drug can transfer its energy to oxygen, generating cellular damaging singlet oxygen.[87] A2E has been repeatedly shown to induce apoptosis when irradiated with blue light,[53,54,55,59] and other pyridinium *bis*-retinoids have been shown in our laboratories to behave in a similar manner. The mechanism implicated in the photoinduced death involves cellular reaction with A2E polyoxidation products generated through the self quenching of singlet oxygen.[55,56,59] Figure 10 shows a schematic of our proposed targeted and triggered drug delivery system. The normal cell has a low expression of the folate receptor (green) and thus minimal uptake of the folate labeled pyridinium *bis*-retinoid (yellow and orange). However, the cancer cell shows significant folate receptor expression and uptakes the drug preferentially. Upon exposure to blue light the cancer cell undergoes apoptosis, while the healthy cell is left unharmed.

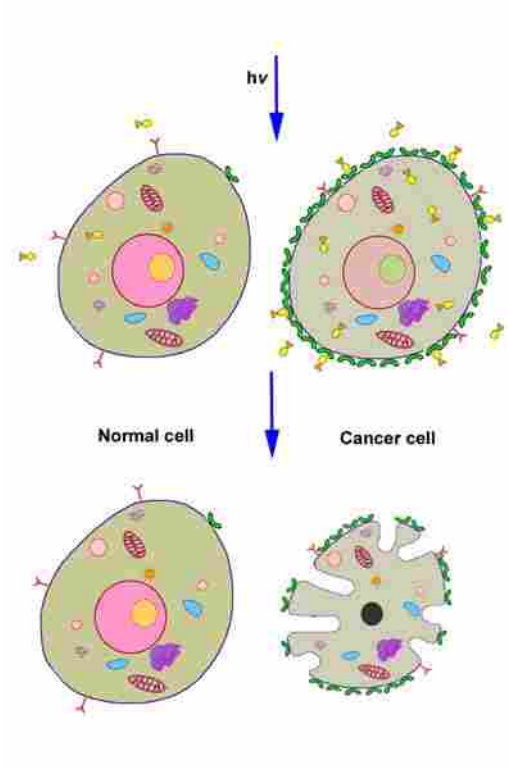

Figure 10. Depiction of Targeted and Triggered Drug Delivery System

Our proposed targeted and triggered drug delivery system offers three advantages over traditional cancer therapies. First, folic acid will be used to specifically target cancer cells. Targeting with folic acid may also decrease the amount of drug needed to induce apoptosis. Unlike other drug delivery systems which are trafficked directly to the lysosome for destruction, thus requiring higher concentrations to elicit fatality, folic acid labeled drugs are recognized by the cell and consequently retained in the cytoplasm where they are most effective.[88] A second advantage is that folic acid is minimally toxic and A2E, in the unoxidized form, is well tolerated at relatively high concentrations (up to 100 μM)[53] compared to typical cancer treatments. Finally, cytotoxicity can be triggered by irradiation only to the affected area, thus minimizing toxicity to surrounding healthy tissue. Based on these three properties, our targeted and triggered drug delivery system could potentially offer a less invasive and toxic alternative to the current slash and burn cancer treatments available.

1.9 References

1. Fine, S. L.; Berger, J. W.; Maguire, M. G.; Ho, A. C. *New Engl. J. Med.* **2000**, *342*, 483–492.
2. Klein, R.; Peto, T.; Bird, A.; Vannewkirk, M. R. *Am. J. Ophthalmol.* **2004**, *137*, 486–495.
3. Kuehn, B. M. *JAMA* **2005**, *293*, 1841–1845.
4. McConnell, V.; Silvestri, G.; *Ulter. Med. J.* **2005**, *74*, 82–92.

5. Bok, D. *J. cell Sci. Suppl.* **1993**, *17*, 189.

6. Young, R. W. *Invest. Ophthalmol. Vis. Sci.* **1976**, **15**, 700.

7. Campochiaro, P. A. *Expert. Opin. Biol. Ther.* **2004**, *4*, 1395–1402.

8. Kijlstra, A,; La Heij, E. C.; Hendrikse F. *Ocul. Immunol. Inflam.* **2005**, *13*, 3–11.

9. Sparrow, J. R.; Boulton, M. *Exp. Eye Res.* **2005**, *80*, 595–606.

10. Wiktorowska-Owczarek, A.; Nowak, J. Z.; *Pol. J. Environ. Stud.* **2006**, *15*, 69–72.

11. Algvere, P. V.; Seregard, S. *Acta. Ophthalmol. Scand.* **2003**, *81*, 427–429.

12. Bressler, N. M.; Silva, J. C.; Bressler, S. B.; Fine, S. L.; Green,W. R. *Retina* **1994**, *14*, 130–142.

13. Dorey, C. K.; Wu, G.; Ebenstein, D.; Garsd, A.; Weiter, J. J. *Invest. Ophthalmol. Vis. Sci.* **1989**, *30*, 1691.

14. Feeney-Burns, L.; Hilderbrand, E. S.; Eldridge, S. *Invest. Ophthalmol. Vis. Sci.* **1984**, *25*, 195.

15. Warburton, S.; Southwick, K.; Hardman, R. M.; Secrest, A. M.; Grow, R. K.; Xin, H.; Wooley, A. T. *Mol. Vis.* **2005**, *11*, 1122–1134.

16. Feeney-Burns, L.; Berman, E. R.; Rothman, H. *Am. J. Ophthalmol.* **1980**, *90*, 783–791.

17. Feeney-Burns, L.; Eldred, G. E. Trans. *Ophthalmol. Soc. U.K.* **1983**, *103*, 416–421.

18. Geng, I.; Wihlmark, U.; Algvere, P. V. *Exp. Eye Res.* **1999**, *69*, 539–546.

19. Boulton, M.; Dontsov, A.; Jarvis-Evans, J.; Ostrovsky, M.; Svistunenko, D. *J. Photochem. Photobiol. B* **1993**, *19*, 201–204.

20. Gaillard, E. R.; Atherton, S. J.; Eldred, G.; Dillon, J. *Photochem. Photobiol.* **1995**, *61*, 448–453.

21. Rozanowska, M.; Jarvis-Evans, J.; Korytowski, W.; Boulton, M. E.; Burke, J. M.; Sarns, T. *J. Biol. Chem.* **1995**, *270*, 18825–18830.

22. Eldred, G. E.; Katz, M. L. *Exp. Eye Res.* **1988**, *47*, 71–86.

23. Eldred, G. E.; Lasky, M. R. *Nature* **1993**, *361*, 724–726.

24. Sakai, N.; Decatur, J.; Nakanishi, K. *J. Am. Chem. Soc.* **1996**, *118*, 1559–1560.

25. Ren, R. X.-F.; Sakai, N.; Nakanishi, K. *J. Am. Chem. Soc.* **1997**, *119*, 3619–3620.

26. Parish, C. A.; Hashimoto, M.; Nakanishi, K.; Dillon, J.; Sparrow, J. *Proc. Natl. Acad. Sci. USA* **1998**, *95*, 14609–14613.

27. Sicre, C.; Cid, M. M. *Org. Lett.* **2005**, *7*, 5737–5739.

28. Tuo J.; Bojanowski, C. M.; Chan, C. C. *Progr. Retin. Eye Res.* **2004**, *23*, 229–249.

29. Traboulsi, E. I. *Am. J. Ophthalmol.* **2005**, *139*, 908–911.

30. Weleber, R. G.; Carr, R. E.; Murphey, W. H. *Arch. Ophthalmol.* **1993,** *111*, 1531–1542.

31. Zhang, X. M.; Yang, Z.; Karan, G.; Hashimoto, T.; Baehr, W.; Yang, X. J.; Zhang, K. *Mol. Vis.* **2003**, *9*, 301–309.

32. Mandal, M. N.; Ambasudhan, R.; Wong, P. W.; Gage, P. J.; Sieving, P. A.; Ayyagari, R. *Genomics* **2004**, *83*, 615–625.

33. Karan, G.; Lillo, C.; Yang, Z.; Cameron, D. J.; Locke, K. G.; Zhao, Y.; Thirumalaichary, S.; Li, C.; Birch, D. G.; Vollmer-Snarr, H. R.; Williams, D. S.; Zhang, K. *Proc. Natl. Acad. Sci. USA* **2005**, *102*, 4164–4169.

34. Allikmet, R.; Singh, N.; Sun, H. *Nat. Genet.* **1997**, *15*, 236–246.

35. Stone, E. M.; Webster, A. R.; Vandenburgh, K. *Nat. Genet.* **1998**, *20*, 328–329.

36. Mata, N. L.; Tzekov, R. T.; Liu, X.; Weng, J.; Birch, D. G.; Travis, G. H. *Invets. Ophthalmol. Vis. Sci.* **2001**, *42*, 1685–1690.

37. Papermaster, D. S.; Schneider, B. G.; Zorn, M. A.; Kraehenbuhl, J. P.; *J. Cell Biol.* **1978**, *78*, 415–425.

38. Azarian, S M.; Travis, G. H.; *FEBS Lett.* **1997**, *409*, 247–252.

39. Illing, M.; Molday, L. L.; Molday, R. S. *J. Biol. Chem.* **1997**, *272*, 10303–10310.

40. Weng, J.; Mata, N. L.; Azarian, S. M.; Tzekov, R. T.; Birch, D. G.; Travis G. H. *Cell* **1999**, *98*, 13–23.

41. Mata, N. L.; Moghrabi, W. N.; Lee, J. S.; Bui, T. V.; Radu, R. A.; Horwitz, J.; Travis, G. H. *J. Biol. Chem.* **2004**, *279*, 635–643.

42. Mata, N. L.; Weng, J.; Travis, G. H. *Proc. Natl. Acad. Sci. USA* **2000**, *97*, 7154–7159.

43. Lui, J.; Itagaki, Y.; Ben-Shabat, S.; Nakanishi, K.; Sparrow, J. R. *J. Biol. Chem.* **2000**, *275*, 29354–29360.

44. Ben-Shabat, S.; Parish, C. A.; Vollmer, H. R.; Itagaki, Y.; Fishkin, N.; Nakanishi, K.; Sparrow, J. R. *J. Biol. Chem.* **2002**, *277*, 7183–7190.

45. Sparrow, J. R.; Parish, C. A.; Hashimoto, M.; Nakanishi, K. *Invets. Ophthalmol. Vis. Sci.* **1999**, *40*, 2988–2995.

46. De, S.; Sakmar, T. P. *J. Gen. Physiol.* **2002**, *120*, 147–157.

47. Schutt, F.; Bergmann, M.; Holz, F. G.; Kopitz, J. *Graefe's Arch. Clin. Exp. Opthalmol.* **2002**, *240*, 983–988.

48. Schutt, F.; Bergmann, M.; Kopitz, J.; Holz, F. G. *Ophthalmologe* **2002**, *99*, 861–865.

49. Finnemann, S. C.; Leung, L. W.; Rodriguez-Boulan, E. *Proc. Natl. Acad. Sci. USA* **2002**, *99*, 3842–3847.

50. Bergmann, M.; Schűtt, F.; Holz, F. G.; Kopitz, J. *The FASEB Journal* **2004**, *18*, 562–564.

51. Suter, M.; Reme, C.; Grimm, C.; Wenzel, A.; Jäättela, M.; Esser, P.; Kociok, N.; Leist, M.; Richter, C. *J. Biol. Chem.* **2000**, *275*, 39625–39630.

52. Shaban, H.; Gazzotti, P.; Richter, C. *Arch. Biochem. Biophys.* **2001**, *394*, 111–116.

53. Sparrow, J. R.; Nakanishi, K.; Parish, C. A. *Invest. Ophthalmol. Vis. Sci.* **2000**, *41*, 1981–1989.

54. Sparrow, J. R.; Cai, B. *Invest. Ophthalmol. Vis. Sci.* **2001**, *42*, 1356–1362.

55. Sparrow, J. R.; Zhou, J.; Cai, B. *Invest. Ophthalmol. Vis. Sci.* **2003**, *44*, 2245–2251.

56. Ben-Shabat, S.; Itagaki, Y.; Jockusch, S.; Sparrow, J. R.; Turro, N. J.; Nakanishi, K. *Angew. Chem. Int. Ed.* **2002**, *41*, 814–817.

57. Sparrow, J. R.; Zhou, J.; Ben-Shabat, S.; Vollmer, H.; Itagaki, Y.; Nakanishi, K. *Invest. Ophthalmol. Vis. Sci.* **2002**, *43*, 1222–1227.

58. Radu, R. A.; Mata, N. L.; Bagla, A.; Travis, G. H. *Proc. Natl. Acad. Sci. USA* **2004**, *101*, 5928–5933.

59. Sparrow, J. R.; Vollmer-Snarr, H. R.; Zhou, J.; Jang, Y. P.; Jockusch, S.; Itagaki, Y.; Nakanishi, K. *J. Biol. Chem.* **2003**, *278*, 18207–18213.

60. Dillon, J.; Wang, Z.; Avalle, L. B.; Gaillard, E. R. *Exp. Eye Res.* **2004**, *79*, 537–542.

61. Jang, Y. P.; Matsuda, H.; Itagaki, Y.; Nakanishi, K.; Sparrow, J. R. *J. Biol. Chem.* **2005**, *280*, 39732–39739.

62. Lamb, L. E.; Ye, T.; Haralampus-Grynaviski, N. M.; Williams, T. R.; Pawlek, A.; Sarna, T.; Simon, J. D. *J. Phys. Chem. B* **2001**, *105*, 11507–11512.

63. Kanofsky, J. R.; Sima, P. D.; Richter, C. *Photochem. Photobiol.* **2003**, *77*, 235–242.

64. Pawlak, A.; Wrona, M.; Różanowska, M.; Zareba, M.; Lamb, L. E.; Roberts, J. E.; Simon, J. D.; Sarna, T. *Photochem. Photobiol.* **2003**, *77*, 253–258.

65. Pawlak, A.; Różanowska, M.; Zareba, M.; Lamb, L. E.; Simon, J. D.; Sarna, T. *Arch. Biochem. Biophys.* **2002**, *403*, 59–62.

66. Ross, J. F.; Chaudhuri, P. K.; Ratnam, M. *Cancer* **1994**, *73*, 2432–2443.

67. Toffoli, G.; Cernigoi, C.; Russo, A.; Gallo, A.; Bagnoli, M.; Boiocchi, M. *Int. J. Cancer* **1997**, *74*, 193–198.

68. Weitman, S. D.; Frazier, K. M.; Kamen, B. A. *J. Neurooncol.* **1994**, *21*, 107–112.

69. Veggian, R.; Fasolato, S.; Menard, S.; Minucci, D.; Pizzetti, P.; Regazzoni, M.; Tagliabue, E.; Colnaghi, M. I. *Tumori* **1989**, *75*, 510–513.

70. Pillai, M. R.; Chacko, P.; Kesari, L. A.; Jayaprakash, P. G.; Jayaram, H. N. *J. Clin. Pathol.* **2003**, *56*, 569–574.

71. Kelley, K. M.; Rowan, B. G.; Ratnam, M. *Cancer Res.* **2003**, *63*, 2820–2828.

72. Kelemen, L. E. *Int. J. Cancer* **2006**, *119*, 243–250.

73. Poss, J. F.; Wang, H.; Behm, F. G.; Mathew, P.; Wu, M.; Booth, R.; Ratnam, M. *Cancer* **1999**, *85*, 348–357.

74. Pan, X. Q.; Zheng, X.; Shi, G.; Wang, H.; Ratnam, M.; Lee, R. J. *Blood* **2002**, *100*, 594–602.

75. Wang, X.; Shen, F.; Freisheim, J. H.; Gentry, L. E.; Ratnam, M. *Biochem. Pharmacol.* **1992**, *44*, 1898–1901.

76. Reddy, J. A.; Low, P. S. *Crit. Rev. Ther. Drug Carrier Syst.* **1998**, *15*, 587–627.

77. Elnakat, H.; Ratnam, M. *Adv. Drug Deliv. Rev.* **2004**, *56*, 1067–1084.

78. Parker, N.; Turk, M. J.; Westrick, E.; Lewis, J. D.; Low, P. S.; Leamon, C. *Anal. Biochem.* **2005**, *338*, 284–293.

79. Pan, X. Q.; Zheng, X.; Shim G.; Wang, H.; Ratnam, M.; Lee, R. J. *Blood* **2002**, *100*, 594–602.

80. Zhao, X. B.; Lee, R. *Adv. Drug Deliv.* **2004**, *56*, 1193–1204.

81. Xu, L.; Pirollo, K. F.; Chang, E. H. *J. Control. Release* **2001**, *74*, 115–128.

82. Lee, R. J.; Low, P. S. *Biochem. Biophys. Acta.* **1995**, *1233*, 134–144.

83. Leamon, C. P.; Pastan, I. *J. Biol. Chem.* **1993**, *268*, 24847–24854.

84. Leamon, C. P.; Low, P. S. *J. Drug Target.* **1994**, *2*, 101–112.

85. Wiedmann, M. W.; Caca, K. *Curr. Pharmaceut. Biotech*. **2004**, *5*, 397–408.

86. Triesscheijn, M.; Baas, P.; Schellens, J. H. M.; Stewart, F. A. *Oncologist*, **2006**, *11*, 1034–1044.

87. Foote, C. S. *Photochem. Photobiol.* **1991**, *54*, 659.

88. Low, P. S. *Adv. Drug Deliv. Rev*. **2004**, *56*, 1055–1058.

CHAPTER 2. INDENTIFICATION OF NEW FLUOROPHORES

In an effort to better define lipofuscin's role in the pathology of AMD and to reconcile the differences in the photoreactivity of lipofuscin and A2E, a central goal of our research is to identify the remaining blue-absorbing lipofuscin chromophores. Similar to the original experiments by Eldred and Katz[1] used to isolate A2E, we also performed extractions on lipofuscin, melanolipofuscin, and human donor RPE samples. The extraction protocol is based on the method reported by Parish *et al.*[2]

2.1 Extraction of Human Lipofuscin, Melanolipofuscin, and RPE

Samples of lipofuscin and melanolipofuscin, melanin pigment fused with lipofuscin granules,[3,4,5] were prepared and donated by Dr. Craig Thulin and researchers. The prepared eye samples were first homogenized and then extracted. The chloroform ($CHCl_3$) soluble material was collected and analyzed by reversed-phase HPLC. The resulting HPLC chromatogram from the melanolipofuscin sample is shown in Figure 1a. A2E, highlighted in red, was identified in the melanolipofuscin extract by its standard retention time and characteristic camel back shaped UV-Vis spectrum. We also observed two other unknown prominent peaks (blue) that were not all-*trans* retinol, retinal, or A2E oxidation products based on comparison to known spectral data. The two peaks presented UV-Vis spectra similar to A2E, but it was determined that they were not isomers due to their large relative peak areas. Iso-A2E, the most abundant isomer, is known to exist in a 1:4 ratio with A2E[2] and other isomers are substantially less prevalent.[6] It was hypothesized that these two peaks belonged to new pyridinium *bis*-retinoid compounds. To test this

hypothesis, a co-injection of the melanolipofuscin extract and synthetic standard A2E was performed to corroborate that the two putative pyridinium *bis*-retinoid peaks did not belong to A2E or its isomers. The resulting co-injection HPLC chromatogram shown in Figure 1b confirms our hypothesis that the unidentified blue-absorbing chromophores are not A2E or any of its isomers. This was concluded from the increase in A2E (red) peak area ratio relative to the putative novel pyridinium *bis*-retinoids (blue) resulting from the co-injected standard.

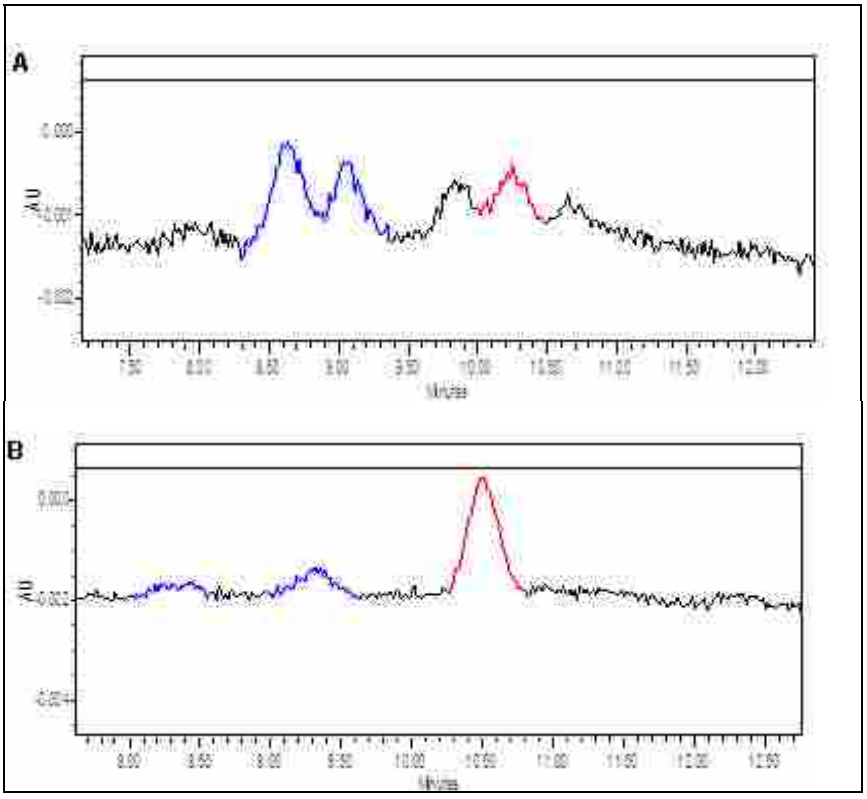

Figure 11. (a) Chromatogram of Melanolipofuscin Extract: A2E (red), New Chromophores (blue); (b) Co-injection with A2E Standard

In addition to observing new pyridinium *bis*-retinoid compounds in lipofuscin, we have also detected a new pyridinium *bis*-retinoid in human donor RPE eye extracts, indicating that the melanolipofuscin fluorophores were not merely an artifact. Figure 2 shows the HPLC chromatogram from one of the RPE eye extracts.

Once again A2E is highlighted in red and the putative pyridinium *bis*-retinoid in blue. Figure 2b shows the unidentified pyridinium *bis*-retinoid's UV-Vis spectrum which has the classic camel back shape similar to A2E.

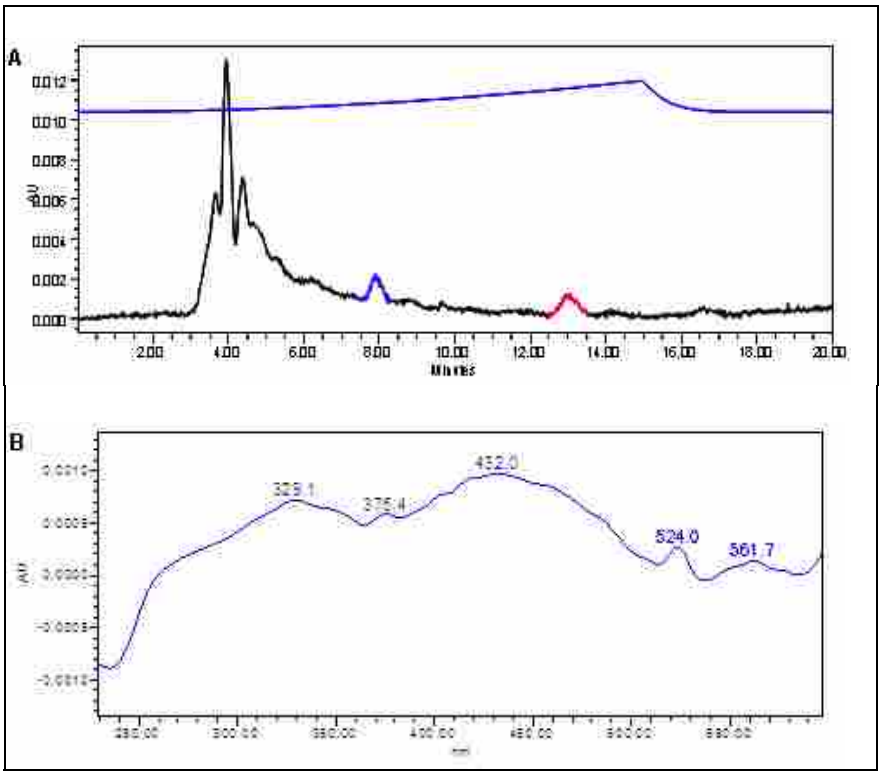

Figure 12. (a) Chromatogram of RPE Extract: A2E (red), New Chromophore (blue); (b) UV-Vis of New Chromophore

While the identity of these putative pyridinium *bis*-retinoids are at present unknown, a common trend can be seen in both the melanolipofuscin and RPE extracts. In each of the HPLC chromatograms the unidentified fluorophores have a shorter retention time than A2E, meaning they are more polar. This information has provided a direction for us in which to start looking. To this end, we began building a pyridinium *bis*-retinoid library combining polar biogenic amines commonly found in the eye with all-*trans* retinal in an attempt to identify these compounds. Figure 3

shows prospective biogenic amines that are presumably more polar than ethanolamine and that are being used in our library.

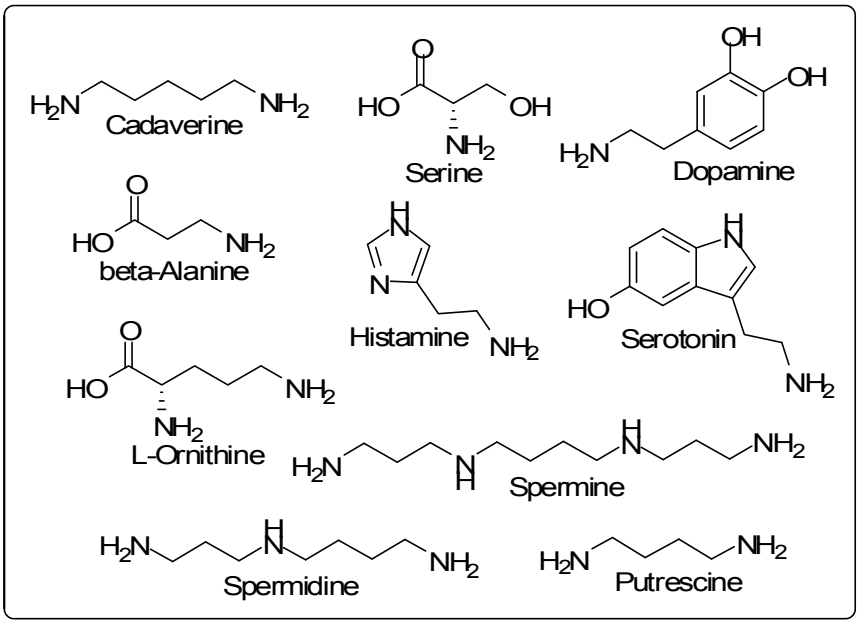

Figure 13. Biogenic Amines to be Used in Pyridinium *Bis*-Retinoid Library

2.2 References

1. Eldred, G. E.; Katz, M. L. *Exp. Eye Res.* **1988**, *47*, 71–86.
2. Parish, C. A.; Hashimoto, M.; Nakanishi, K.; Dillon, J.; Sparrow, J. *Proc. Natl. Acad. Sci. USA* **1998**, *95*, 14609–14613.
3. Feeney-Burns, L. *Invest. Ophthalmol. Vis. Sci.* **1978**, *17*, 583–600.
4. Schraermeyer, U.; Stieve, H. *Cell Tissue Res.* **1994**, *276*, 273–279.
5. Schraermeyer, U.; Peters, S.; Thumann, G.; Kociok, N.; Heimann, K. *Exp. Eye, Res.* **1999**, *68*, 237–279.

6. Ben-Shabat, S.; Parish, C. A.; Vollmer, H. R.; Itagaki, Y.; Fishkin, N.; Nakanishi, K.; Sparrow, J. R. *J. Biol. Chem.* **2002**, *277*, 7183–7190.

CHAPTER 3. STUDIES OF PYRIDINIUM *BIS*-RETINOID A2-DOPAMINE

Upon the discovery of potential new pyridinium *bis*-retinoids in human melanolipofuscin and RPE extractions, our focus turned to identifying these biological compounds by constructing a library of pyridinium *bis*-retinoids. In beginning to build our library, one of the new amines of choice was dopamine (**21**, Figure 1). Dopamine was selected as a starting point for two reasons. First, the resulting amino retinoid would presumably be more polar than A2E on reversed-phase HPLC, thus correlating to the new amino retinoid compounds observed. Second, dopamine has the ability to generate free radicals.[1,2,3] The ability of dopamine to generate reactive oxygen species, known as dopamine toxicity, was an attractive property for our targeted and triggered cancer drug delivery system. Theoretically, more free radicals generated would result in more cytotoxic oxidation products and hopefully increased cell fatality.

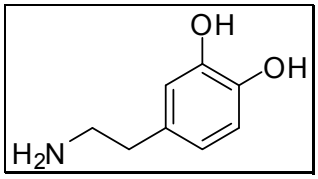

Figure 14. Dopamine (**21**)

3.1 Synthesis of A2-Dopamine

The proposed route for constructing the amino retinoid library was to use a biomimetic method reacting all-*trans* retinal with the desired amine. A biomimetic route was chosen over total synthesis for three fundamental reasons. First, current multi-step A2E total syntheses report low overall yields (around 14 %),[4] while the biomimetic method gives A2E in one-step in 49% yield.[5] The second reason is that a

biomimetic approach is a simple one step and one pot reaction, compared to a ten step total synthesis.[1] Finally, the amines are generally economical and readily available. All-*trans* retinal (**2**) can be easily synthesized from inexpensive vitamin A propionate (**22**) or purchased directly, making the overall synthesis even easier.

The first step in constructing our amino retinoid library was to synthesize the starting material all-*trans* retinal (**2**) from vitamin A propionate (Scheme 1). Vitamin A propionate (**22**) was hydrolyzed to retinol (**5**) with potassium carbonate (K_2CO_3) in a 10:1 methanol (MeOH), tetrahydrofuran (THF) solution.[6] The resulting retinol (**5**), typically isolated in 80 % yield, was then oxidized by manganese dioxide (MnO_2) to give all-*trans* retinal in 85 % yield (**2**).[7]

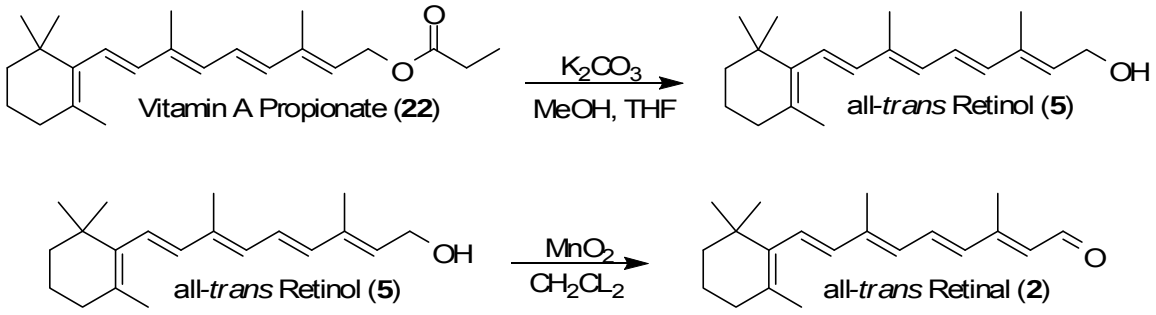

Scheme 3. Synthesis of all-*trans* Retinal (**2**)

With the starting material in hand, we had two biomimetic options for synthesizing the dopamine retinoid compound. Pezzela *et al.*[8] had previously reported a synthesis for the dopamine *mono*-retinoid (A1D) using a 0.1 M phosphate buffer at pH 7.4 with 1-2% w/w sodium dodecylsulfate (SDS) to mimic the eye's biological environment. The second option for synthesizing the dopamine retinoid compound was to use the standard conditions for synthesizing A2E reported by Parish *et al.*[5] This method combined all-*trans* retinal and the desired amine in ethanol and

acetic acid. Because Pezzela[8] only reported formation of the *mono*-retinoid it was presumed that both methods would yield only A1D and not the pyridinium *bis*-retinoid. Theoretically, both the tetrahydroisoquinoline retinoid, A1D, and pyridinium *bis*-retinoid, A2-dopamine (A2D), have a chance of forming. Once dopamine (**1**) has attacked the aldehyde (**2**) to form the Schiff base intermediate **23**, there are two diverging pathways that can follow (Scheme 2). The Schiff base intermediate **23** can either undergo a [1, 5] H-shift, as in the case of A2E, giving the secondary amine **24**. The secondary amine **24** can subsequently react with another molecule of all-*trans* retinal to give the pyridinium *bis*-retinoid A2D (**25**). Alternatively, intermediate **23** can follow another pathway involving a Pictet-Spengler reaction where the electron donating hydroxy groups of dopamine facilitate the attack of the Schiff base adduct to give tetrahydroisoquinoline products **26** and **27**, collectively referred to as A1D.

Three reactions were initially used in the synthesis of the dopamine retinoid compound to discover conditions which optimized yield and purity. Two of the three reactions were carried out under the Parish[5] method which combined dopamine (HCl) and all-*trans* retinal in ethanol. An equivalent of acetic acid (AcOH) was added to only one of the two reaction flasks to see if it improved yields. The third reaction combined dopamine (HCl) and all-*trans* retinal in 0.1 M phosphate buffer (pH 7.4) with 1.5% w/w SDS. All reactions were stirred at room temperature, in the dark to minimize any decomposition or photoisomerization of materials.

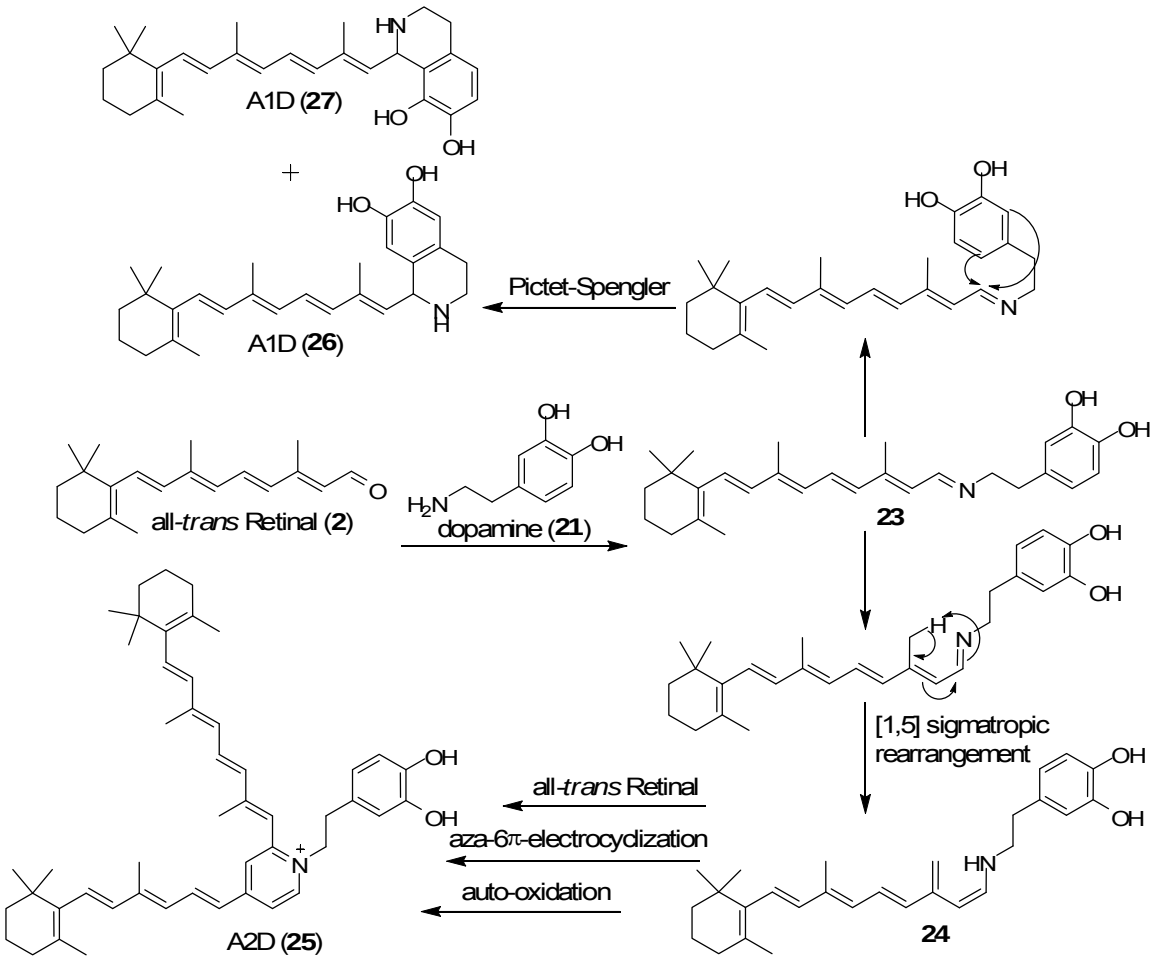

Scheme 4. Two Pathways in the Reaction of all-*trans* Retinal and Dopamine

Surprisingly, the two biomimetic methods gave drastically different outcomes. According to the fast atom bombardment-mass spectrometry (FAB-MS) results, the two reactions using the standard A2E protocol (Method I, Figure 2) gave only the anticipated A1D (420 m/z, **26** and **27**) products. The reaction containing acetic acid returned more product. However, the physiological conditions reported by Pezzella[8] (Method II, Figure 2) gave the previously unreported pyridinium *bis*-retinoid, A2D (684 m/z, **25**), as the major amino retinoid product.

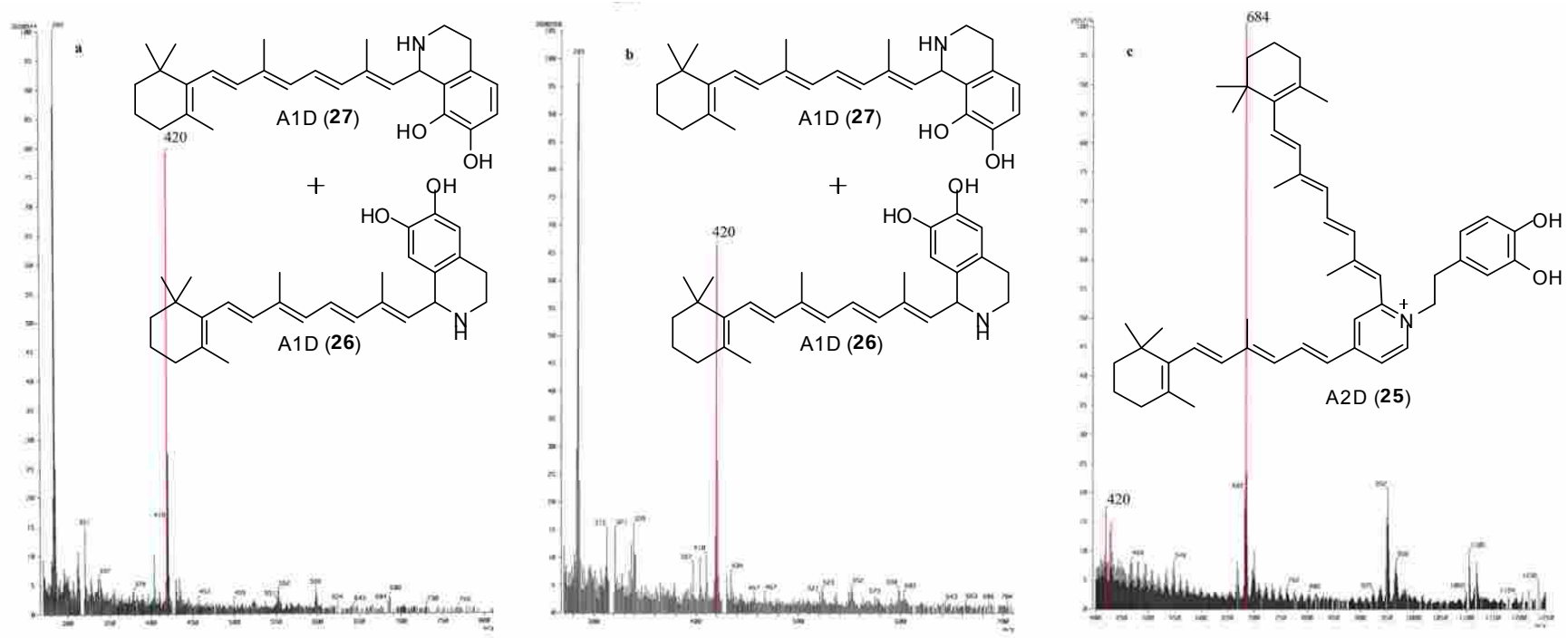

Figure 15. A2D Synthesis FAB-MS Results (a) Method I with Acetic Acid, (b) Method I without Acetic Acid, (c) Method II

Limited attempts were made to alter the outcomes of the two methods by varying amounts of all-*trans* retinal. One equivalent of all-*trans* retinal was used to select for the tetrahydroisoquinoline retinoid products, while two equivalents were used to encourage the formation of the pyridinium *bis*-retinoid. Regardless of the conditions used, the outcomes were the same. Method I still gave the *mono*-retinoid with two equivalents of retinal, and Method II yielded the pyridinium *bis*-retinoid with only one equivalent.

The surprising discovery of A2D proved advantageous since one of the purposes of constructing our library is to identify the pyridinium *bis*-retinoid compounds seen in the human eye extractions. To this end, A2D was synthesized according to Pezzella's[8] conditions, extracted from the aqueous buffer, purified by column chromatography, and repurified by chromatotron. A2D was isolated in 20 % yield and the identity was confirmed by UV-Vis, high resolution electrospray ionization mass spectrometry (HR-ESI-MS), and $^{1}H/^{13}C$ NMR. Proton and carbon NMRs revealed the dodecyl sulfate anion to be the counterion to A2D. Figure 3 shows a comparison of the A2D UV-Vis spectrum (a) and its near identical resemblance to the camel backed shape spectrum of A2E (b).

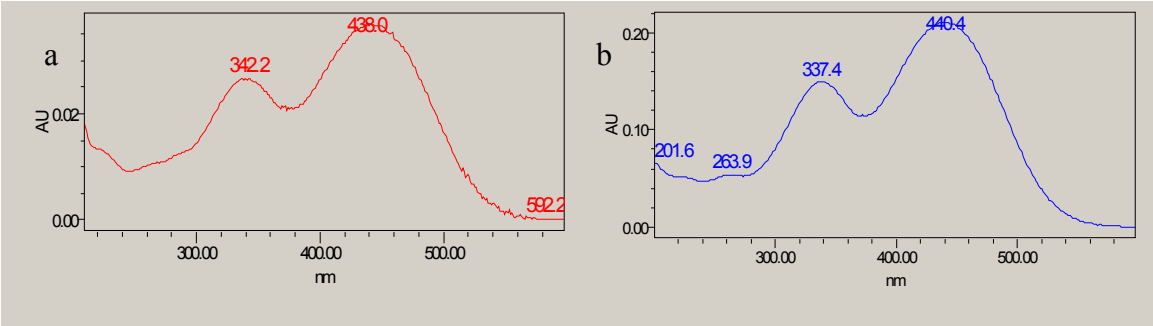

Figure 16. Comparison of UV-Vis Spectra (a) A2D, (b) A2E standard.

In summary, we were able to biomimetically synthesize, isolate, and characterize the pyridinium *bis*-retinoid A2D. The dopamine *bis*-retinoid was isolated in 20 % yield. While this is lower than the 50 % yield reported for biomimetically synthesized A2E, it is

still more economical than the ten step and 14 % overall yield total synthesis alternative. In addition, we demonstrated that the two different biomimetic approaches gave two different amino retinoid products. In fact, the conditions used by Pezzella[8] actually yielded A2D (**25**) as the main amino retinoid product, contrary to that reported. It is unclear as to why the two biomimetic methods gave different results since both used protic solvents (Method I: ethanol; Method II: water) to run the reaction. The outcome in Method II was presumably a consequence of either the buffer or SDS that favored the formation of the pyridinium *bis*-retinoid. With the finding that the biologically relevant conditions reported by Pezzella actually yield the pyridinium *bis*-retinoid over the tetrahydroisoquinolines, one might hypothesize that the *bis*-retinoid would form preferentially to the *mono*-retinoid in the lipid rich aqueous environment of the eye.

3.2 A2D Photochemical Experiments

With A2-Dopamine in hand the next step in our project was to test the pyridinium *bis*-retinoid for potential photooxidation capabilities. If A2D demonstrated photoinduced oxygen uptake similar to A2E not only could it potentially play a role in the pathology of AMD, but it could also make an effective phototoxin for our targeted and triggered drug delivery system. Because dopamine is known to generate reactive oxygen species it was hoped that A2D would be oxidized more efficiently than A2E. To test this hypothesis A2D was dissolved in a 10% dimethylsulfoxide (DMSO) solution in water. The sample was irradiated in a two sided polystyrene visible cuvette using a dichroic blue filter. Aliquots of the irradiated A2D were taken every hour for five hours and submitted for electrospray ionization-mass spectrometry (ESI-MS) analysis.

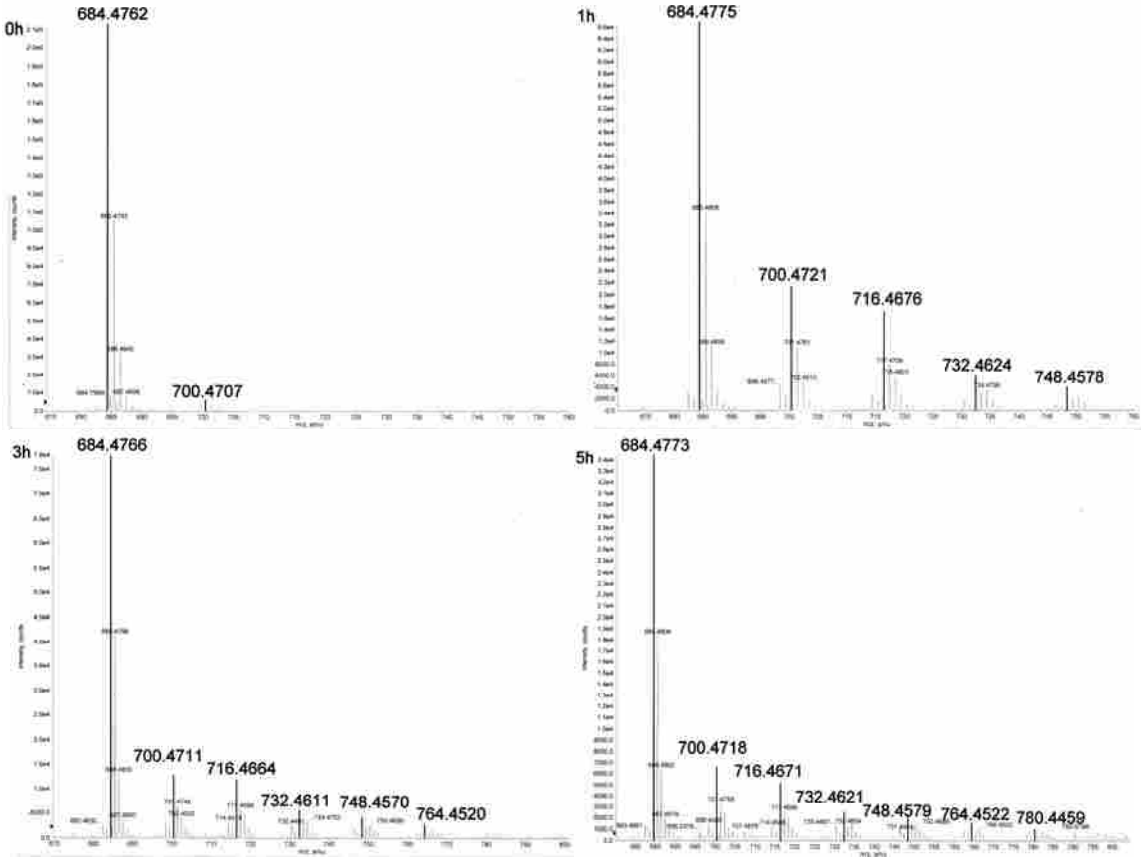

Figure 17. A2D Irradiation ESI-MS Results for Hours 0, 1, 3 and 5

The ESI-MS irradiation results for hours one, three, and five are shown in Figure 4. Beginning with time = 0, the pure sample solution shows one single clean product peak at *m/z* 684 belonging to the pyridinium *bis*-retinoid A2D. After one hour of blue light exposure one can observe the appearance of four oxidation products in increments of *m/z* 16 starting from the M^+ peak. The first peak (700), exactly *m/z* 16 greater than A2D, corresponds to the addition of one oxygen atom. The second (716), third (732), and fourth (748) peaks are associated with the addition of two, three, and four oxygen atoms to the pyridinium *bis*-retinoid arms. Further blue light exposure results in a decrease of the original oxidation products (*m/z* 700 and 716), and simultaneously yields

additional product peaks at *m/z* 764, after three hours, and 780 after five hours of irradiation. These results correspond to the formation of polyoxidative species with at least six oxygen atoms added onto the A2D retinoid arms.

While A2D does appear to yield polyoxidative species similar to A2E when irradiated with blue light, its oxidation mechanism differs in several aspects. For instance, A2D's most abundant oxidation product is *m/z* 700, corresponding to the addition of one oxygen atom. Typically, A2E forms the *bis*-oxo preferentially to the *mono*-oxo A2E. Also, when A2E is irradiated with blue light it is almost completely consumed. However, from mass spectrometry data it appears that the majority of A2D oxidation takes place within the first hour of light exposure. From this point it appears that only the *mono* and *bis*-oxo A2D, not the starting material, are further oxidized to form the polyoxidative A2D species. This is concluded from the decrease in *m/z* 700 and 716 peak ratios compared to the virtually unchanging A2D peak (684). This result can be explained by the fact that conjugation in the A2D oxidation products has been broken, and therefore they are more likely to react with singlet oxygen over the original A2D.

Finally, A2E has been shown to generate nine photooxidation products by mass spectrometry, compared to A2D's six. It was initially hypothesized that upon irradiation with blue light, epoxidation would occur at all nine double bonds on the *bis*-retinoid arms of A2E, forming a nonaoxirane.[9] However, the feasibility of the formation of a nonaoxirane was questioned due to the instability of a molecule containing nine epoxides. More recently it was suggested that epoxidation begins at the 5,6 double bond of amino *bis*-retinoids, and in some cases rearranges to form a 5,8-furanoid product.[10,11] In addition to this, it was found that the more highly oxygenated *bis*-retinoid products are

likely polyperoxide species resulting from a [4+2] cycloaddition between singlet oxygen and two double bonds, instead of epoxidation occurring at every double bond.[11] Based on this information, we conclude that the observed oxo-A2D products are also a consequence of epoxidation and [4+2] cycloadditions with singlet oxygen. Figure 5 shows a selection of potential A2D oxidation products such as the epoxide (**28**), *bis*-furan (**29**), peroxyexpoxide (**30**), and the *bis*-peroxy-A2D (**31**). Clearly it would be impossible to determine by NMR the exact structure of these A2D photooxidation products due to the small quantities, instability, and multiple isomers of the species formed. The structure of the oxo-A2D products are speculative based on the current findings, which are still heavily debated in the literature.

Unfortunately, it appears that A2D does not oxidize as efficiently as A2E. However, it has been demonstrated that some A2D photooxidation does take place *in vitro*, and therefore is likely to occur *in vivo* and could potentially play a role in the observed phototoxicity of lipofuscin. Additionally, while A2D may not be as photoreactive as A2E, its oxidation properties make it useful in our targeted and triggered drug delivery system.

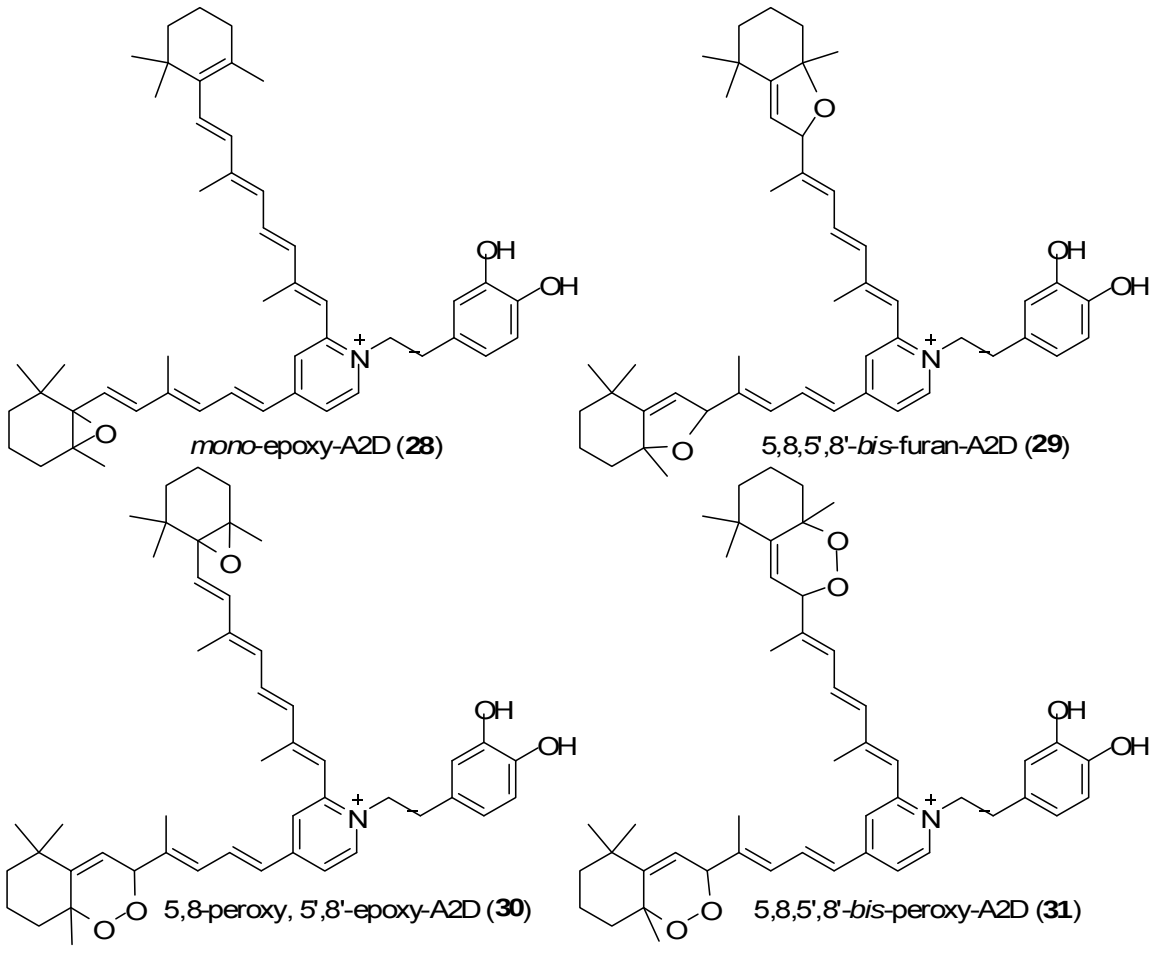

Figure 18. Potential A2D Photooxidation Products

3.3 Coupling of Folic Acid to A2D

In addition to identifying new amino *bis*-retinoids in human eyes, our project included using the library of synthesized amino retinoid compounds as potential anti-cancer therapies. Once A2D had been isolated and its potential photooxidation demonstrated, the next step was to tether A2D to folic acid (**20**) yielding folic acid-A2-dopamine (FA-A2D). The coupling of A2D to folic acid would allow us to specifically target cancer cells, while leaving healthy normal cells untouched. Our plan to accomplish this task, shown in Scheme 3, was to activate the α and γ carboxylic acid groups of folic acid with dicyclohexylcarbodiimide (DCC), using 4-dimethylaminopyridine (DMAP) as the catalyst. It was anticipated that the reaction would potentially give at least four FA-A2D products (**32**, **33**, **34, 35**) resulting from dopamine's two different hydroxyl groups potentially attacking either the α or γ carboxylic acid of folic acid. Initial attempts to selectively protect one of the carboxylic acids were not made because the starting materials were costly. The purpose of this reaction was to see if it was possible to directly link folic acid to a pyridinium *bis*-retinoid, as the coupling of folic acid to this type of compound had never been reported in the literature.

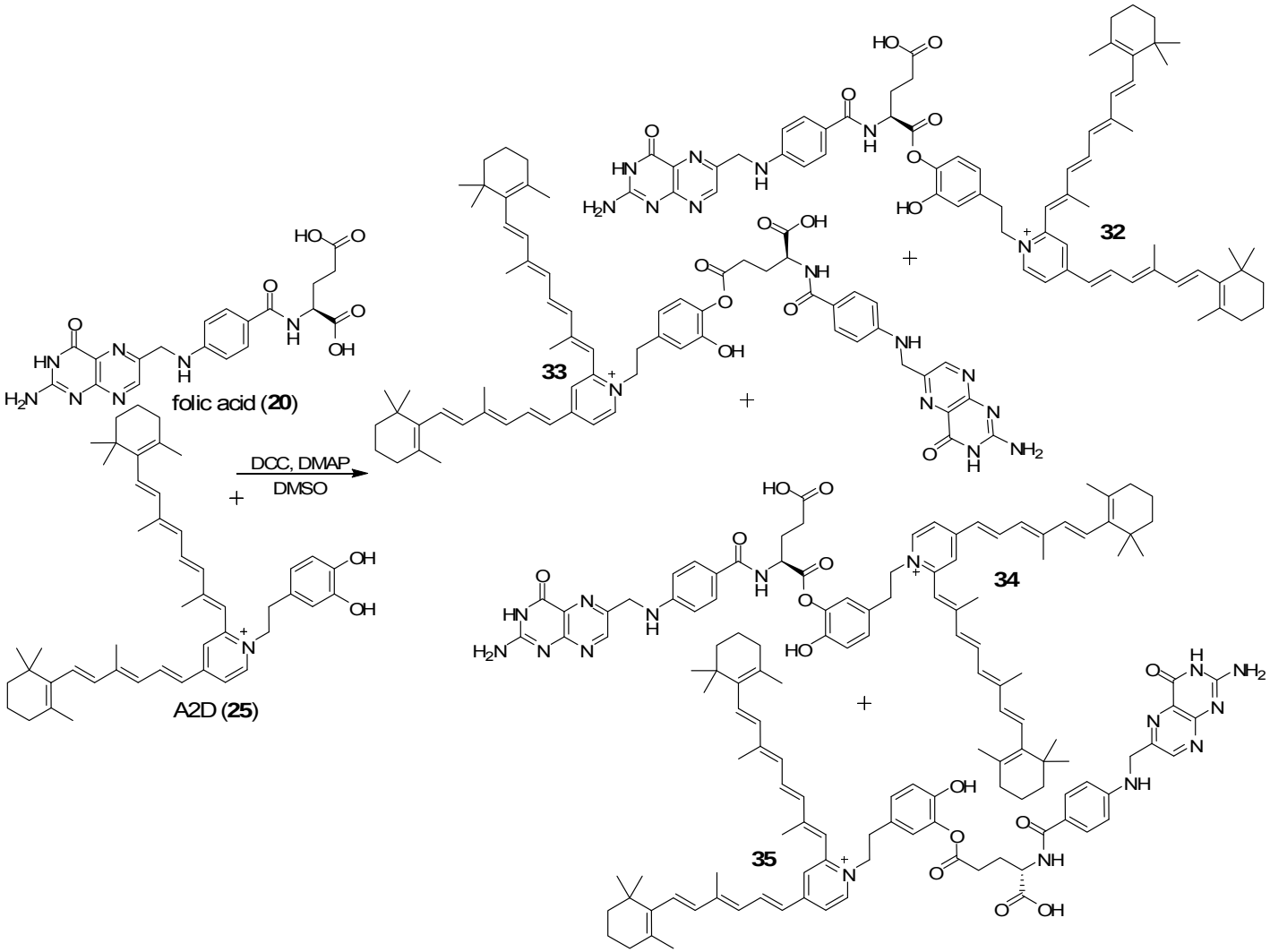

Scheme 5. Reaction of Folic Acid and A2D

The FA-A2D reaction was carried out in dark and dry conditions under N_2 by first activating folic acid (**20**) with DCC, followed by addition of the catalyst, DMAP, and the pyridinium *bis*-retinoid, A2D (**25**). Large excesses of folic acid, DCC, and DMAP were used in this first attempt to ensure the reaction would go to completion. The reaction's progress was tracked for 24 hours by HPLC starting at 5 minutes. From the HPLC results in Figure 6 (1), it seems that there is a series of initial complexes forming between folic acid and A2D after only 5 minutes of reaction time. This is evidenced by the formation of several new peaks (A, C, and D) with corresponding UV spectra that appear to be a combination of folic acid (λ_{max}=283 nm) and A2D (λ_{max}= 339.8, 441.6 nm, DMSO). Peak B corresponds to the starting material A2D.

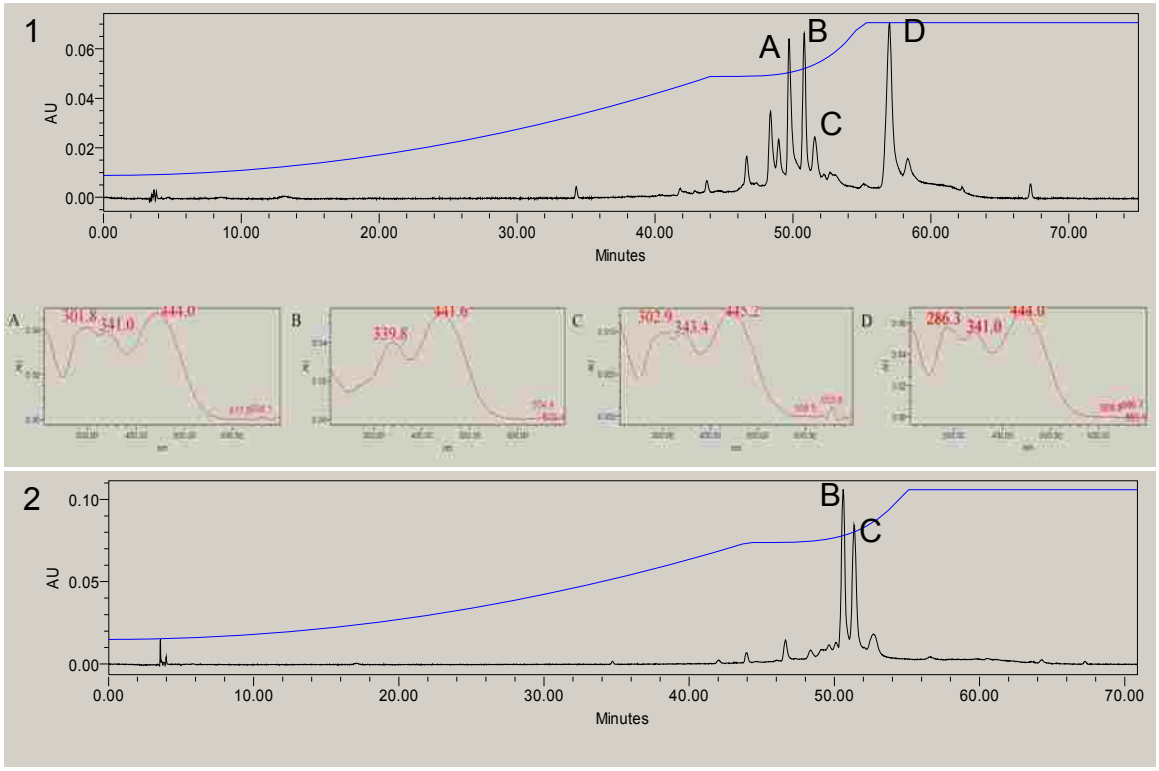

Figure 19. HPLC Chromatogram and Corresponding UV-Vis Spectra from FA-A2D Reaction (1) time=5 minutes, (2) time= 24 hours

Figure 7 illustrates the UV-Vis spectra of starting materials, folic acid (red) and A2D (green), and the initially proposed folic acid-A2D complex (purple). Although the purple spectrum looks like it may be the FA-A2D complex, because of the nice overlay with the starting materials, we were skeptical because ester bond formation is typically not immediate. This skepticism was supported by HPLC results after 24 hours of reaction time (2) where only peak C remains and has increased in area. Peak C represents the only resulting FA-A2D product.

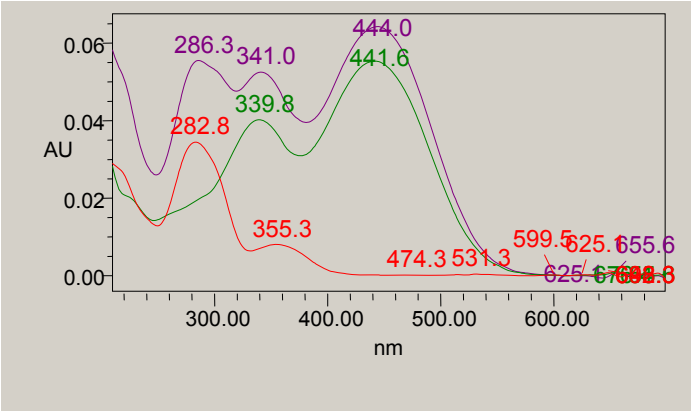

Figure 20. Comparison of UV-Vis Spectra: Folic Acid (red), Dopamine (green), and Initially Proposed FA-A2D (purple)

To further confirm the success of the folic acid A2D linkage, a crude product sample was submitted for MS (FAB) analysis shown (Figure 8). While the mass spectrum of the crude product mixture has a large 685 peak, it also shows a small 1108 peak indicating that the desired folic acid amino retinoid compound did indeed form. The size of the peak in the MS is not considered to be an indication of the amount of product. A molecule of this size could be easily broken up during bombardment. In addition, it is typically difficult to visualize folic acid using any form of MS.

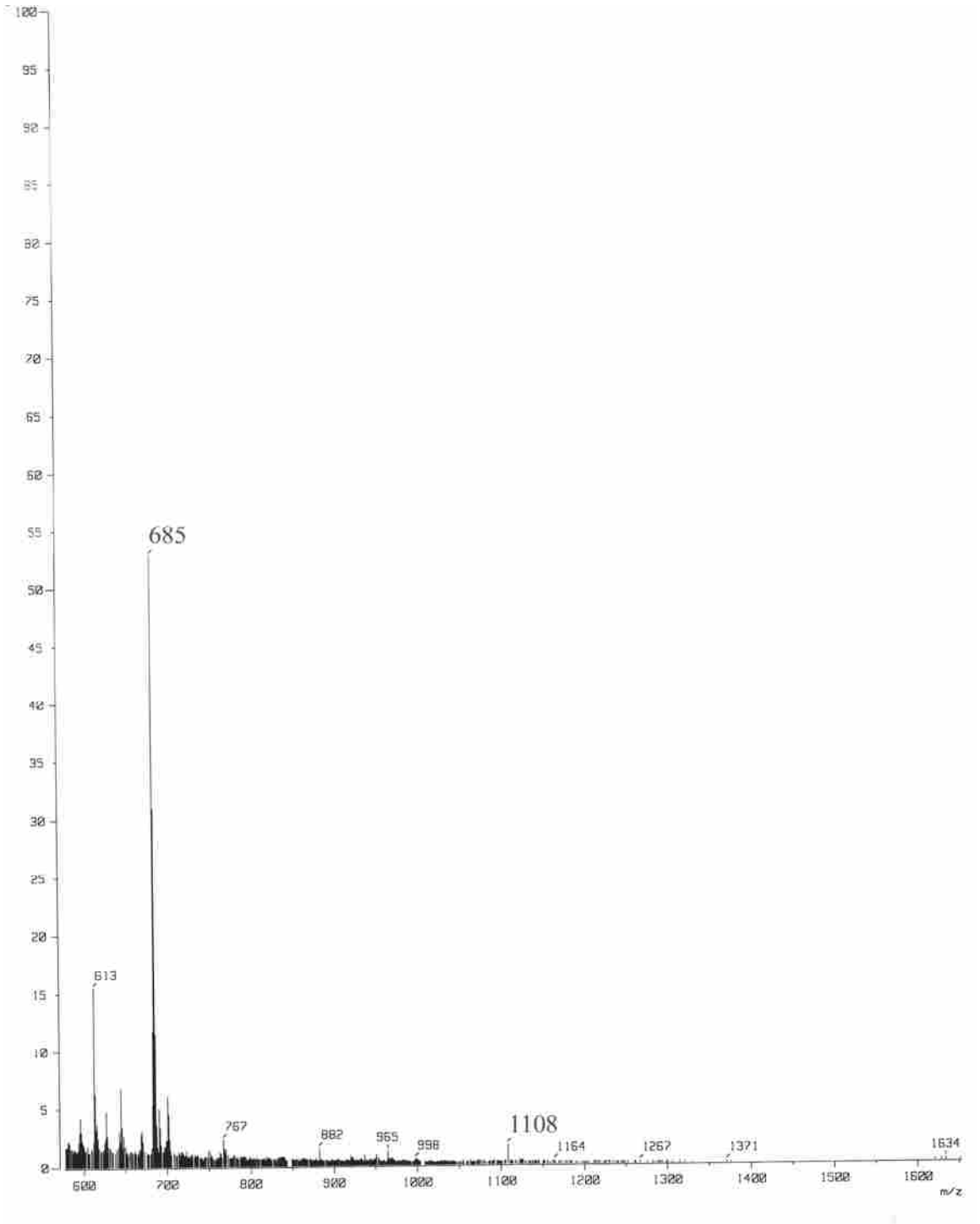

Figure 21. FAB-MS of Crude Folic Acid Dopamine Reaction Products

MS and HPLC evidence indicated some success with at least partial conversion of A2D to the folic acid derivative. Unfortunately, however, complete reaction of the starting material was never achieved and coupling was not consistently reproducible.

There are three possible reasons why the linkage of the pyridinium *bis*-retinoid to folic acid was not reproducible and did not go to completion. The first reason is that it might be sterically difficult for two large molecules to physically come together and form a tether, slowing the kinetics of the reaction. Second, the length of the linker between A2D and folic acid may not have been long enough, possibly causing steric problems after bond formation and making the FA-A2D unusually susceptible to hydrolysis. Finally, the ester bond might not have been a strong enough bond under these conditions. Perhaps only an amide bond will be strong enough to hold these two large molecules together. Further investigation is warranted to determine the cause of reaction failure.

3.4 References

1. Jones, D. C.; Gunasekar, P. G.; Borowitz, J. L.; Isom, G. E. *J. Neurochem.* **2000**, *74*, 2296–2304.
2. Offen, D.; Ziv, I.; Sternin, H.; Melamed, H.; Melamed, E.; Hochman, A. *Exp. Neurol.* **1996,** *141*, 32–39.
3. Zeevalk, G. D.; Bernard, L. P.; Nicklas, W. J. *J. Neurochem.* **1998**, *70*, 1421–1430.
4. Sicre, C.; Cid, M. M. *Org. Lett.* **2005**, *7*, 5737–5739.

5. Parish, C. A.; Hashimoto, M.; Nakanishi, K.; Dillon, J.; Sparrow, J. *Proc. Natl. Acad. Sci. USA* **1998**, *95*, 14609–14613.
6. Duffy, J. A.; Teal, J. J.; Garrison, M. S.; Serban, G. P. *PCT Int. Appl.* 9516659, **1995**.
7. Sollaolie, G.; Girradin, A.; Lang, G. *J. Org. Chem.* **1989**, *54*, 2620–2628.
8. Pezzella, A.; Prota, G. *Tetrahedron Lett.* **2002**, *43*, 6719–6721.
9. Ben-Shabat, S.; Itagaki, Y.; Jockusch, S.; Sparrow, J. R.; Turro, N. J.; Nakanishi, K. *Angew. Chem. Int. Ed.* **2002**, *41*, 814–817.
10. Dillon, J.; Wang, Z.; Avalle, L. B.; Gaillard, E. R. *Exp. Eye Res.* **2004**, *79*, 537–542.
11. Jang, Y. P.; Matsuda, H.; Itagaki, Y.; Nakanishi, K.; Sparrow, J. R. *J. Biol. Chem.* **2005**, *280*, 39732–39739.

CHAPTER 4. STUDIES OF PYRIDINIUM *BIS*-RETINOID A2-CADAVERINE

The next biogenic amine of choice for our pyridinium *bis*-retinoid library was the diamine cadaverine (**36**, Figure 1). A diamine was selected in order to help decipher why the coupling of folic acid to A2D failed. A diamine would enable an amide bond with folic acid which would be stronger than the ester linkage made with A2D. In addition, cadaverine was specifically chosen for its 5 carbon linker that would provide steric relief between the large pyridinium *bis*-retinoid and folic acid. With these two variables changed, we could determine if it was possible to directly link folic acid to a pyridinium *bis*-retinoid. Ultimately, the efficacy of our targeted and triggered cancer drug delivery system depends on the success of the coupling of folic acid to one of our anti-cancer compounds. Not only could cadaverine solve the folic acid linking problem, but A2-cadaverine (A2C) is also suspected to be one of the novel pyridinium *bis*-retinoids found in the human eye extractions, based on preliminary MS studies. Thus, two long term goals of our research can be accomplished.

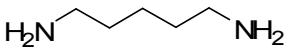

Figure 22. Cadaverine (**36**)

4.1 Synthesis of A2-Cadaverine

A biomimetic approach was once again chosen for the synthesis of A2C for the same reasons as listed for A2D. The biomimetic synthesis is an easy one pot reaction compared to a ten step total synthesis. Also, the biomimetic approach is generally more economical than a total synthesis of pyridinium *bis*-retinoids. Accordingly, the starting material all-*trans* retinal was synthesized in the same manner as previously reported

(Chapter 3, Scheme 1). The biomimetic method of choice, however, did differ from that used to synthesize A2D. The Parish[1] method was used to make A2C, in which all-*trans* retinal (**2**) and cadaverine (**36**) were combined in ethanol and acetic acid. Pezzella's[2] more physiological method was forgone because the formation of a Pictet Spengler product wasn't a possibility, and the Parish method was simpler and more straightforward. The synthesis of A2C (**37**) is shown in Scheme 1.

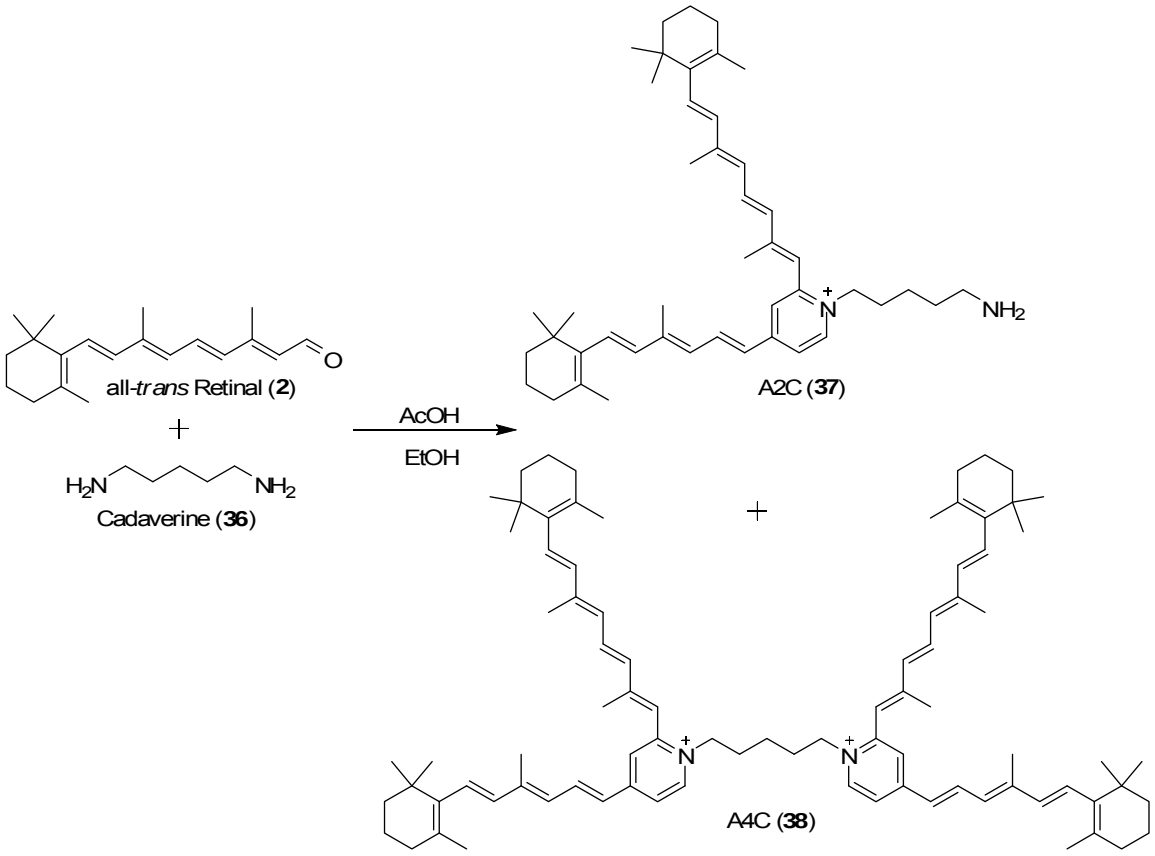

Scheme 6. Synthesis of A2C (**37**)

While cadaverine does not have an electron rich phenyl group to produce an alternate Pictet Spengler product like dopamine, it is a diamine and can therefore potentially react with four molecules of all-*trans* retinal to form the *tetra*-retinoid A4C (**38**). Though A2C and A4C are interesting both as potential anti-cancer agents and toxic

retinoids implicated in AMD, we initially chose to simplify by using one equivalent of all-*trans* retinal to avoid the formation of A4C. Diamines had not previously been used in this type of synthesis and presented added purification challenges.

One equivalent of all-*trans* retinal was combined with one equivalent of cadaverine and acetic acid in ethanol. The reaction was stirred in a dark sealed round bottom flask for two days. The crude A2C was then purified by column chromatography using varying concentrations of MeOH, methylene chloride (CH_2Cl_2), and trifluoroacetic acid (TFA). The isolated A2C was repurified by chromatotron and recovered in 5 % yield. UV-Vis spectroscopy, HR-ESI-MS, and proton and carbon NMRs confirmed the identity of the pure (≈ 92%) A2C. Carbon NMR indicated that the trifluoroacetate anion (δ 116.3, 162 ppm) was the counterion to A2C.

Five percent was a surprisingly low yield for the A2C compound, even for using only one equivalent of all-*trans* retinal. Once A2C had been successfully isolated and purified, we could experiment with reaction variables to find conditions that would optimize the yield. The number of equivalents of all-*trans* retinal was the first condition to be varied, followed by the number of equivalents of acetic acid, and then the reaction time. Table 1 shows a comparison of the different conditions attempted and the yields obtained.

Table 1. Comparison of A2C (37) Reaction Conditions and Yields

Reaction	*all-trans* Retinal (eq.)	Acetic Acid (eq.)	Time (hours)	Yield
A.	1	1	48	5 %
B.	2	1	48	2 %
C.	1	1.5	48	11 %
D.	1	1	60	7 %
E.	1	1.5	60	12 %

The first variation to the synthesis was to increase the equivalents of all-*trans* retinal from one to two. However, in reaction B, as shown in Table 1, the yield actually decreased from five to two percent. This made little sense because the synthesis of any amino *bis*-retinoid compound requires two equivalents of all-*trans* retinal and initially only one was used (reaction A). Because poor yields were obtained when two equivalents of all-*trans* retinal were used, only one equivalent was used in future reactions.

The second variable altered in the synthesis of A2C was the amount of acetic acid. Acetic acid was only increased by fifty percent in reaction C to one and a half equivalents. Reasoning for the conservative increase in acetic acid was that Parish[1] reported the one-step preparation of A2E to be very sensitive to the overall pH of the mixture. With this said, it was anticipated that because cadaverine is more basic than ethanolamine that it would tolerate an increase in acid. The assumption was correct and the additional acid more than doubled the amount of A2C recovered.

Encouraged by the improved yields, the final control variable altered was the reaction time. There was a delicate balance in deciding how much to increase the reaction length. Increased reaction time should theoretically lead to more product. However, the longer reaction time would also lead to additional isomerization and decomposition of the products and starting material all-*trans* retinal. It was decided that an additional twelve hours of stirring would lead to higher A2C yields while minimizing the amount of isomerization and decomposition. Reactions D and E were both stirred for 60 hours and trial E was used to test the effect of the extra 0.5 equivalent of acetic acid. As reported in Table 1 both reactions, D and E, showed an increased yield compared to

their 48 hour counterparts. Reaction D, in which one equivalent of acetic acid was used, resulted in an increase from five to seven percent versus Reaction A. However, in Reaction E (1.5 equivalents of AcOH) only a slight increase in yield was observed of twelve percent compared to Reaction C's eleven percent A2C recovery.

Overall, it was determined that using one and a half equivalents of acetic acid and stirring for 48 hours produced A2C with the best purity and yield. It was surprising to discovery that increasing the amount of all-*trans* retinal from one equivalent to the required two (compared to one equivalent of cadaverine) actually had an ill effect on the yield. Perhaps this can be attributed to the formation of the A4C product. However, evidence for the formation of the A4C product was never found during mass spectrometry analysis of crude aliquots. Of course the A4C product, due to its large size, could easily be broken up during mass spectrometry and never be detected. An additional explanation for poor yields is that cadaverine's second amine is far more nucleophilic than ethanolamine's hydroxyl group and thus can alternatively form various Schiff base products instead of the desired pyridinium *bis*-retinoids.

Unlike the two equivalents of all-*trans* retinal, the added acid yielded better than expected results. There are two possible explanations for this phenomenon. First, acid was added in the initial A2E reaction to serve as a catalyst. Cadaverine is basic and therefore tolerated the extra acid better, which led to an increase in reaction rate. The second explanation is that the added acid rendered the primary amine on A2C less nucleophilic, and therefore less likely to form unwanted side products. While the biomimetic synthesis of A2C might not have produced good yields, it was the simplest method for our purposes.

4.2 A2C Photochemical Experiments

The next step in determining whether A2C may be cytotoxic was to test the isolated A2C for potential photoreactivity. If A2C is a major cytotoxin in the RPE, then it will likely be through photochemical mechanisms. Moreover, if biogenic diamines prove to be the best option for tethering *bis*-retinoids to folic acid, then they too must have A2E's capability to generate photooxidation products in order for our cancer treatment to be viable.

The photooxidation of the diamine *bis*-retinoid A2C was carried out by dissolving the pure compound in a ten percent DMSO solution. A two sided polystyrene visible cuvette filled with the dissolved A2C was irradiated with light using a 442 nm interference filter. Aliquots of the irradiated compound were taken once every hour for five hours and analyzed by HPLC and ESI-MS. Figure 2 shows a picture of the setup used in the pyridinium *bis*-retinoid irradiation experiments.

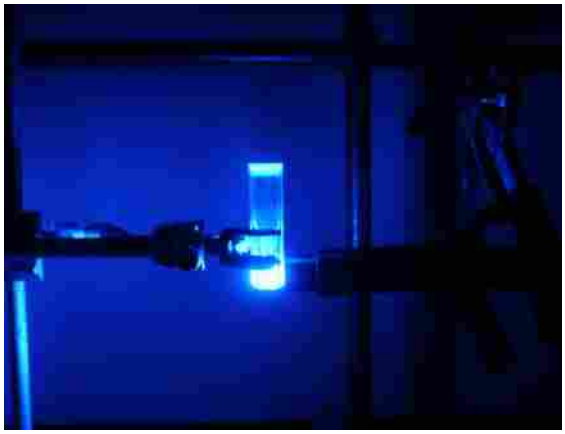

Figure 23. Photochemical Experiment Setup

The HPLC and ESI-MS results are illustrated in Figures 3 and 4 for samples taken at zero, one, three, and five hours of irradiation. From the first HPLC chromatogram in Figure 3 before irradiation has commenced, one can see a single clean A2C (A) peak with

minor isomer products. After exposure to blue light for one hour there is an emergence of two peaks (B and C) in addition to A2C (A). Corresponding UV-Vis spectra indicate that peak C is not significantly blue shifted and is a result of the expected photoisomerization. Its UV-Vis spectrum resembles the typical 13-*cis* isomer of A2E and suggests that peak C may be the 13-*cis* isomer of A2C, which assumes a steady state ratio with all-*trans* A2C throughout the remaining irradiation. Peak B has an interesting corresponding UV-Vis spectrum that is blue shifted nearly 35 nm compared to that of peak A, indicating loss of conjugation and reaction at a double bond. In addition to having an interesting UV-Vis, peak B also has a shorter retention time than A2C on reversed phase HPLC, meaning that this new photo product is more polar than its predecessor.

The most dramatic change in HPLC evidence occurs between one and three hours of irradiation time. According to the three hour chromatogram, the initial photoproduct (peak B) has almost doubled its area, while the A2C peak has suffered a significant loss. In addition to the drastic change in A and B peak ratios, two new non-oxidative product peaks have appeared, suggesting decomposition or isomerization due to light. The final HPLC chromatogram observed after five hours of irradiation demonstrates the extent to which photo reactivity occurs. The starting *bis*-retinoid (peak A) has been almost completely consumed, leaving only various photo, isomer, and side products. Even the blue shifted product (peak B) is no longer the dominant peak.

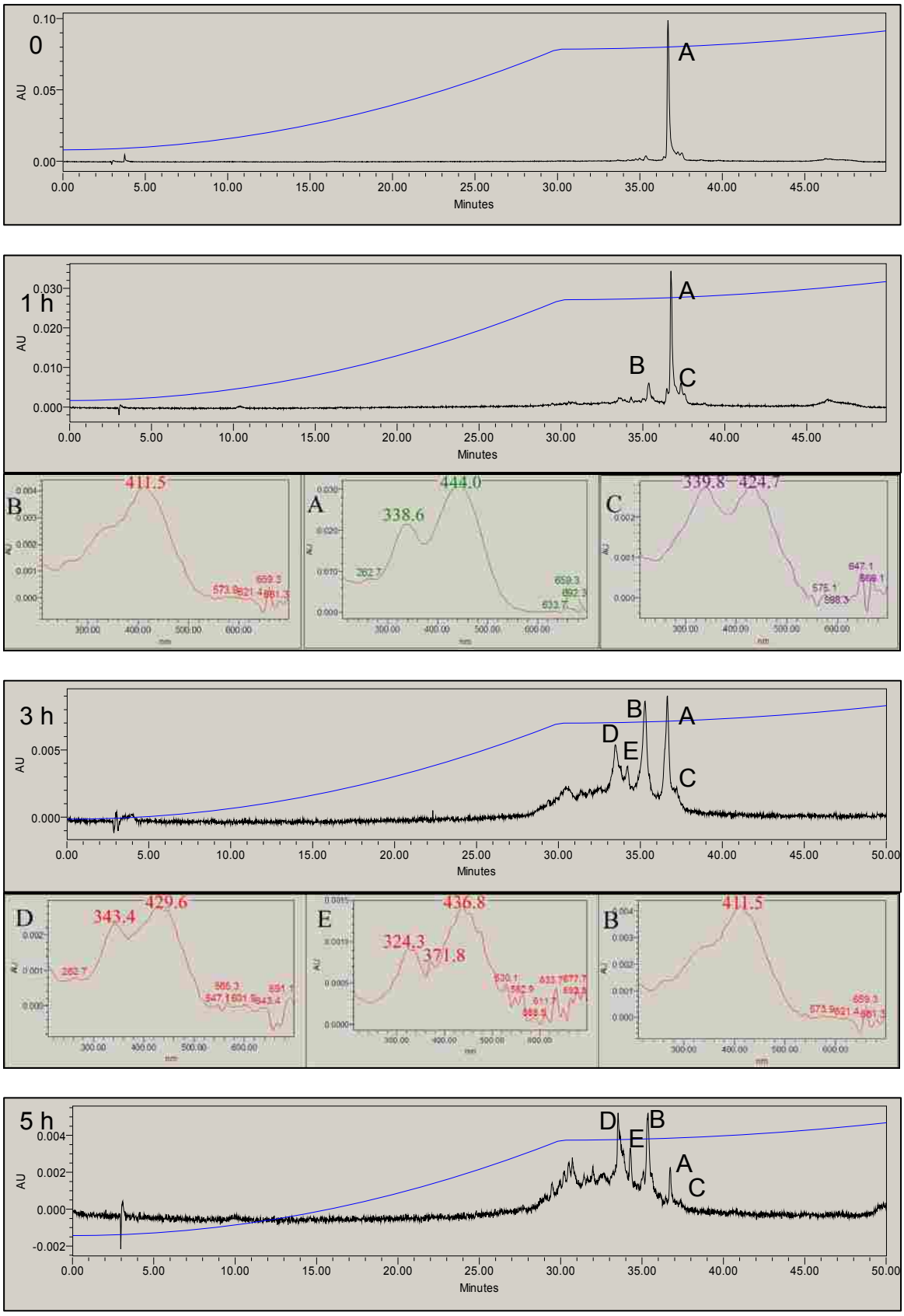

Figure 24. A2C Photochemistry HPLC Chromatograms at 0, 1, 3, and 5 Hours

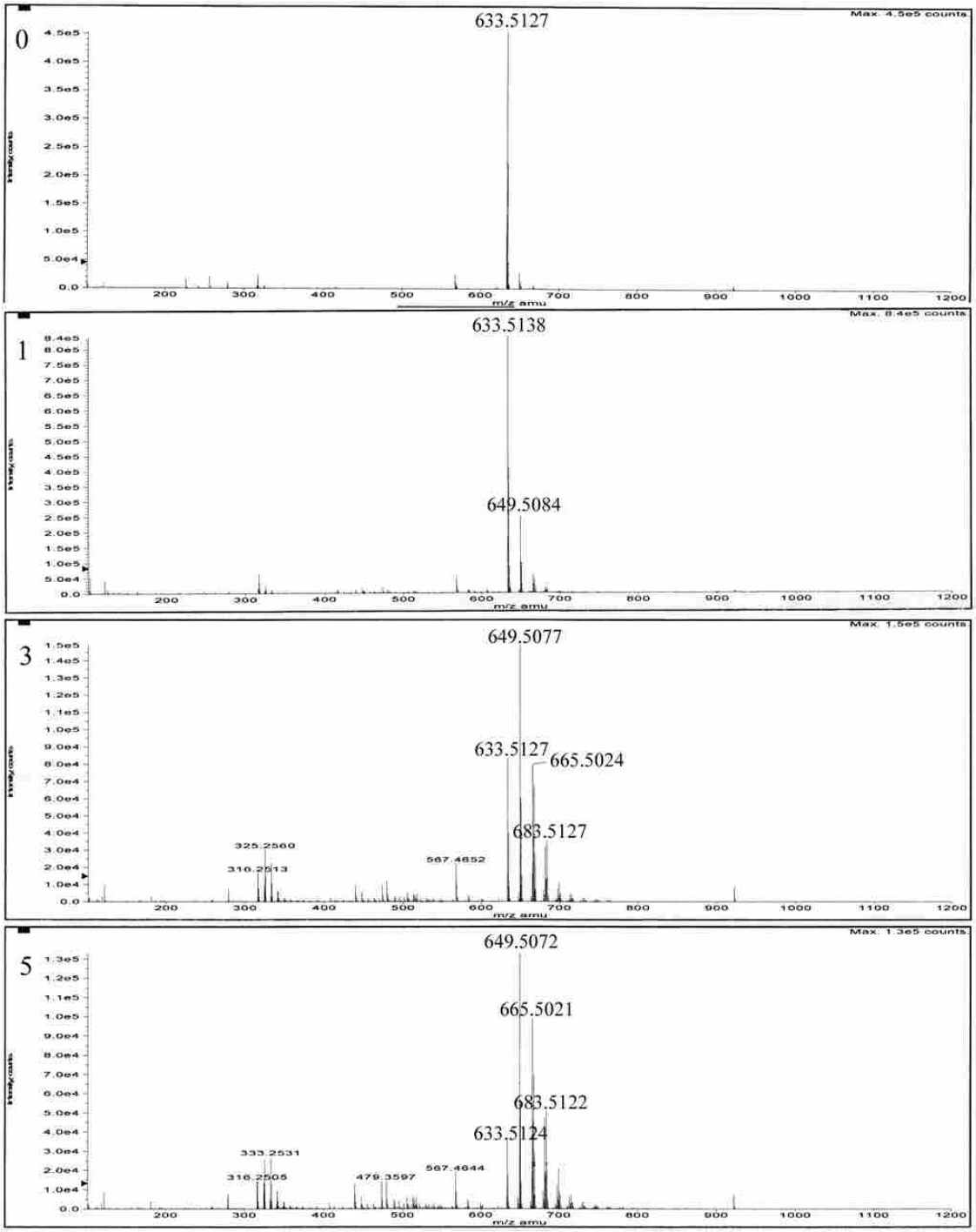

Figure 25. A2C Light Experiment ESI-MS Results for 0, 1, 3, and 5 Hours

The MS results in Figure 4 echo that observed on HPLC chromatograms. Starting after one hour of irradiation there is an emergence of a product peak of *m/z* 649, differing from the M^+ by *m/z* 16. This new peak visualized in MS correlates to the appearance of

the HPLC photo-product having a shorter retention time and blue shifted UV-Vis spectrum. MS and HPLC evidence combined suggest that this new product is a result of the addition of oxygen to the double bonds on the longer retinoid arm of A2C. Thus, the hypsochromic UV-Vis shift is due to loss of conjugation, and the shorter retention time is a consequence of increased polarity from the added oxygen.

Similar to that seen in the HPLC chromatograms, the most radical change in solution composition according to MS occurs between one and three hours of irradiation. Not only is there a complete reversal in the *m/z* 633 and *m/z* 649 peak ratios, indicating a loss of A2C, but two new oxidation products appear at *m/z* 665 and *m/z* 683 . The *m/z* 665 is exactly 32 mass units greater than the starting material A2C, corresponding to the addition of two oxygens. The second product peak at *m/z* 683 is 50 atomic mass units greater than A2C, and 2 mass units larger than the expected *tris*-oxo peak of *m/z* 681, suggesting insertion of three oxygens and two additional hydrogens.

Finally, after five hours of light exposure we once again observe further decrease in the parent A2C ion, almost to complete extinction, and an increase of photooxidation products, including a new peak at *m/z* 699. Interestingly, the new *m/z* 699 product peak is exactly 16 atomic mass units greater than the 683 peak at three hours of irradiation, suggesting the addition of just one oxygen atom to the third photooxidation product. In addition to the disappearance of the A2C parent ion and the new observed oxidation peak, one can also observe the formation of up to five more minor oxidation peaks in increments of *m/z* + 16. This makes a total of nine photooxidation products, with up to nine oxygens incorporated into the *bis*-retinoid arms.

Likewise, A2E has also been shown to generate nine photooxidation products by MS.[3] As discussed in Chapter 3 it was recently suggested that A2E epoxidation begins at the 5,6 double bond of amino *bis*-retinoids, and in some cases rearranges to form a 5,8-furanoid product.[4,5] Also, it was found that the more highly oxygenated *bis*-retinoid products are likely polyperoxide species resulting from a [4+2] cycloaddition with singlet oxygen.[5] Based on this information, we conclude that the observed oxo-A2C products are similar to those observed with A2D and are also a consequence of epoxidation and [4+2] cycloadditions with singlet oxygen.

While A2C did show extensive photoreactivity similar to A2E, it did differ in the most abundant species formed. Typically, the most dominant A2E photoproduct observed incorporates two oxygen atoms, but as seen by HPLC evidence in Figure 3 and MS in Figure 4, the most abundant is the mono-oxygenated A2C product.[3,5] Even though A2C does not appear to generate the *bis*-oxo as the main oxidation product, it does generate polyoxidative species, which should be cytotoxic based on A2E literature precedence.

In addition to the multiple photooxidation products evidenced by MS, there are also other unknown products observed in HPLC, namely peaks D and E in Figure 3. The UV-Vis spectra corresponding to peaks D and E do not exhibit the classic 40 nm hypsochromic shift seen in oxidized pyridinium *bis*-retinoids. However, these unaccounted peaks could easily arise from isomerization or a reaction between an unstable oxidation product and a nucleophile, such as the amine from cadaverine. Another incongruency between A2E and A2C found through HPLC analysis is that the most common site for oxidation of A2E is on the short retinoid arm. However, from peak

B's corresponding UV-Vis spectrum one can see that the preferred oxidation site of A2C is on the longer retinoid arm. This is concluded because A2C's λ_{max} is shifted from 444 to 411 as compared to the shift from 337 to 297 observed with oxo- A2E.[4] The structure of the oxo-A2C products have not been determined by NMR data and are speculative based on the current literature. However, for our purpose it was only necessary to demonstrate similar potential photooxidation capabilities of A2C.

4.3 Coupling of Folic Acid to A2C

Once A2-Cadaverine's potential phototoxicity had been confirmed, the ultimate test of our proposed targeted and triggered cancer drug therapy came down to coupling folic acid with the synthesized A2C. Other attempts in our lab at tethering pyridinium *bis*-retinoids to folic acid had failed. It was essential for the diamine *bis*-retinoid, A2C, to form the desired folic acid-A2-cadaverine (FA-A2C) product for our proposed chemotherapy system to be viable. The approach used to obtain the folic acid product was the same standard coupling conditions, shown in Scheme 2, used in the FA-A2D synthesis. Once again, folic acid's α and γ carboxylic acid groups were not selectively protected because the purpose of this initial attempt was to see if a connection between folic acid and A2C was possible.

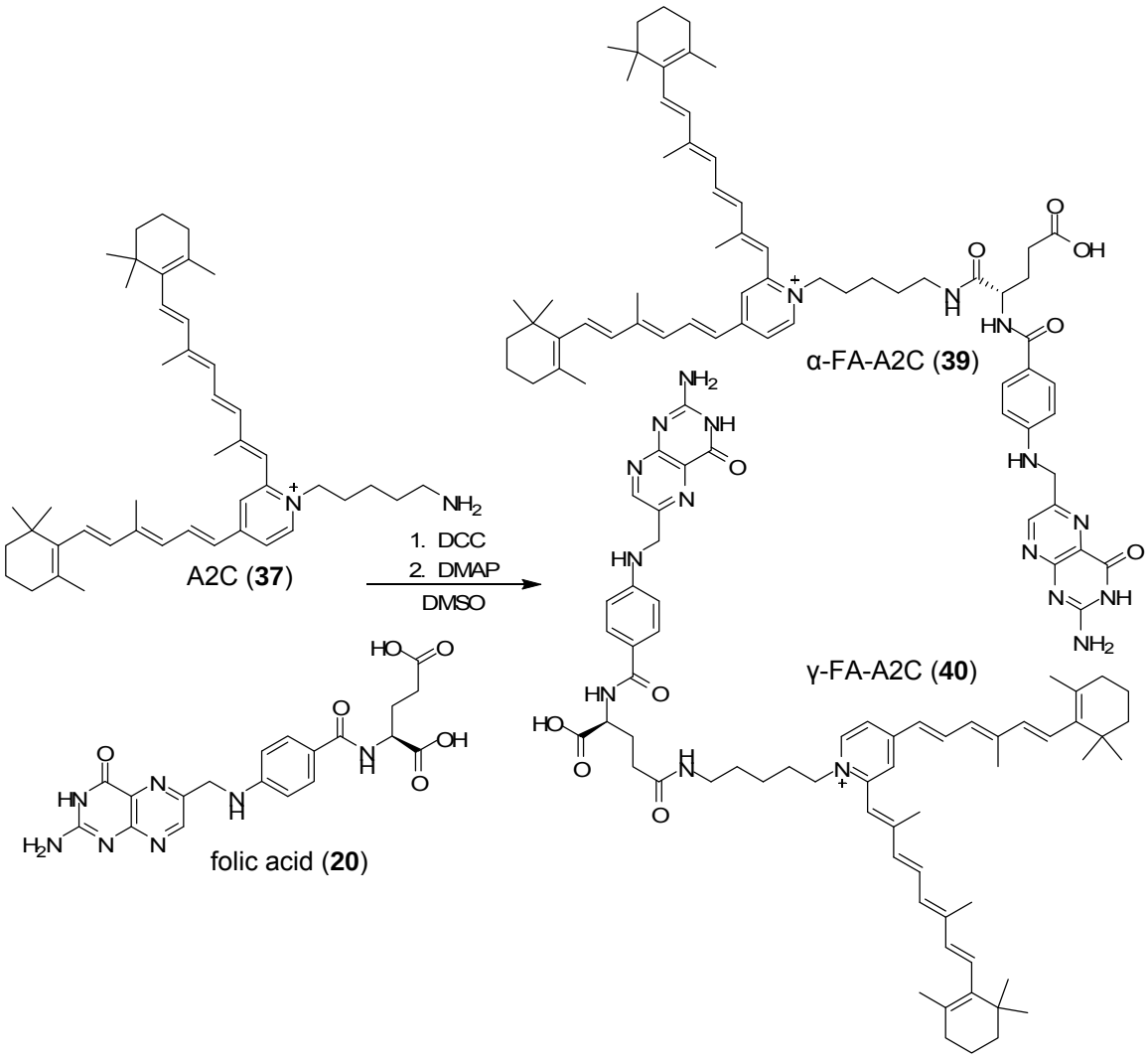

Scheme 7. Reaction of Folic Acid and A2C

Folic acid was first activated with DCC, stirred in dark and dry conditions for six hours. Following this, A2C and DMAP were dissolved in DMSO and transferred *via* syringe to the activated folic acid. The reaction was stirred for 15 hours and progress was tracked by HPLC. The A2C and folic acid reaction was successful. HPLC analysis (Figure 5) revealed the formation of two major products nearly equal in area with almost identical retention times and UV-Vis spectra. These major products were accompanied by two minor products also equal in area with similar, yet slightly blue shifted, UV-Vis

spectra. The four new peaks' corresponding UV-Vis spectra appeared to be a combination of folic acid and A2C, similar to that observed in the A2D coupling. Figure 6 shows the combination UV-Vis spectra belonging to the two main products, along with the UV-Vis spectra of the starting materials (folic acid and A2C). From the two identical UV-Vis spectra the main product peaks were believed to be a result of the formation of α-FA-A2C (**39**) and γ-FA-A2C (**40**) products. Logically, the two minor product peaks were assigned to be the 13-cis isomers of the α and γ tethered A2C derivatives.

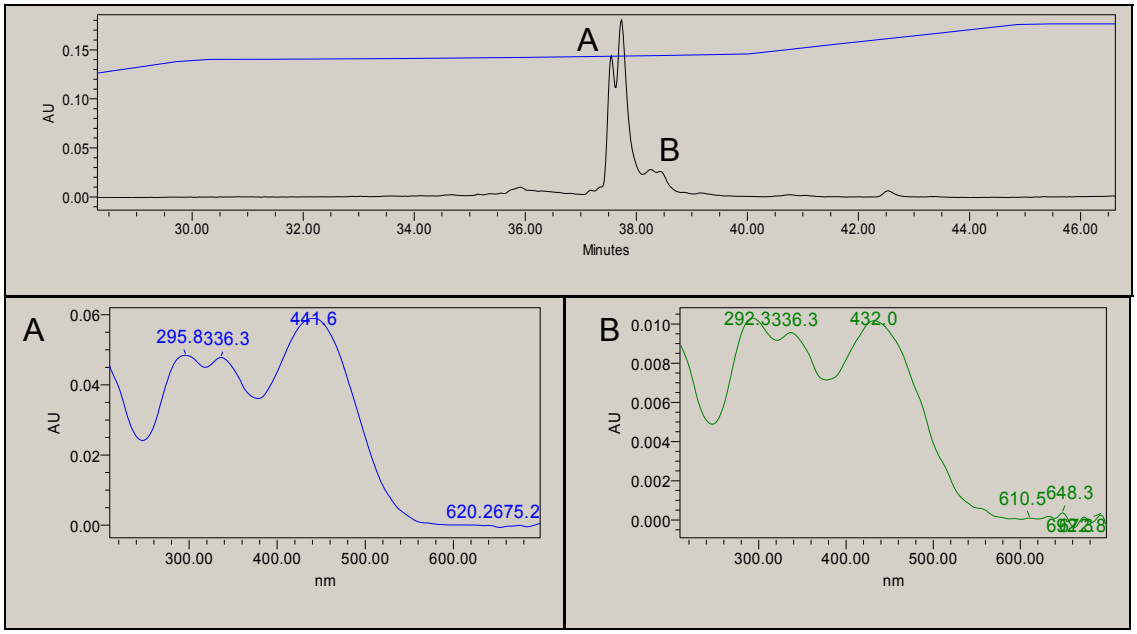

Figure 26. FA-A2C Reaction HPLC Chromatogram and Corresponding UV-Vis Spectra

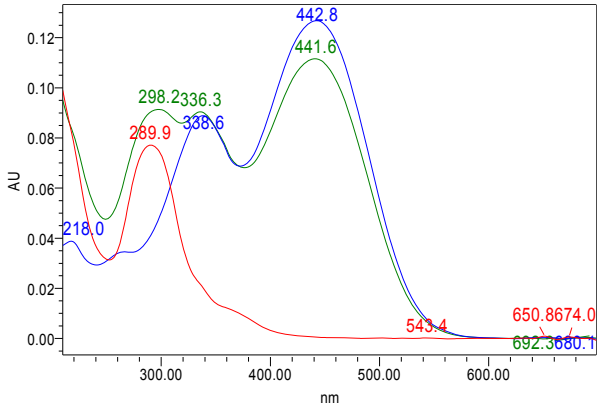

Figure 27. Comparison of Folic Acid (red), A2C (blue), and FA-A2C (green) UV-Vis Spectra

Not only did HPLC tracking reveal reaction success, but it also proved that the products were stable and did not mysteriously disappear or revert back to starting material over time, a common problem with A2D and other pyridinium *bis*-retinoids. After 15 hours of stirring, the reaction was quenched with chilled distilled water. Upon the addition of water, a red crystalline-like precipitate formed. The precipitate was subsequently collected, filtered, washed with water, methanol, ether, and finally dissolved in a 5:95 MeOH/CH_2Cl_2 solution. Working with the desired FA-A2C product revealed that it was stable enough to be chromatographed multiple times. The folic acid targeted compound was first purified by column chromatography using CH_2Cl_2 with five percent MeOH followed by increasing concentrations of MeOH in CH_2Cl_2. The coveted folic acid A2C material was obtained with a 20:80:0.005 MeOH/CH_2Cl_2/TFA solution. Both ^{1}H NMR and ESI-MS confirmed the successful formation and isolation of the folic acid linked A2C drug. As seen with the FA-A2C UV-Vis spectra, the ^{1}H NMR also appeared to be a combination of both folic acid and A2C proton NMRs. Proton NMR also showed the α and γ folic acid labeled compounds to be recovered with reasonable purity for a combined yield of 75 %. From this point the two FA-A2C products could be

further separated into the α and γ counterparts by chromatotron using a 25:75 MeOH/CH_2Cl_2 solution. However, while separation was possible, it usually came at a high price of decreased yields.

The addition of folic acid to a pyridinium *bis*-retinoid is a significant chemical derivatization and it was unknown how this change would affect the photochemical characteristics of A2C. The added folic acid could potentially quench excited states, provide new oxidative sites, or cause no significant change at all. Consequently, preliminary photochemistry experiments were commenced on the combined α and γ FA-A2C products. Irradiation was conducted under the same conditions used for the photooxidation of A2C. The material was dissolved in a DMSO/H_2O solution and irradiated with a 442 nm interference filter in a two sided polystyrene visible cuvette. Aliquots of the blue light irradiated sample were taken for HPLC and MS analysis. Surprisingly, after just one hour of blue light exposure there was not any original FA-A2C remaining according to HPLC or ESI-MS results. Only unrecognizable photoproducts remained in solution. Figure 7 shows a comparison between FA-A2C stock solution and the FA-A2C sample after one hour of irradiation. From the photograph one can observe a significant change in color from bright orange to pale yellow after one hour of blue light exposure, indicating that extensive photobleaching has occurred.

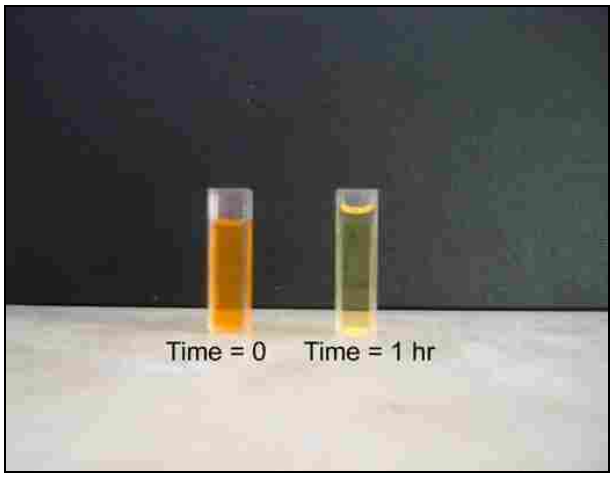

Figure 28. Before and After Irradiation of FA-A2C with Blue Light

It appears from photochemistry experiments that the FA-A2C derivative is substantially more light sensitive than the original A2C molecule. Even exposure to ambient light seems to induce photooxidation. Figure 8 shows a comparison of two UV-Vis spectra resulting from an FA-A2C solution exposed to small amounts of ambient light. The blue spectrum corresponds to the FA-A2C. The red spectrum is similar in shape to the blue, but shows a large characteristic hypsochromic shift from 440 to 416 nm and is believed to be the result of a photooxidation FA-A2C product. Similar to that observed with A2C, oxidation also seems to occur on the long retinoid arm of FA-A2C.

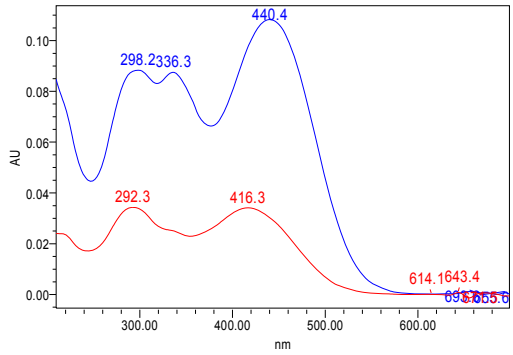

Figure 29. Comparison of FA-A2C (blue) and Proposed FA-A2C Ambient Light Photoproduct (red)

In conclusion, the synthesis and isolation of the folic acid tethered pyridinium *bis*-retinoid, FA-A2C, was a success. We demonstrated that the direct linkage of folic acid to a pyridinium *bis*-retinoid in a one pot process was in fact possible and the products were attainable in good yields, proving that there was hope for our targeted and triggered cancer drug delivery system. Not only was the FA-A2C product easily isolated, but the α and γ tethered products could also be separated by chromatotron, eliminating the extra steps involved with selectively protecting the carboxylic acids. Unfortunately, the current separation procedure returns the α and γ products in low yields, but refinement of the procedure should improve the quantities recovered. Attempts will not be made to selectively protect the α or γ carboxylic acid groups of folic acid. Not only does this eliminate unnecessary steps, but both products are also biologically interesting for cellular assays.

Additionally, it was found that FA-A2C was exceptionally stable at room temperature and could be chromatographed multiple times with minimal decomposition. The stability of this folic acid tethered pyridinium *bis*-retinoid suggests that other folic acid labeled drugs from our pyridinium *bis*-retinoid library might also be stable and could be simply purified by column chromatography. It remains to be determined why the reaction between folic acid and A2C was a success, while the reaction with A2D failed. The success may have been a result of the added stability of the amide bond compared to a weaker FA-A2D ester bond. Success may have also been made possible by the relief of steric congestion provided by cadaverine's five carbon linker between folic acid and the pyridinium *bis*-retinoid, or perhaps a combination of both variables could have been the cause of success. Further investigation into this matter is currently underway.

Finally, preliminary photochemistry experiments suggest that FA-A2C may be a more potent phototoxin than A2C. This was an unexpected, yet fortuitous outcome. It was initially anticipated that because folic acid is a vitamin and had been reported to have some antioxidative capabilities that it was going to deleteriously alter the photochemical properties of A2C.[6] However, FA-A2C was completely destroyed after one hour of irradiation with blue light. Also, it appeared that photooxidation could be induced even from ambient light. A possible explanation for this phenomenon has recently been proposed by Jakus *et al.*[7] wherein they relate that some antioxidants exhibit pro-oxidant activity when combined with photodynamic therapy. The authors speculate that the addition of antioxidants onto sensitizer molecules could provide effective new cancer treatments.

Another likely cause of the observed photochemical reactivity is that folic acid is known to decompose upon exposure to light and it has been reported that singlet oxygen may participate in this mechanism.[8,9] Perhaps the photosensitivity of folic acid and A2C synergistically combine to produce singlet oxygen which subsequently reacts with A2C to form various photooxidation products. Additional experimentation with shorter and less intense irradiation intervals is needed to determine the mechanism and products involved in photodegradation. If the hypothesis that A2C and folic acid synergistically produce singlet oxygen is true, then the FA-A2C derivative could be a cytotoxin. This fortuitous outcome could potentially mean less drug, light intensity, and exposure time necessary to induce apoptosis and eventually an all-around less invasive cancer treatment.

4.4 References

1. Parish, C. A.; Hashimoto, M.; Nakanishi, K.; Dillon, J.; Sparrow, J. *Proc. Natl. Acad. Sci. USA* **1998**, *95*, 14609–14613.
2. Pezzella, A.; Prota, G. *Tetrahedron Lett.* **2002**, *43*, 6719–6721.
3. Ben-Shabat, S.; Itagaki, Y.; Jockusch, S.; Sparrow, J. R.; Turro, N. J.; Nakanishi, K. *Angew. Chem. Int. Ed.* **2002**, *41*, 814–817.
4. Dillon, J.; Wang, Z.; Avalle, L. B.; Gaillard, E. R. *Exp. Eye Res.* **2004**, *79*, 537–542.
5. Jang, Y. P.; Matsuda, H.; Itagaki, Y.; Nakanishi, K.; Sparrow, J. R. *J. Biol. Chem.* **2005**, *280*, 39732–39739.
6. Gliszcyńska-Świglo, A. *Food Chem.* **2007**, *101*, 1480–1483.
7. Jakus, J.; Farkas, O. *Photochem. Photobiol. Sci.* **2005**, *4*, 694–698.
8. Vorobey, P.; Steindal, A. E.; Off, M. K.; Vorobey, A.; Moan, J. *Photochem. Photobiol.* **2006**, *82*, 817–822.
9. Thomas, A. H.; Suárez, G.; Cabrerizo, F. M.; Martino, R.; Capparelli, A. L. *J. Photochem. Photobiol. A* **2000**, *135*, 147–154.

CHAPTER 5. FUTURE WORK AND CONCLUSIONS

5.1 Identification of New Pyridinium *Bis*-Retinoids in Human RPE

We have observed new putative pyridinium *bis*-retinoids in melanolipofuscin and human RPE eye extracts. These have yet to be identified due to the small quantities of material. However, it is known from HPLC analysis that these unidentified compounds are more polar than A2E and this information has provided a general direction from which to continue the investigation. Eldred[1] initially used 250 human donor eyes which provided 100 micrograms of material for the elucidation of A2E. Similarly, it will require a large amount of material to identify other pyridinium *bis*-retinoids. The extraction procedure will be scaled up to accommodate at least a hundred donor eyes. The most promising method for the identification of these new compounds will be the use of LC-MS wherein the compound's UV-Vis spectrum can be obtained simultaneously with the high resolution *m/z* and molecular formula. From this point, standards can be used for further structural elucidation, opening the door to additional photophysical, chemical, and toxicity studies in relation to lipofuscin and AMD.

We have also begun the construction of our pyridinium *bis*-retinoid library for the purpose of identifying the unknown compounds found in the eye. We have successfully synthesized, isolated, and characterized the pyridinium *bis*-retinoids A2C and A2D, and plan to continue expanding the selection of amino *bis*-retinoid standards. Unfortunately, neither A2D nor A2C have yet been identified as the novel eye compounds, but we are still pursuing this. Another promising pyridinium *bis*-retinoid to consider for our library is A2-Serine (Figure 1, **41**). The biosynthesis of A2E involves the condensation of all-*trans* retinal with phosphatidylethanolamine,[2,3] one of the most

prominent lipids in photoreceptor cells. Another abundant lipid present in photoreceptor cells, though four times less common than phosphatidylethanolamine (**42**), is phosphatidylserine.[4,5] All-*trans* retinal would likely react with phosphatidylserine within the photoreceptor membrane eventually resulting in A2-serine. This reaction is not only a plausible outcome, but it would also result in a pyridinium *bis*-retinoid compound that would be more polar than A2E, corresponding to that observed in the HPLC analysis of eye extracts.

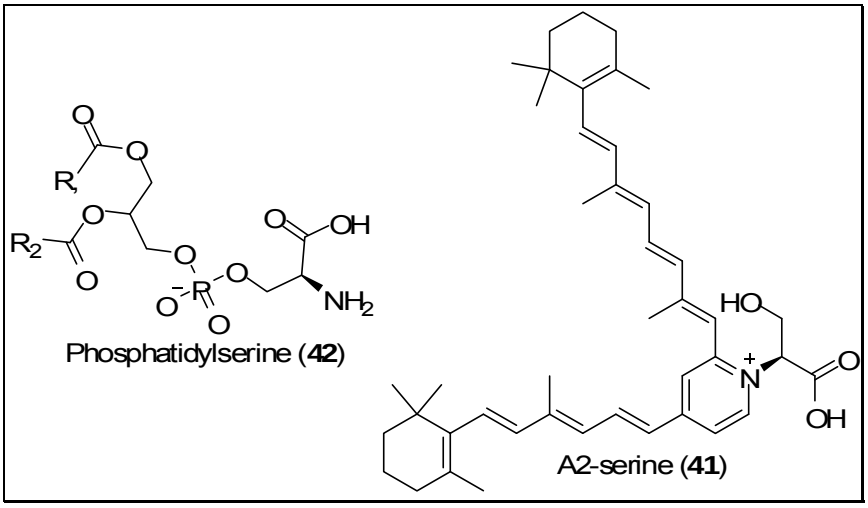

Figure 30. Potential Biogenic Amine and Corresponding Pyridinium *Bis*-Retinoid

5.2 Additional Development of a Targeted and Triggered Cancer Treatment

While A2D and A2C have not yet been identified as the new pyridinium *bis*-retinoid present in human eye extractions, they may fulfill a second purpose: the development of our targeted and triggered drug delivery system. We attempted to tether folic acid to A2D through an ester bond, but the results were not reproducible. We next moved to A2C as a potential cancer therapeutic. The coupling of folic acid to A2C was a success and the product was isolated through column chromatography in good yields.

Both α-FA-A2C and γ-FA-A2C (Figure 2, **39** and **40**) products formed and were separated *via* chromatotron. However, the yields diminished significantly upon isolation. One of our immediate concerns is to improve the isolation method of the α and γ products. From this point several projects will arise. For instance, competition assays need to be performed to prove that the folic acid labeled derivatives are uptaken preferentially to the original A2C. This will be done by incubating cancer cells with folic acid, A2C, α-FA-A2C and γ-FA-A2C. The corresponding cells will then be extracted using the human RPE extraction protocol and the amount of compound present quantified by HPLC. These experiments are underway in our laboratory.

Also, preliminary photochemistry experiments suggested that FA-A2C could be a more potent phototoxin than originally anticipated. Additional irradiation experiments will be executed to confirm this hypothesis wherein the duration of light exposure will be shortened. Instead of samples taken over a five hour period, aliquots will be taken every ten minutes for one hour. Finally, once potential photooxidation has been demonstrated, cancer cell assays will be conducted comparing the efficiency of A2C, α-FA-A2C and γ-FA-A2C at inducing apoptosis. Cells will be incubated with either A2C, α-FA-A2C, γ-FA-A2C, folic acid, or culture media and then subsequently irradiated with blue light. Controls wells will be used and include the same components mentioned, with the exception that these cells will be kept in the dark. Cell viability will be assessed 24 hours post irradiation. These experiments are also underway in our laboratory.

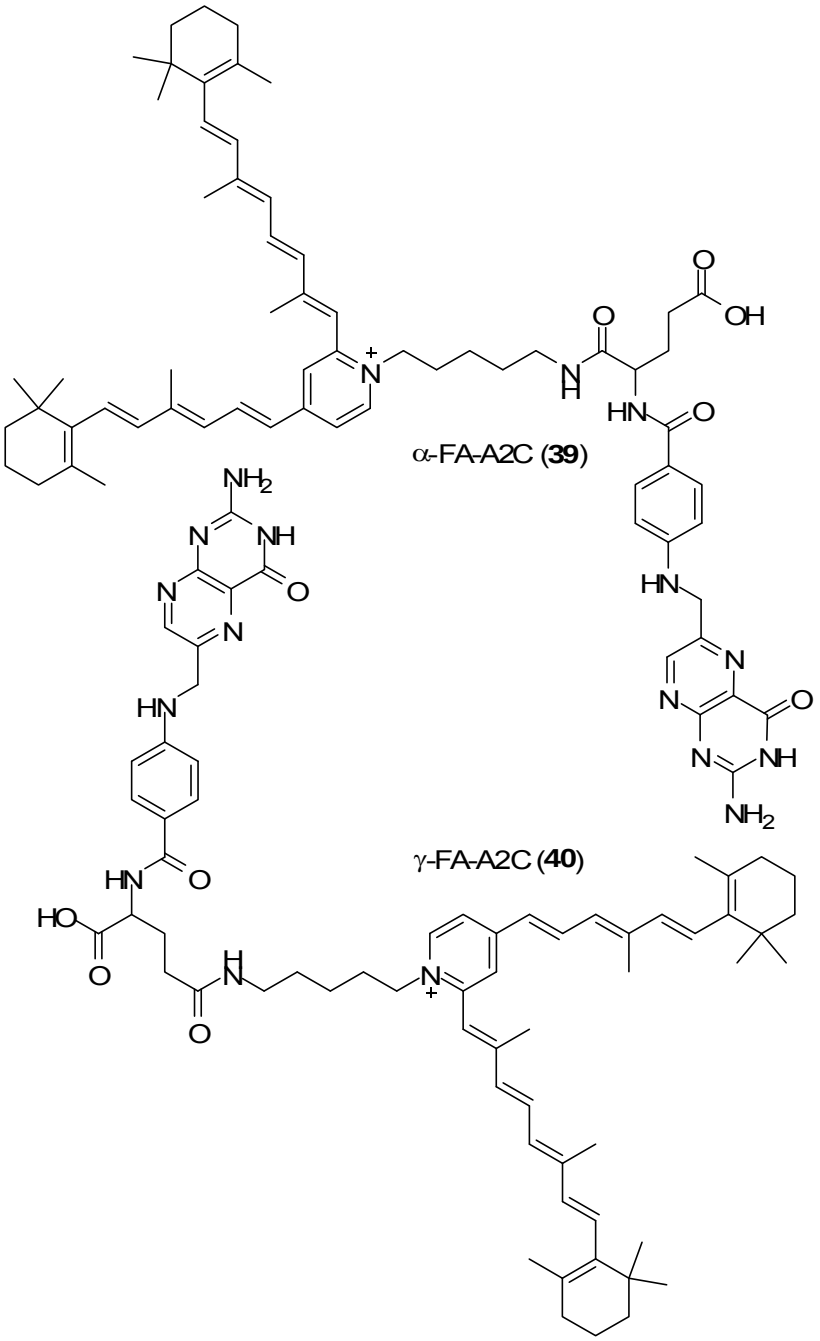

Figure 31. Folic Acid and A2C Coupled Products

5.3 Conclusion

In summary, through melanolipofuscin and human RPE eye extractions, we have observed putative new pyridinium *bis*-retinoids, which may play a role in the etiology of

age-related macular degeneration. In order to characterize these observed biological compounds we have begun to create an amino-retinoid library by synthesizing A2D and A2C. As our library has a dual purpose, these two pyridinium *bis*-retinoids were also reacted with folic acid in an attempt to create a targeted and triggered cancer treatment. While the isolation of FA-A2D failed, the reaction with A2C was successful. Additionally, preliminary photochemical experiments suggest that FA-A2C is substantially more photoreactive than A2C. This surprising discovery could potentially lead to less drug, light, and exposure time required to induce cancer cell death, and an overall less toxic and invasive treatment for cancer patients.

5.4 References

1. Eldred, G. E.; Lasky, M. R. *Nature* **1993**, *361*, 724–726.
2. Mata, N. L.; Weng, J.; Travis, G. H. *Proc. Natl. Acad. Sci. USA* **2000**, *97*, 7154–7159.
3. Liu, J.; Itagaki, Y.; Ben-Shabat, S.; Nakanishi, K.; Sparrow, J. R. *J. Biol. Chem.* **2000,** *275*, 29354–29360.
4. Anderson, R. E.; Maude, M. B. *Biochemistry* **1970**, *9*, 3624–3628.
5. Shichi, H. *Biochemistry of Vision* **1983**, pp. 122–142, Academic Press, New York.

CHAPTER 6. EXPERIMENTAL AND SPECTROSCOPIC DATA

6.1 General Methods

DMSO was dried *via* a solvent drying system using activated alumina. All other solvents and materials were obtained from Fluka or Aldrich and used as purchased, unless otherwise indicated. All extractions and reactions were performed in the dark at room temperature. Column chromatography was carried out using Sorbent Technologies 40-63 μm silica gel. HPLC and UV-Vis data were obtained on a Waters 600 HPLC system equipped with either a Cosmosil Packed Column $5C_{18}$-P-MS 4.6 x 250 mm or Phenomenex Synergi Max 250 x 4 mm column as indicated, with a Waters 2998 photodiode array detector. Chromatographic solvents were HPLC grade H_2O with 0.1% TFA and acetonitrile (ACN). MS data was obtained on an Agilent Technologies Multimode Electrospray APCI mass spectrometer running in ES+APCI+mode. ^{1}H NMR spectra were obtained on a Varian Unity Inova 500 MHz spectrometer using tetramethylsilane (0.00 ppm) as an internal reference. Signals are reported as follows, s (singlet), d (doublet), t (triplet), q (quartet), quin (quintet), dd (doublet of doublets), dt (doublet of triplets), bs (broad singlet), m (multiplet). Coupling constants are reported in hertz (Hz). ^{13}C NMR spectra were obtained on the Varian spectrometer operating at 125 MHz, with tetramethylsilane as an internal standard.

6.2 Extraction Procedure Experimental Details

Human RPE were obtained from the Utah Lion's Eye bank and provided by Dr. Paul Bernstein of the Moran Eye Institute in Salt Lake City, UT. Lipofuscin and melanolipofuscin preparations were provided by Dr. Craig Thulin of Brigham Young

University (currently at Utah Valley State College). Lipofuscin, melanolipofuscin, and donor RPE were stored at -80 °C until extracted. None of the RPE or eyes used for lipofuscin and melanolipofuscin preparations had an ophthalmologic history.

To a homogenizer were added human RPE, lipofuscin, or melanolipofuscin in 1:1 $CHCl_3$/MeOH (2 mL) and 0.01 M phosphate buffered saline (PBS) (1 mL). RPE tissues, lipofuscin, or melanolipofuscin were homogenized in a Kimble-Kontes Tenbroeck tissue grinder. The homogenate was transferred to the appropriate sized separatory funnel. The tissue grinder was rinsed with 1:1 $CHCl_3$/MeOH (2 mL) and 0.01 M PBS (1 mL), followed by $CHCl_3$ (5 mL) and CH_2Cl_2 (5 mL). Rinses were added to the separatory funnel. The organic layer was collected and the aqueous phase extracted 3 times with 1:1 $CHCl_3/CH_2Cl_2$ (10 mL). The combined organic extracts were dried over anhydrous sodium sulfate, concentrated *in vacuo*, and loaded onto a cotton and C_{18} silica gel pipette column system. The material was eluted with 0.1% TFA in MeOH. The collection was concentrated *in vacuo* and dissolved in a minimal amount of 1:1.5 MeOH/CH_2Cl_2 for HPLC analysis. Aliquots were examined by HPLC (Cosmosil Packed Column $5C_{18}$-P-MS 4.6 x 250 mm) running a gradient from 16% H_2O in ACN with 0.5% TFA to 100% ACN with 0.5% TFA.

Sample runs were examined for retinal, retinol, A2E, *iso*-A2E, and other pyridinium *bis*-retinoid compounds. In human RPE, A2E and *iso*-A2E were found at approximately 13.0 and 14.2 minutes, respectively. A peak at 8 minutes showed UV-Vis absorbances at λ_{max} 329 nm and 432 nm. A2E and isomers were found in melanolipofuscin by UV-Vis at approximately 10.3 and 10.7 minutes for A2E and *iso*-A2E, respectively. Peaks were found at 8.6 and 9.0 minutes with λ_{max} 341.0 nm, 433.2

nm and 339.8 nm, 430.8 nm, respectively. **Human RPE**. A2E: UV-Vis: λ_{max} 337.4 nm, 445 nm (lit. 336 nm, 439 nm, MeOH)[1], Iso A2E: UV-Vis: λ_{max} 331.5 nm, 433.2 nm (lit. 335 nm, 430 nm, MeOH).[1] **Melanolipofuscin**. A2E: UV-Vis: λ_{max} 339.8 nm, 433.2 nm (lit. 334 nm, 439 nm, MeOH)[1], Iso A2E: UV-Vis: λ_{max} 331.5 nm, 423.5 nm (lit. 335 nm, 430 nm, MeOH).[1]

6.3 Synthesis Experimental Details

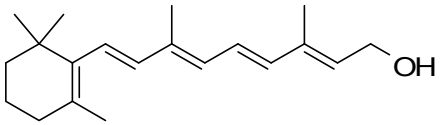

(2*E*,4*E*,6*E*,8*E*)-3,7-Dimethyl-9-(2,6,6-trimethylcyclohex-1-enyl)nona-2,4,6,8-tetraen-1-ol, all-*trans* retinol (5).[2] To a solution of vitamin A propionate (**22**, 6.71 g, 19.6 mmol) in MeOH (20 mL) and THF (2 mL) was added K_2CO_3 (3.29 g, 23.8 mmol). The solution was stirred in the dark at room temperature for four hours. To this solution was added 1:1 hexanes/Et_2O (100 mL). The resulting unwanted solid was removed by filtration and the product was concentrated *in vacuo*. The residue was purified by chromatography (SiO_2, 10% EtOAc in hexanes) to give **5** (4.49 g, 15.7 mmol, 80%) as a yellow oil.

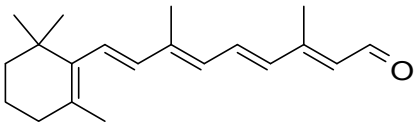

(2*E*,4*E*,6*E*,8*E*)-3,7-Dimethyl-9-(2,6,6-trimethylcyclohex-1-enyl)nona-2,4,6,8-tetraenal, all-*trans* retinal (2).[3] To a solution of all-*trans* retinol (**5**, 4.49 g, 15.7 mmol) in CH_2Cl_2 (50 mL) was added MnO_2 (20.3 g, 223 mmol). The reaction was stirred in the dark at room temperature for 5 hours and then the excess MnO_2 was removed by

filtration through celite. The product was concentrated *in vacuo* and the residue purified by chromatography (SiO_2, 3% EtOAc in hexanes) to give a yellow oil. Chilling and addition of hexanes (5 μL) to the product yielded **2** (3.82 g, 13.4 mmol, 85%) as an orange crystal.

Dopamine Reaction Study. Method I, Reaction I. To a solution of all-*trans* retinal (**2**, 0.0580 g, 0.204 mmol) in ethanol (3 mL) were added dopamine hydrochloride (**21**, 0.0331 g, 0.175 mmol) and acetic acid (10.5μL). The resulting solution was stirred for 48 hours in the dark. The crude reaction mixture was analyzed using FAB techniques with an NBA matrix. A1D (**26**, **26**) LRMS (FAB) *m/z* 420.

Method I, Reaction II. To a solution of all-*trans* retinal (**2**, 0.0579 g, 0.204 mmol) in ethanol (3 mL) was added dopamine hydrochloride (**21**, 0.0335 g, 0.177 mmol). The resulting solution was stirred for 48 hours in the dark. The crude reaction mixture was analyzed using FAB techniques with an NMB matrix. A1D (**26**, **27**) LRMS (FAB) *m/z* 420.

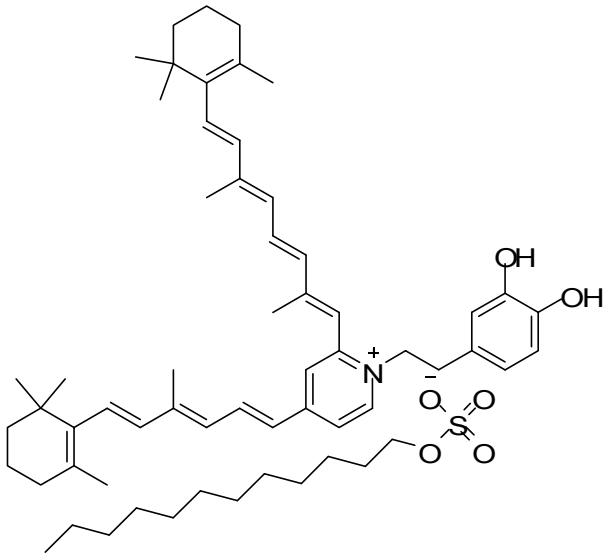

2-[2,6-Dimethyl-8-(2,6,6-trimethyl-1-cyclohexen-1-yl-)-1*E*,3*E*,5*E*,7*E*-octatetraenyl-1-(3,4-dihydroxyphenyl)-4-[4-methyl-6-(2,6,6,-trimethyl-1-cyclohexen-1-yl)-1*E*,3*E*,5*E*-hexatrienyl]-pyridinium dodecyl sulfate (A2-dopamine, A2D, 25). Method II. To a solution of all-*trans* retinal (**2**, 0.0598 g, 0.210 mmol) in 0.1 M phosphate buffer, pH 7.4, with 1.5 % w/w SDS (9 mL) was added dopamine hydrochloride (**21**, 0.0333 g, 0.176 mmol). The reaction was stirred in the dark with a sealed cap for 48 hours and the aqueous layer was extracted with CH_2Cl_2 (5 x 10 mL). The combined organic extracts were concentrated *in vacuo*. Purification of the residue by chromatography (SiO_2, 0-5% MeOH in CH_2Cl_2 gradient elution), followed by chromatotron (5% MeOH in CH_2Cl_2) to yield **25** (0.0199 g, 0.0210 mmol, 20%) as a red solid: ^{1}H NMR ($CDCl_3$, 500 MHz) δ 0.88 (DS: 3H, t, J = 6.75, CH_3), 1.05 (12H, s, 4 x CH_3) 1.25 (DS: 18H, m, 9 x CH_2), 1.39 (DS: 2H, m, CH_2), 1.49 (4H, m, 2 x CH_2), 1.63 (4 H, m, 2 x CH_2), 1.71 (3H, m, C=CCH_3), 1.74 (3H, s, C=CCH_3), 2.05(4H, s, 2 x C=CCH_3), 2.05 (3H, s, C=CCH_3), 2.11 (3H, s, C=CCH_3), 2.12 (3H, s, C=CCH_3), 2.97 (2H, bs, CH_2Ar), 4.12 (DS: 2H, bs, CH_2OSO_3), 4.17 (2H, bs, CH_2N), 6.07 (1H, s,

HC=C), 6.08 (1H, s, HC=C), 6.18-6.25 (4H, m, HC=C), 6.28 (1H, s, ArH), 6.33 (1H, s, ArH), 6.37 (1H, d, *J* = 6.0, ArH), 6.42 (1H, d, *J* =15, HC=C), 6.50 (1H, s, HC=C), 6.54 (1H, s, HC=C), 6.62 (1H, d, *J* = 7.5, HC=C), 7.02 (1 H, dd, *J* =11.5, 14.5, HC=C), 7.51 (1H, bs, pyrArH), 7.62 (1H, dd, *J* = 12.0, 14.5, pyrArH), 8.57 (1H, bs, pyrArH); ^{13}C NMR ($CDCl_3$, 125 MHz) δ 13.15-39.87 (30C, 10 x CH_3, 18 x CH_2, 2 x $C(CH_3)_2$), 58.180 (CH_2N), 68.30 (CH_2OSO_3), 114.51-152.55 (29C, 18 x C=C, 11 x ArC); UV-Vis (CH_2Cl_2) λ_{max} 342.2 nm, 438.0 nm; HRMS (ESI^+) *m/z* 684.4785 (M^+, $C_{48}H_{62}NO_2$ requires 684.4781).

A2D Photochemical Experiments. To a vial of DMSO (2 mL) was added A2D (0.0070 g) and H_2O (18 mL). A sample of the resulting solution (4 mL) was placed in a two sided, 10 mm, polystyrene vis-cuvette. The cuvette was irradiated with blue light (dichroic blue filter, 400-500 nm). Aliquots of the sample (100 μL) were taken for ESI-MS analysis every hour for five hours.

Folate A2-dopamine (FA-A2D). To an oven dried round bottom flask were added folic acid (**20**, 0.0653 g, 0.148 mmol), 1,3-dicyclohexylcarbodiimide (DCC) (0.0805 g, 0.390 mmol), and DMSO (3 mL). The resulting mixture was stirred in the dark under N_2 for 12 hours. To this flask *via* syringe was added A2D (**25**, 0.0200 g, 0.0211 mmol) and 4-dimethylaminopyridine (DMAP) (0.0286 g, 0.234 mmol) in DMSO (3 mL). The combined reaction mixture was stirred in the dark under N_2 for 24 hours. Aliquots were taken at 5 minutes and 24 hours of reaction time for analysis *via* HPLC (Phenomenex Synergi Max column, 250 x 4.0 mm) using a gradient from 90% H_2O with 0.1% TFA in ACN to 100% ACN. Partial conversion to the presumed product was

observed at 24 hours. UV-Vis (DMSO) λ_{max} 302.9 nm, 343.4 nm, 445.2 nm; LRMS (FAB) *m/z* 1108.

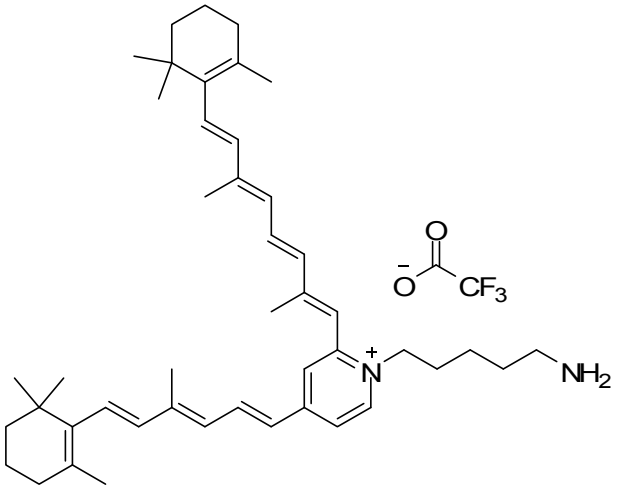

2-[2,6-Dimethyl-8-(2,6,6-trimethyl-1-cyclohexen-1-yl-)-1*E*,3*E*,5*E*,7*E*-octatetraenyl-1-(5-aminopentyl)-4-[4-methyl-6-(2,6,6,-trimethyl-1-cyclohexen-1-yl)-1*E*,3*E*,5*E*-hexatrienyl]-pyridinium 2,2,2-trifluoroacetate (A2-cadaverine, A2C, 37). To a solution of all-*trans* retinal (**2**, 0.2686 g, 0.9444 mmol) in ethanol (5 mL) was added cadaverine (**36**, 0.0922 g, 0.902 mmol) and acetic acid (54.2 μL, 0.903 mmol), and the resulting solution was stirred at room temperature in the dark for 48 hours. The solvent was removed *in vacuo*, and the residue was purified by column chromatography (SiO_2, 0-40% MeOH in CH_2Cl_2 gradient, further elution with 40:60:0.005 MeOH:CH_2Cl_2:TFA), followed by use of the chromatotron (13% MeOH in CH_2Cl_2) to afford A2C **37** (0.0388 g, 0.0519 mmol, 11%) as a red solid: ^{1}H NMR (CD_3OD, 500 MHz) δ 1.04 (6H, s, 2 x CH_3), 1.05 (6H, s, 2 x CH_3), 1.49 (2H, m, CH_2), 1.50 (4H, m, 2 x CH_2), 1.65 (4H, m, 2 x, CH_2), 1.70 (2H, m, $CH_2(CH_2NH_2)$), 1.72 (3H, s, C=CCH_3), 1.74 (3H, s, C=CCH_3), 1.91 (2H, quin, J = 6.3, $CH_2(CH_2N)$), 2.03 (3H, s, C=CCH_3), 2.05 (4H, m, 2 x C=CCH_2), 2.16 (3H, s, C=CCH_3), 2.18 (3H, s, C=CCH_3), 2.93 (2H, t, J = 7.5, CH_2NH_2), 3.31 (2H, s,

NH_2), 4.44 (2H, t, *J* = 7.5, CH_2N), 6.18 (1H, d, *J* = 17.0, C=CH), 6.25 (1H, d, *J*=10, C=CH), 6.28 (1H, d, *J* = 17.0, C=CH), 6.35 (1H, d, *J* = 15.0, C=CH), 6.42 (1H, d, *J* = 10.0, C=CH), 6.55 (1H, d, *J* =15.0, C=CH), 6.65 (1H, d, *J* =15.0, C=CH), 6.67 (1H, s, C=CH), 6.76 (1H, d, *J* =15.0, C=CH), 7.13 (1H, dd, *J* = 15.1, 11.7, C=CH), 7.86 (1H, s, ArH), 7.94 (1H, m, ArH), 8.00 (1H, dd, *J* = 15.1, 11.7, C=CH) 8.61 (1H, d, *J* = 6.84, ArH); ^{13}C NMR (CD_3OD, 125 MHz) δ 11.77-39.63 (20C, 9 x CH_3, 9 x CH_2, 2 x $C(CH_3)_2$), ≈47 (CH_2NH_2), 56.70 (CH_2N), 116.3 (CF_3), 118.79-153.56 (23C, 18 x C=C, 5 x ArC), 162 ($COCF_3$); UV-Vis (DMSO) λ_{max} 338.6 nm, 444.0 nm; HRMS (ESI^+) *m/z* 633.5148 (M^+, $C_{45}H_{65}N_2$ requires 633.5148).

A2C Photochemical Experiments. To a vial of DMSO (2 mL) was added A2C (0.0047 g) and H_2O (18 mL). A sample of the resulting solution (4 mL) was placed in a two sided, 10 mm, polystyrene vis-cuvette. The cuvette was irradiated with blue light (442 nm interference filter). Aliquots of the sample (100 μL) were taken for HPLC analysis (Phenomenex Synergi Max column, 250 x 4.0 mm) running a gradient from 90% H_2O with 0.1% TFA in ACN to 100% ACN and ESI-MS analysis every hour for five hours.

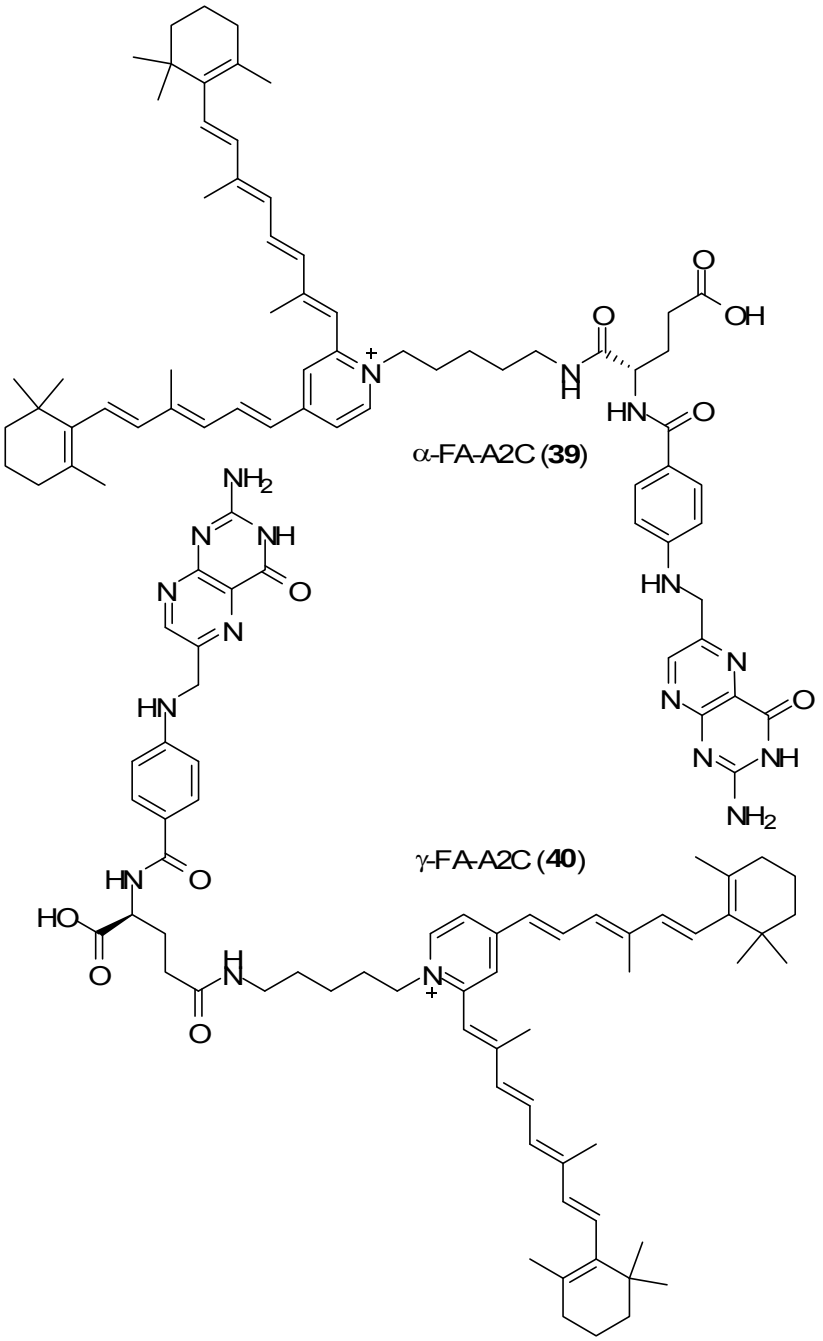

1-(5-((S)-2-(4-((2-Amino-4-oxo-3,4-dihydropteridin-6-yl)methylamino)benzoamino)-4-carboxybutanamido)pentyl)-2-((1*E*,3*E*,5*E*,7*E*)-2,6-dimethyl-8-(2,6,6-trimethylcyclohex-1-enyl)octa-trimethylcyclohex-1-enyl)hexa-1,3,5-trienyl)pyridinium (α-Folic Acid-A2-cadaverine, α-FA-A2C, 39). 1-(5-((S)-4-(4-((2-Amino-4-oxo-3,4-dihydropteridin-6-yl)methylamino)benzamido)-4-

carboxybutanamido)pentyl)-2-((1*E*,3*E*,5*E*,7*E*)-2,6-dimethyl-8-(2,6,6-trimethylcyclohex-1-enyl)octa-1,3,5,7-tetraenyl)-4-((1*E*,3*E*,5*E*)-4-methyl-6-(2,6,6-trimethylcyclohex-1-enyl)hexa-1,3,5-trienyl)pyridinium (γ-Folic Acid-A2-cadaverine, γ-FA-A2C, 40). To an oven dried round bottom flask were added folic acid (**20**, 0.0630 g, 0.143 mmol), DCC (0.0488 g, 0.237 mmol), and DMSO (5 mL). The solution was stirred in the dark under N_2 at room temperature for 6 hours. To this reaction *via* syringe was added A2C (**37**, 0.0468 g, 0.0626 mmol) and DMAP (0.0074 g, 0.0606 mmol) in DMSO (5 mL). The resulting red solution was stirred at room temperature under N_2 in the dark for 15 hours. The reaction was quenched by addition of chilled H_2O (5 ml) which resulted in the formation of a red precipitate. The solid was filtered and washed successively with H_2O (200 mL), MeOH (10 mL), Et_2O (30 mL), and CH_2Cl_2 (10 mL). The solid was dissolved with 10% MeOH in CH_2Cl_2 and concentrated *in vacuo*. Purification of the residue by chromatography (SiO_2, 5-20% MeOH in CH_2Cl_2 gradient, further elution with 20:80:0.005 MeOH:CH_2Cl_2:TFA) gave the combined α and γ products **39**, **40** (0.0541 g, 0.0462 mmol, 74%) as a red solid: ^{1}H NMR (d_6-DMSO, 500 MHz) δ 1.04 (6H, s, 2 x CH_3), 1.05 (6H, s, 2 x CH_3), 1.25 (2H, m, CH_2), 1.41 (2H, m, $CH_2(CH_2NHCO)$), 1.43 (4H, m, 2 x CH_2), 1.57 (4H, m, 2 x CH_2), 1.69 (3H, s, C=CCH_3), 1.71 (3H, s, C=CCH_3), 1.85 (2H, quin, *J*=6.3, $CH_2(CH_2NH_2)$), 1.98 (1H, m, $CH_2(CH_2COOH)$), 2.00 (3H, s, C=CCH_3), 2.01 (1H, m, $CH_2(CH_2COOH)$), 2.02 (4H, m, 2 x C=CCH_2), 2.07 (3H, s, C=CCH_3), 2.10 (2H, d, *J*=50, $CH_2(COOH)$), 2.14 (3H, s, C=CCH_3), 3.02 (2H, t, *J*=7.5, CH_2NHCO), 4.21 (1H, bs, CH(COOH)), 4.37 (2H, m, CH_2N), 4.48 (2H, d, *J*=3.4, $CH_2(NHAr)$), 6.20 (1H, d, *J*=17.0, C=CH), 6.28 (2H, m, C=CH), 6.44 (2H, m, C=CH), 6.65 (1H, d, *J*=15.0, C=CH), 6.62 (2H, d, *J*=10, ArH), 6.65

(1H, d, *J*=15.0, C=CH), 6.72 (1H, s, C=CH), 6.77 (1H, d, *J*=15.0, C=CH), 6.90 (1H, m, NH(Ar)), 7.05 (1H, dd, *J*=15.1, 11.7, C=CH), 7.09 (1H, bs, HO(Ar)), 7.63 (2H, d, *J*=10.0, ArH), 7.82 (1H, s, ArH), 8.00 (1H, s, NH(COAr)), 8.05 (1H, m, ArH), 8.05 (2H, m, C=CH), 8.61 (1H, s, ArH), 8.72 (1H, d, *J*=6.84, ArH), 11.90 (1H, bs, HO(CO)); HRMS (ESI^+) *m/z* 1056.6438 (M^+, $C_{45}H_{65}N_2$ requires 1056.6439).

Separation of α and γ FA-A2C products by chromatotron was achieved with (25% MeOH in CH_2Cl_2) giving two red products in low yields: α-UV-Vis (DMSO) λ_{max} 293.5 nm, 336.3 nm, 441.6 nm; γ-UV-Vis (DMSO) λ_{max} 294.6 nm, 336.3 nm, 439.2 nm.

6.4 References

1. Parish, C. A.; Hashimoto, M.; Nakanishi, K.; Dillon, J.; Sparrow, J. *Proc. Natl. Acad. Sci. USA* **1998**, *95*, 14609–14613.
2. Duffy, J. A.; Teal, J. J.; Garrison, M. S.; Serban, G. P. *PCT Int. Appl.* 9516659, **1995**.
3. Sollaolie, G.; Girradin, A.; Lang, G. *J. Org. Chem.* **1989**, *54*, 2620–2628.

6.5 Selected NMR Spectra

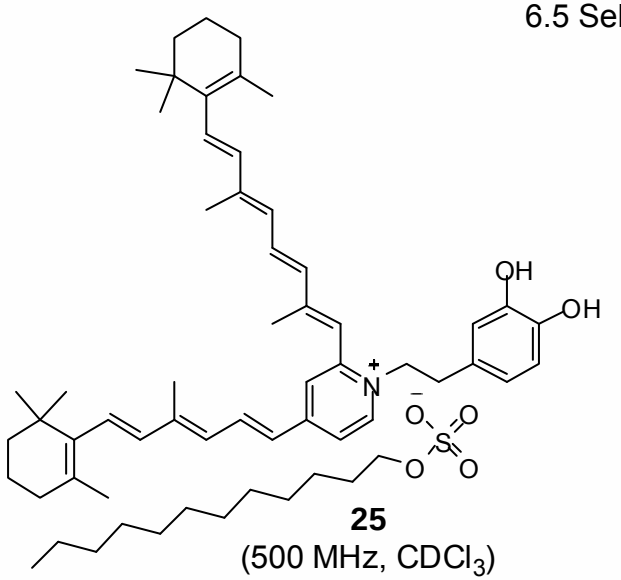

25

(500 MHz, $CDCl_3$)

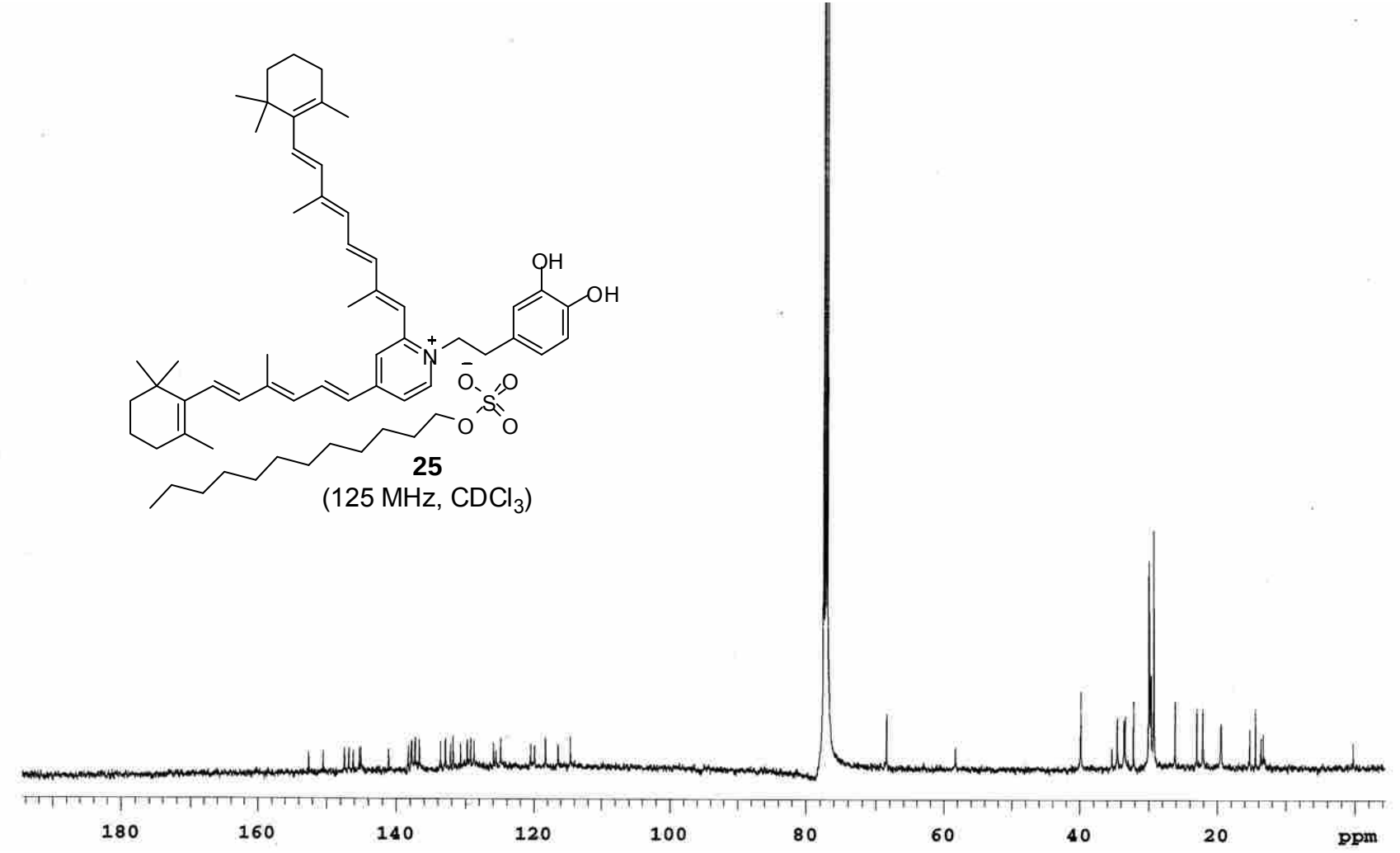

25

(125 MHz, $CDCl_3$)

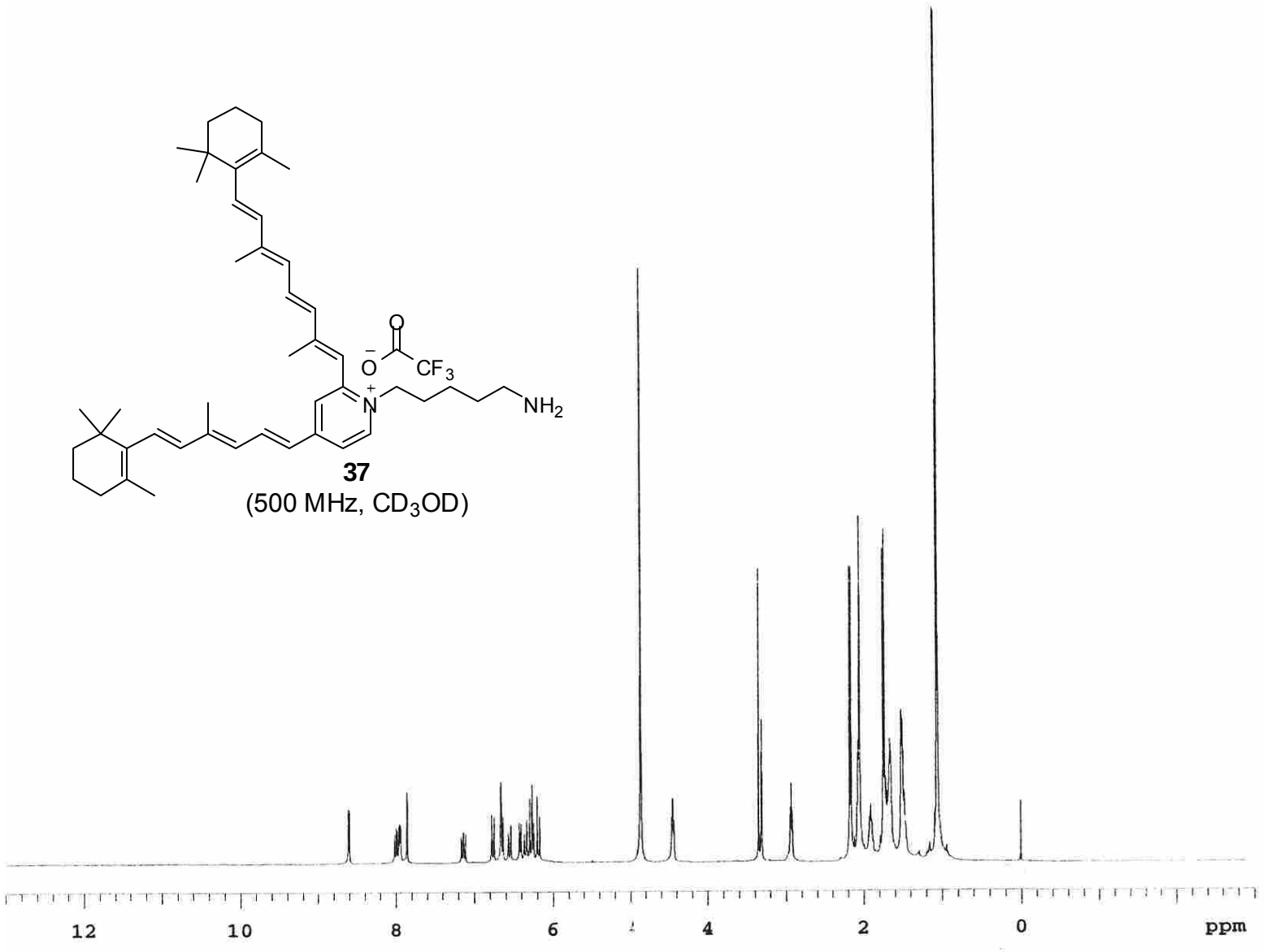

37

(500 MHz, CD_3OD)

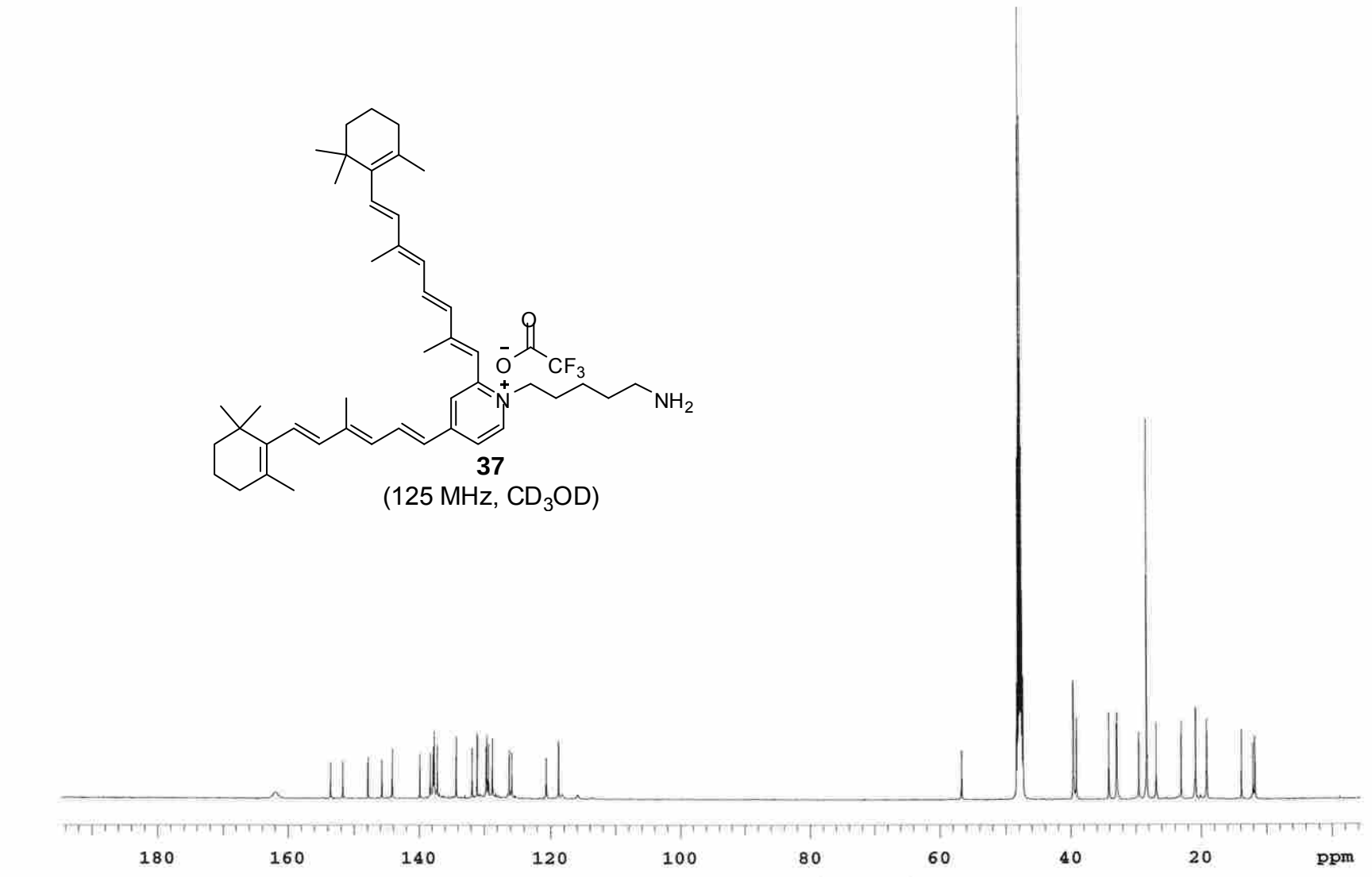

37

(125 MHz, CD_3OD)

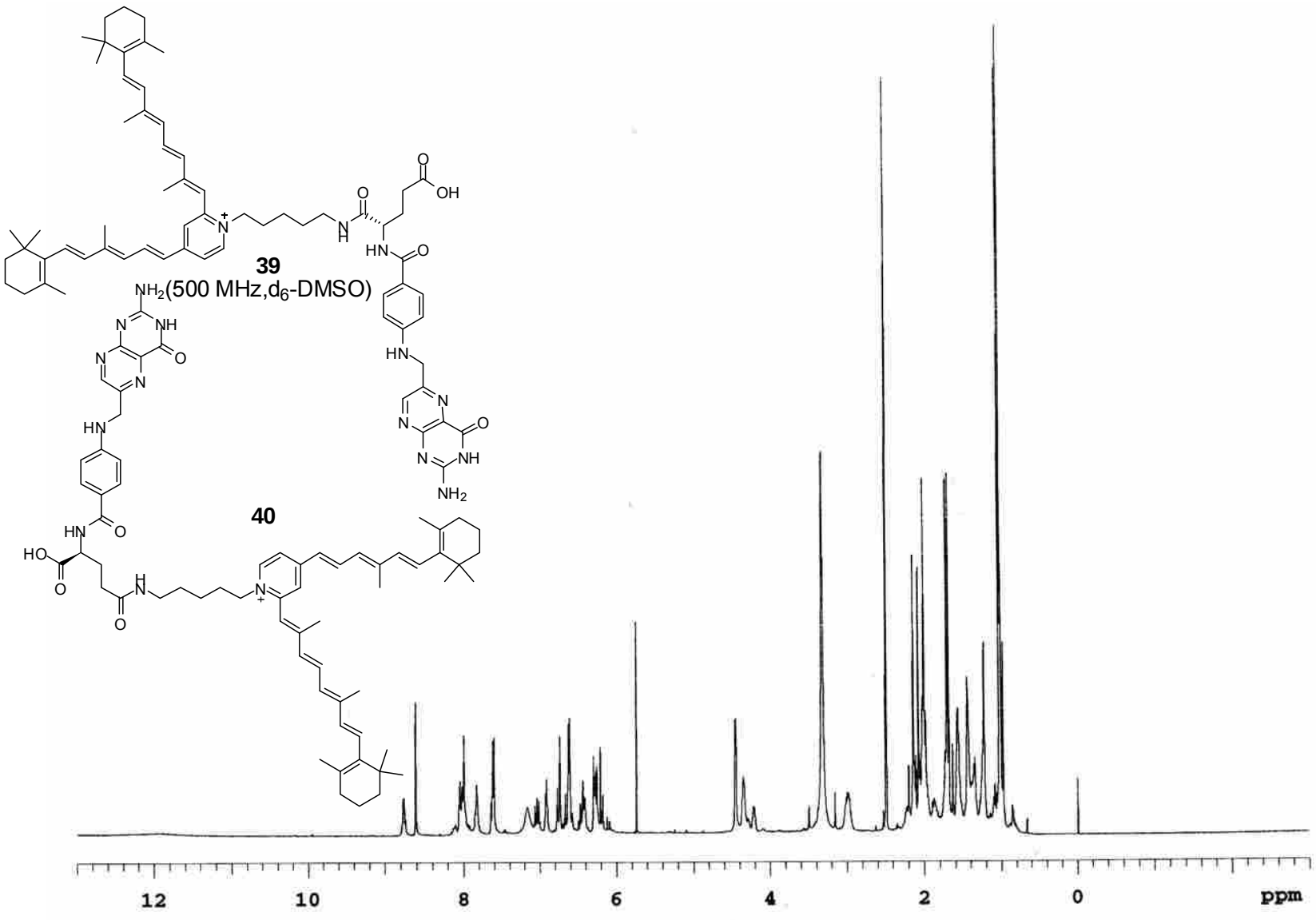
39
NH2(500 MHz,d6-DMSO)
40
12
10
8
6
4
2
0
ppm